

INFRARED STUDIES OF CARBON MONOXIDE

AND HYDROGEN ADSORBED ON

SILICA SUPPORTED METAL CATALYSTS

A thesis presented to the

UNIVERSITY OF CAPE TOWN

in fulfilment of the requirements for the degree of

DOCTOR OF PHILOSOPHY

by

MARTIN JAMES HEAL

School of Chemistry,

University of Cape Town,

Rondebosch, Cape,

South Africa.

September 1976.

The copyright in this thesis is held by the
University of Cape Town.
Reproduction in any form or by any means
may be made for study purposes only, and
not for publication.

The copyright of this thesis vests in the author. No quotation from it or information derived from it is to be published without full acknowledgement of the source. The thesis is to be used for private study or non-commercial research purposes only.

Published by the University of Cape Town (UCT) in terms of the non-exclusive license granted to UCT by the author.

A C K N O W L E D G E M E N T S

I would like to express my sincere thanks to my supervisors :
Professor E. C. Leisegang, and Dr. R. G. Torrington for their
invaluable guidance and friendship throughout the course of this
work.

I would also like to thank my colleagues for their useful comments,
and in particular Charles Ledger and John Cordiner for their help
in constructing the laboratory apparatus. I am indebted to the
University of Cape Town for financial assistance during the course
of this study.

Finally, I wish to thank Miss M. Dreyer for kindly typing the
manuscript.

(ii)

S U M M A R Y

The interaction of carbon monoxide and hydrogen on silica supported nickel, cobalt, and iron catalysts was studied using infrared spectroscopy. The products occurring in the gas phase, as well as spectra of adsorbed CO surface species in the frequency range 2300 - 1700 cm^{-1} for different order of addition of the two reactants was examined. Bulk powdered samples and conventional thin transparent sample discs were used to study either the products in the gas phase or the adsorbed CO species respectively. It was found that :

(a) for nickel catalysts.

(i) The bands found at 2080 cm^{-1} (on CO preadsorption), and at 2074 cm^{-1} (on H_2 preadsorption and on treatment with a CO/ H_2 mixture), can be assigned to co-adsorbed surface species having the structures $\text{Ni}(\text{CO})_X$ and $\text{H}_Z \text{Ni}(\text{CO})_Y$ respectively, where $4 > X > Y > 1$, $Z \geq 1$.

(ii) The band attributed to linearly held adsorbed CO, either at 2080 cm^{-1} when at room temperatures or at lower frequencies on evacuation or heating, was correlated with methane formation. Previously only "bridged" CO ligands were thought to be responsible.

(iii) A band which occurred at 2055 cm^{-1} was correlated with the formation of $\text{Ni}(\text{CO})_4$. It was found that gaseous $\text{Ni}(\text{CO})_4$ was formed rapidly at room temperatures when only CO was present or providing the catalyst was pretreated with CO prior to the addition of H_2 .

(iv) Heating the system caused bands attributed to adsorbed CO to shift to lower frequencies. On cooling, the frequency shift occurred in the opposite direction but followed a different path, i.e., as the

(iii)

distribution obtained at the higher temperatures persisted the adsorbed CO was considered to become "frozen". On further heating and cooling this shift became temperature reversible. The "frozen" CO was attributed, in part, to a side reaction in which CO₂ was formed. The CO₂ effectively prevented the adsorption of more than one CO ligand per metal site.

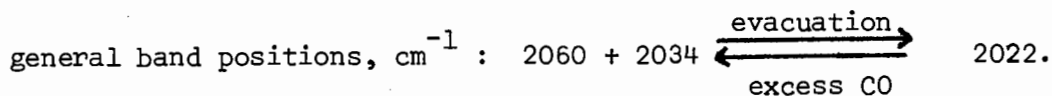
(v) Methane was formed at temperatures above $190 \pm 5^{\circ}\text{C}$, slightly lower than that found for cobalt ($195 - 215^{\circ}\text{C}$) and iron catalysts ($>220^{\circ}\text{C}$), when all these catalysts were subjected to similar experimental conditions.

(vi) A by-product, CO₂, was formed providing CO had been preadsorbed prior to the addition of H₂. This suggested that different "active" sites became available, and its formation was considered to proceed via either a carbide or surface oxygen species. The lower formation temperature limit (about 100°C) for CO₂ corresponded closely with the temperature of dissociation of CO.

(b) for cobalt catalysts.

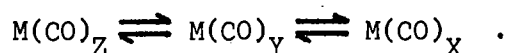
(i) Cobalt displayed a degree of "activity" in between that shown by nickel and iron. This was reflected in the main infrared band ascribed to linearly held CO ligands which decreased in frequency across the series Fe, Co, Ni.

(ii) A reversible band frequency shift was observed for CO on cobalt under varying conditions according to the equation:



(iv)

(iii) The multiplicity and frequencies of infrared bands given by CO chemisorbed onto Co/SiO₂ catalysts can be explained in terms of the CO : metal ratio, whereas only their shape is dependent on "external" forces such as ligand-ligand interactions, metal to metal distances, and the nature of the adsorption sites, e.g., planes, corners, and edges. The interpretation included bridged CO ligands, as the lower the CO frequency the lower the CO : metal ratio; and could also be applied to CO on nickel catalysts. The bands found above 2000 cm⁻¹ were attributed to the species M(CO)_Z, M(CO)_Y, and M(CO)_X corresponding to the frequencies 2060, 2034, and 2022 cm⁻¹ respectively, and where Z > Y > X ≥ 1. Evidence to support this hypothesis was obtained by varying the CO pressure, evacuation, temperature effects, and the addition of H₂. For example, the expected equilibria were given on varying the CO pressure, namely :



(iv) A band observed at 2181 cm⁻¹ was attributed to weakly chemisorbed CO with some CO existing in a physisorbed state. The chemisorbed species was considered to be adsorbed onto cobalt oxide surfaces. Similar conclusions were reached for the 2169 cm⁻¹ band given by CO on iron.

(v) Evidence showed that linear CO groups were involved in methane formation, similar to that found for nickel catalysts. Methane formation was dependent on both time and temperature. Also an intermediate complex, formed between M - CO and H₂ was considered to be stable within the temperature range 125 - 195°C.

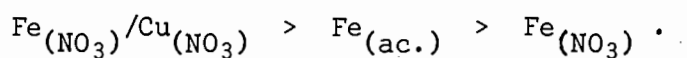
(v)

(c) for iron catalysts.

(i) Iron catalysts showed a tendency to chain propagation, forming ethane and propane in much larger amounts than were formed on nickel and cobalt.

(ii) The preadsorption of hydrogen prevented chain propagation from occurring, either by co-adsorption or by blocking specific adsorption sites.

(iii) Fe/Cu catalysts prepared from the nitrates were more "active" than iron catalysts prepared from the nitrate or acetate. Catalytic activity was of the order:



Longer reduction times and higher temperatures increased catalytic activity.

(iv) A band at 2030 cm^{-1} was assigned to linear CO chemisorbed species which were firmly held on the metal surface.

C O N T E N T S

	<u>PAGE</u>
ACKNOWLEDGEMENTS	(i)
SUMMARY	(ii)
CONTENTS	(iv)
CHAPTER 1. INTRODUCTION	1
1.1 Catalysis	1
1.2 Molecular Bonding in Carbon Monoxide and Metal Carbonyls	4
1.3 The Use of Infrared Spectroscopy in the Study of Adsorbed Molecules	7
CHAPTER 2. LITERATURE REVIEW.	10
2.1 Introduction	10
2.2 Infrared Spectra of Carbon Monoxide and other Gases Adsorbed onto Nickel	15
2.3 Infrared Spectra of Carbon Monoxide and other Gases Adsorbed onto Iron	28
2.4 Infrared Spectra of Carbon Monoxide and other Gases Adsorbed onto Cobalt.	36
O B J E C T I V E S	39
CHAPTER 3. EXPERIMENTAL METHODS AND PROCEDURE.	42
3.1 Apparatus	42
3.1.1 The Infrared Spectrometer	42
3.1.2 The <i>in situ</i> Cell	43
3.1.3 The Reactor	48
3.1.4 The Differential-Pulley System	50
3.1.5 The Die	52
3.1.6 The Vacuum Line	52

	<u>PAGE</u>
3.2 Gas Purification	54
3.3 Adsorbent Preparation	55
3.3.1 Nickel, Iron, and Cobalt Catalysts for Use in the Reactor.	55
3.3.2 Nickel, Iron, and Cobalt Catalysts for Use in the <i>in situ</i> Cell	57
3.4 Procedure	60
3.4.1 Procedure - Reactor Experiments	60
3.4.2 Procedure - <i>in situ</i> Cell Experiments	64
3.4.3 Experiments on the Rate of Carbon Monoxide Diffusion	67
CHAPTER 4. RESULTS	70
4.1 The Reactions of CO and H ₂ on Silica Supported Nickel Catalysts	70
4.1.1 Reactor Experiments - Nickel	70
4.1.2 <i>In situ</i> Cell Experiments - Nickel	81
4.2 The Reactions of CO and H ₂ on Silica Supported Iron Catalysts	108
4.2.1 Reactor Experiments - Iron	108
4.2.2 <i>In situ</i> Cell Experiments - Iron	112
4.3 The Reactions of CO and H ₂ on Silica Supported Cobalt Catalysts	118
4.3.1 Reactor Experiments - Cobalt	118
4.3.2 <i>In situ</i> Cell Experiments - Cobalt	121
4.4 Mass Spectroscopy Results	132

	<u>PAGE</u>
CHAPTER 5. DISCUSSION OF RESULTS AND CONCLUSIONS	138
5.1 Introduction	138
5.2 Nickel Catalysts	143
5.3 Iron Catalysts	154
5.4 Cobalt Catalysts	158
APPENDIX 1.	167
Experiments on the Rate of Diffusion of Carbon Monoxide	
APPENDIX 2.	172
The Silica Disc Reference	
APPENDIX 3.	175
Calibration of the Infrared Spectrometer	
LIST OF TABLES.	
Table 1. Vacuum Line - Ratio of Volumes	52
Table 2. Catalysts Used in the Reactor	56
Table 3. Catalysts Used in the <i>in situ</i> Cell	59
Table 4. Results Demonstrating the Rate of Diffusion of Carbon Monoxide - 1.	168
Table 5. Results Demonstrating the Rate of Diffusion of Carbon Monoxide - 2.	170
Table 6. Mass Spectra of Products given by Fe, Co, and Ni Catalysts.	136
Chart 1. Sample Preparation Techniques.	14
LIST OF FIGURES	
Figure 1. Infrared <i>in situ</i> Cell	45
Figure 2. Infrared <i>in situ</i> Cell, end-on view	46
Figure 3. Sample holder with sample disc in position.	47

	<u>PAGE</u>
Figure 4. The Reactor	49
Figure 5. Time - temperature curves, when using the differential pulley system	51
Figure 6. The vacuum line : schematic diagram	53
Figure 7. Spectrum of products at 400°C from CO followed by H ₂ adsorbed on Ni/SiO ₂ .	71
Figure 8. Plot of absorbance as a function of temperature, at 3017,5 cm ⁻¹ , from the interaction of CO and H ₂ on Ni/SiO ₂ .	73
Figure 9. Spectrum of products at 400°C from a CO/H ₂ mixture adsorbed on Ni/SiO ₂ .	75
Figure 10. Spectrum of products at 400°C from H ₂ followed by CO adsorbed on Ni/SiO ₂ .	77
Figure 11. Spectrum of products at 400°C from CO adsorbed on Ni/SiO ₂ .	78
Figure 12. Spectrum of products at 400°C from CO _{ads} . and H ₂ on Ni/SiO ₂ .	79
Figure 13. Plot of absorbance as a function of temperature at 2063,6 cm ⁻¹ due to adsorbed CO on Ni/SiO ₂ .	82
Figure 14. Spectrum of CO adsorbed on Ni/SiO ₂ for both CO alone and CO followed by H ₂ .	84
Figure 15. Spectrum of CO adsorbed on Ni/SiO ₂ for both H ₂ followed by CO and a CO/H ₂ mixture.	86
Figure 16. Spectra of CO adsorbed on Ni/SiO ₂ during heating.	87
Figure 17. Effect of heating on the spectrum for a CO/H ₂ mixture adsorbed on Ni/SiO ₂ .	89

	<u>PAGE</u>
Figure 18. Plot of band B frequency as a function of temperature, for CO on Ni/SiO ₂ .	90
Figure 19. Effect of evacuation on the spectrum for CO adsorbed on Ni/SiO ₂ .	92
Figure 20. Effect of evacuation on the spectrum for a CO/H ₂ mixture adsorbed on Ni/SiO ₂ .	93
Figure 21. Plots of absorbance as a function of temperature at 2030 cm ⁻¹ .	94
Figure 22. Plot of absorbance as a function of temperature at 2056 cm ⁻¹ .	96
Figure 23. Spectra of CO adsorbed on Ni/SiO ₂ during heating.	98
Figure 24. Spectra of CO adsorbed on Ni/SiO ₂ on cooling.	99
Figure 25. Spectra of CO adsorbed on Ni/SiO ₂ on re-heating.	100
Figure 26. Plot of band B frequency as a function of temperature for CO adsorbed on Ni/SiO ₂ .	102
Figure 27. Spectrum of CO adsorbed on an aged/sintered Ni/SiO ₂ disc.	104
Figure 28. Spectrum of CO adsorbed on an oxidised Ni/SiO ₂ sample disc.	106
Figure 29. Spectrum of products at 400°C from CO and H ₂ adsorbed on Fe/Cu/SiO ₂ .	110
Figure 30. Fragmentation pattern of products from CO and H ₂ adsorbed on Fe/Cu/SiO ₂ .	133
Figure 31. Effect of CO pressure on Band B at 2169 cm ⁻¹ for CO on Fe/Cu/SiO ₂ .	114

	<u>PAGE</u>
Figure 32. Effect of evacuation on the spectrum for CO adsorbed on Fe/Cu/SiO ₂ .	116
Figure 33. Spectrum of products at 400°C from CO followed by H ₂ adsorbed on Co/SiO ₂ .	120
Figure 34. Fragmentation pattern of products from CO and H ₂ adsorbed on Co/SiO ₂ .	134
Figure 35. Fragmentation pattern of products from CO and H ₂ adsorbed on Ni/SiO ₂ .	135
Figure 36. Plot of absorbance as a function of temper- ature at 3017,5 cm ⁻¹ due to adsorbed CO and H ₂ on Co/SiO ₂ over a 2 hr. period.	122
Figure 37. Effect of evacuation on the spectrum of CO adsorbed on Co/SiO ₂ .	124
Figure 38. Plot of absorbance as a function of temper- ature at 2020 cm ⁻¹ for CO and CO + H ₂ on Co/SiO ₂ .	126
Figure 39. Effect on the spectra on varying CO pressure.	127
Figure 40. Effect of H ₂ on band A for CO on Co/SiO ₂ .	129
Figure 41. Spectrum of CO adsorbed on an aged/sintered Co/SiO ₂ disc.	131
Figure 42. Spectrum of a thin SiO ₂ disc.	173
REFERENCES:	176

CHAPTER 1.

INTRODUCTION

1.1 CATALYSIS.

Catalysis has become very important as a stage of process in a large percentage of manufactured goods¹. Consequently the nature of the catalyst and catalytic processes have been the source of extensive study for many years. A catalyst can be defined as a substance which increases the rate of attainment of equilibrium in a reacting system without causing any alteration in the free energy changes involved. It achieves this by becoming temporarily involved in the reaction. The effect of a catalyst has been found to be a kinetic one and not a thermodynamic one, which not only lowers the activation energy of a reaction² but also determines which path is taken.

There are two systems in catalysis: (i) homogeneous catalysis, in which the catalyst and reactants are in the same phase, and (ii) heterogeneous or contact catalysis, whereby the catalyst is in a different phase from the reactants. Many of the important industrial catalytic processes employ heterogeneous catalysts and these may be divided into two groups; (a) metals of the transition series; and (b) non-metals, which can be classified under the sub-headings, semiconductors, and insulators. Heterogeneous catalysis chiefly involves chemisorption of the adsorbate onto the adsorbent, i.e. the formation of chemical bonds between the two phases. This is accompanied by a loss or decrease in entropy, and also a decrease

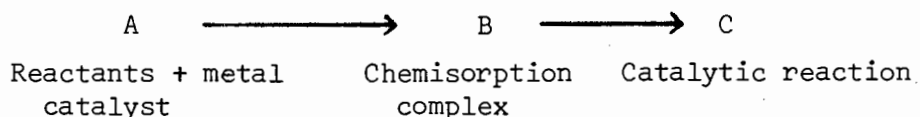
in free energy. Hence, from the Second Law of thermodynamics given by $\Delta G = \Delta H - T\Delta S$, it follows that the process of adsorption is exothermic³. Some interesting aspects of the chemisorption of gases by transition metals are given below:

1. Chemisorption is usually an 'activated' process proceeding at a finite rate⁴ which in turn increases with temperature⁵.
2. Chemisorption is specific, i.e. it can be expressed as a function of the chemical properties of both adsorbent and adsorbate. Frequently heterogeneous catalysts are specific for particular groups of reactions.
3. Only monolayer thickness of the adsorbate is attained, and the fraction of the surface covered is large even at low pressures^{6,7}.
4. As the number of gas molecules adsorbed increases the fraction of the surface covered increases and the heat of adsorption, ΔH_{ads} , decreases⁸. This is considered to be due in part to 'active' spots or centres on the surface which adsorb preferentially, indicating the heterogeneity of the surface⁹⁻¹¹.

There are three chief factors which influence catalytic activity, namely:

- a) the geometric factor;
- b) the electronic factor;
- c) the effect of imperfections, or 'active centres' on the surface.

These have been dealt with elsewhere¹²⁻²¹, but will nevertheless play an important part in this work. A heterogeneous catalytic reaction can be represented symbolically²²:



Thus the situations that arise and which can be studied are:

- (1) the transition from state A to B; (2) the identification of the chemisorption complexes, their reactivity and role in the particular catalytic reaction; (3) the reaction mechanism going from state B to C; and (4) the liberation of the reaction products from the surface or their stability on the surface. Infrared spectroscopic methods may provide information on the chemisorption complexes, (2).

The objective in catalysis research is to understand the phenomenon of catalysis to the extent that catalysts can be 'tailor-made' to meet specific requirements. The elucidation of mechanisms in catalysed reactions is of considerable importance, and infrared spectroscopy has been of great value in observing the interactions and perturbations that occur at the surface during adsorption. Of particular interest is the reaction of carbon monoxide and hydrogen on an iron catalyst in the synthesis of paraffinic and olefinic hydrocarbons, known as the Fischer-Tropsch process²³. Nickel and cobalt catalysts were used initially because of their known 'activity' in hydrogenation reactions^{107,23}. Now iron catalysts are used, being less expensive, but the process does require medium industrial pressures of 15 - 20 atmospheres. Several mechanisms have been proposed for this process²³⁻²⁶, based on studies using heterogeneous catalysts. Ferreira^{27,28} studied this process using infrared techniques; however, several problems remain unsolved, for this and analogous systems.

1.2 MOLECULAR BONDING IN CARBON MONOXIDE AND METAL CARBONYLS.

Carbon monoxide chemisorbed onto d-group transition metals forms complexes which are closely related to those of metal carbonyl compounds. The infrared spectra of CO and other small molecules on specific metals will be discussed in the literature review, Chapter 2. However, a brief description will be given here of the molecular bonding in the CO molecule and metal carbonyls together with their infrared spectra.

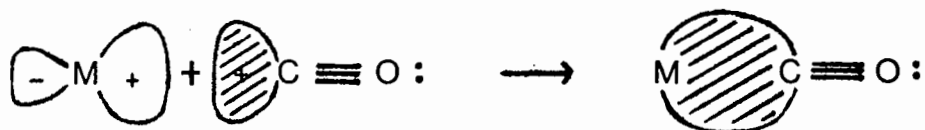
A characteristic of d-group transition metals is their ability to form complexes with neutral molecules, e.g. CO, and molecules with delocalised π orbitals such as pyridine. Various types of complex exist from binary molecular compounds, e.g. $\text{Cr}(\text{CO})_6$, to mixed species, e.g. $\text{Co}(\text{CO})_3\text{NO}$, to complex ions, e.g. $[\text{Fe}(\text{CN})_5\text{CO}]^{3-}$.

Usually the metal atoms are in a low positive, zero, or low negative oxidation state. Consequently donor atoms of the ligands stabilise these low oxidation states via their vacant orbitals in addition to lone pairs of electrons. The vacant antibonding ligand orbitals accept electron density from filled metal orbitals forming a π bond which supplements the σ bond arising from lone-pair donation, i.e. high electron density on the metal atom (of necessity in low oxidation states) can be delocalised onto ligands. This ability of ligands to accept electron density into low-lying empty π orbitals can be called ' π acidity', where acidity is used in the Lewis sense. The most important π acceptor ligand is CO, and many of its complexes are not only of structural interest, but are also important in industry in catalytic reactions. Furthermore, CO acts as a weak donor ligand

to the metal by forming very weak dative bonds, which can be represented by the structure, $O \equiv C \rightarrow M^{29}$.

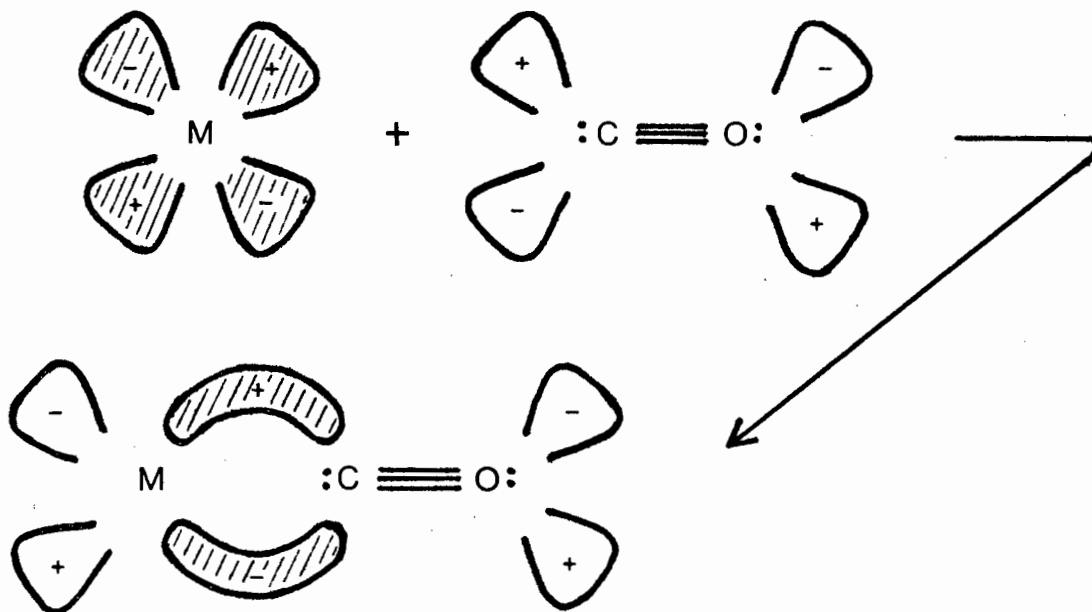
The multiple nature of the metal carbonyl bond is shown diagrammatically³⁰:

(1)



formation of a carbon to metal σ -bond using an unshared electron pair on the carbon.

(2)

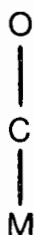


formation of a metal to carbon π -bond.

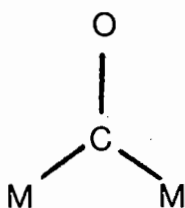
This bonding mechanism is synergic, since the drift of metal electrons into CO orbitals will tend to make the CO negative and hence increase its basicity via the σ orbital of carbon; at the same time

the drift of electrons to the metal in the σ bond tends to make the CO positive, thus enhancing the acceptor strength of the π orbitals. Thus the effects of a σ bond formation strengthen the π bonding and vice versa. Dipole moment studies indicate that the moment of an M-C bond is very low, about 0,5D, suggesting a close approach to electro-neutrality.

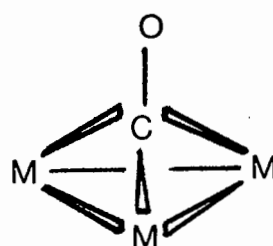
Evidence for the above is given by bond lengths³¹ and infrared spectroscopy. Changes in the metal to carbon bonding can be inferred and correlated from infrared spectra, and the molecular structure can be determined from the frequency position of the absorption bands together with the number and relative intensities of these bands³². Three CO to metal structures are exhibited by metal carbonyls:



(a) Terminal,
(linear) groups.



(b) Bridging
groups.



(c) Triply-bridging
groups.

Examples of compounds which possess terminal groups are nickel tetracarbonyl, $\text{Ni}(\text{CO})_4$, and chromium hexacarbonyl, $\text{Cr}(\text{CO})_6$, which show bands in the infrared at frequencies of 2057 and 1986 cm^{-1} respectively. A polynuclear carbonyl containing bridged and terminal carbonyl groups is iron enneacarbonyl, $\text{Fe}_2(\text{CO})_9$. For this compound infrared bands are found at frequencies 2082, 2019, and 1829 cm^{-1} . The two bands at higher frequencies can be attributed to active modes for the six terminal ligands, and the low frequency band to one active

mode for the three bridging groups. The validity of the theory that all low frequency bands, i.e. those found below 2000 cm^{-1} , are due solely to bridging groups was questioned by Cotton and Wilkinson in 1957³³, and further data ³⁴⁻⁴⁰ provided evidence which can be summarised as follows:

Bands appearing above 2000 cm^{-1} in the infrared spectra of metal carbonyls usually belong to terminal groups, and those below 2000 cm^{-1} may be attributed to 'bridged' species or may arise from the following: (1) a combination band of other fundamentals, which may be enhanced in intensity by Fermi resonance with a fundamental carbonyl mode; (2) the presence of a formal negative charge on the carbonyl; (3) the presence of electron-donor substituents, or substituents which will not engage in π -bonding with the metal.

1.3 THE USE OF INFRARED SPECTROSCOPY IN THE STUDY OF ADSORBED MOLECULES.

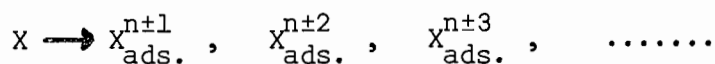
Surface properties differ from bulk properties due to the nature of the crystalline surface. Surface atoms, unlike internal atoms, have an asymmetrical distribution of forces which do not exist in a state of maximum entropy. This state can be relieved either by rearrangement of the surface atoms or by adsorption onto the surface of foreign substances. Thus the surface forces must change the symmetry of an adsorbed molecule. Minor variations in the characteristic vibrational frequencies of an adsorbed molecule arise from local differences in molecular environment, and these quantitative changes can be detected by the change in the molecule's infrared

spectrum.

Therefore infrared techniques have proved extremely useful in observing small molecules adsorbed onto metal surfaces. Data has been provided for the elucidation of structures of complexes; and mechanisms for catalytic processes can be predicted with reasonable accuracy. Furthermore, the use of infrared spectroscopy has since led to several theories on the prediction of catalytic activity.

Mayers (1958)⁴¹ proposed the concept of 'matching vibrations'. This was based on the assumption that if the frequency of the bond that must be broken to initiate catalytic reactivity is similar to that of the bond formed between the catalyst and reactant then a transfer of energy takes place readily and catalytic activity is observed. Thus the vibrations most likely to cause correct fragmentation in product formation have almost identical frequencies.

The theory of 'intermedions' was proposed by Gardner and Petrucci (1960)^{42,43}, from infrared data of CO adsorbed on various metals. The possibility that an intermediate in electronic structure existed between the species CO_{free} and CO^+ was examined. They modified a concept, first proposed by Wolkenstein⁴⁴, stating that an electron-transfer mechanism occurs on adsorption in which the adsorbate has the forms:



Hence n , which has a value <1 , was considered a property of the metal adsorbent and known as the 'polarisation fraction'.

The following relationship was shown^{45,46} between vibrational frequency of some adsorbed CO species and the number of valance

electrons:

$$[2269,96 \pm \nu(\text{CO})][12,1182 - E(\text{CO})] = 268,31 \text{ cm}^{-1}$$

where $E(\text{CO})$ is the number of valance electrons, and $\nu(\text{CO})$ the vibrational frequency of the CO species. Values of $E(\text{CO})$ were calculated using observed $\nu(\text{CO})$ values of CO adsorbed onto various metals, and so assigned either to 'intermedions' or carbonyls. 'Intermedions' were assumed to be the species responsible for catalytic activity. However, bands attributable to these had only been detected for CO adsorbed on metals with partially vacant d-orbitals. Nevertheless, the above hypothesis provided a measure of catalytic activity.

Several different infrared techniques have been employed in the study of adsorbed species and these, together with a review on the adsorption of CO and other molecules on metals, will now be discussed in the following chapter. The references ⁴⁷⁻⁵⁶ were used to obtain a working knowledge on the subjects of catalysis and infrared spectroscopy.

CHAPTER 2.

LITERATURE REVIEW

2.1 INTRODUCTION

Until the advent of X-ray and ultraviolet photoelectron spectroscopy, infrared had been the only spectroscopic method able to provide information as to the structure of adsorbed species on metal surfaces. Infrared still provides the basis of most investigations, and as a tool in surface chemistry invites much interest. The various techniques used, together with the type of information obtainable, have been widely reviewed^{176,57,58}. Naturally these techniques have their own limitations but the most significant is the difficulty of attaining reproducible results. Observations frequently show that infrared spectra of an adsorbate are dependent in part on the sample preparation as well as conditions, times and temperatures, used within a specific preparation. Illustrated in Chart 1 are the chief methods of sample preparation.

Other limitations of infrared methods are: Firstly, surface studies are often confined to narrow spectral regions due primarily to strong absorption of the solid adsorbent to which the molecules are bound. Large frequency shifts and changes in spectral intensities can occur in the adsorbed state which are not comparable to solvent or substituent effects. These may be caused by the asymmetric surface electric field⁵⁹. Also normal vibrations of adsorbed species may interact with lattice vibrations of the adsorbent, resulting in lateral interactions through a mechanical coupling via the adsorbent lattice⁶⁰.

Another important limitation is the difficulty of obtaining pure metal surfaces. This can almost be achieved by using ultra-high vacuum techniques at pressures of 10^{-11} - 10^{-12} Torr.

Nevertheless, apart from the above, infrared can provide direct evidence on the molecular structure of adsorbed species. It is particularly valuable where hydrogen bonding interactions occur. Infrared measures the vibrational and rotational states of molecular systems, which depend on the masses and stereochemical arrangements of the constituent atoms and on the force constants of the connecting bonds, hence the value of infrared techniques in gas/solid surface studies.

The change from the "model" system (studied in the laboratory) to the "real" one (an industrial catalytic process) must be quantitative only²², e.g. the area of the active surface and the number (not the type) of active chemisorption complexes is changed on going from the former system to the latter one. Therefore ideally experiments should be performed on both well defined surfaces and the industrial catalyst, the objective being to prove whether the basic reaction mechanism is the same in both cases. This does pose its own problems. However, although "model" systems are often far removed from industrial catalytic systems they are relatively simple, experimentally inexpensive, and open to investigations which are essentially involved with the chemical properties of the catalyst and not its physical properties.

Relatively complex catalysts are used by S.A.S.O.L. in the Fischer-Tropsch synthesis but they are basically of the 'inert oxide support' type catalysts. Therefore simple silica supported

metal catalysts were studied in this work, although they too have their limitations. Scattering due to the adsorbent may occur, but can be reduced if the particle size is reduced⁶¹. Ideally supported metal particles should be 10 to 100 Å in diameter with 30 to 30 000 metal atoms per particle⁵⁷. With small particles most of the metal atoms are exposed to the surface, whereas about $\frac{1}{10}$ th become exposed for a 100 Å particle. For practical purposes it is necessary to compromise between increasing the sample thickness, which increases the intensity of the absorption bands, and decreasing the thickness to achieve sufficient infrared transmission.

The structure of supported metal catalysts is of prime importance and the mean size, or size distribution, of metal particles has been determined by gas chemisorption, electron microscopy, and X-ray diffraction methods. Studies have also been concerned with establishing whether specific activity of metal crystallites is a function of their size⁶², and it was concluded that specific activity is a constant over a large range of average particle sizes for a number of different processes. It has been suggested⁶³ that some electron transfer occurs between the metal and its support, which modifies the metal's electronic structure and therefore its activity; and indeed, valency induction has been shown to occur⁶⁴. Several other methods have been used to study the nature and structure of supported metal catalysts, e.g. electrical conductivity, contact potential methods on nickel-chromia catalysts⁶⁵, and Mössbauer spectroscopy^{66,70}. Also the ease of reduction of supported metal catalysts does depend on the nature of the support, and a detailed study has been given of supported NiO catalysts⁶⁷.

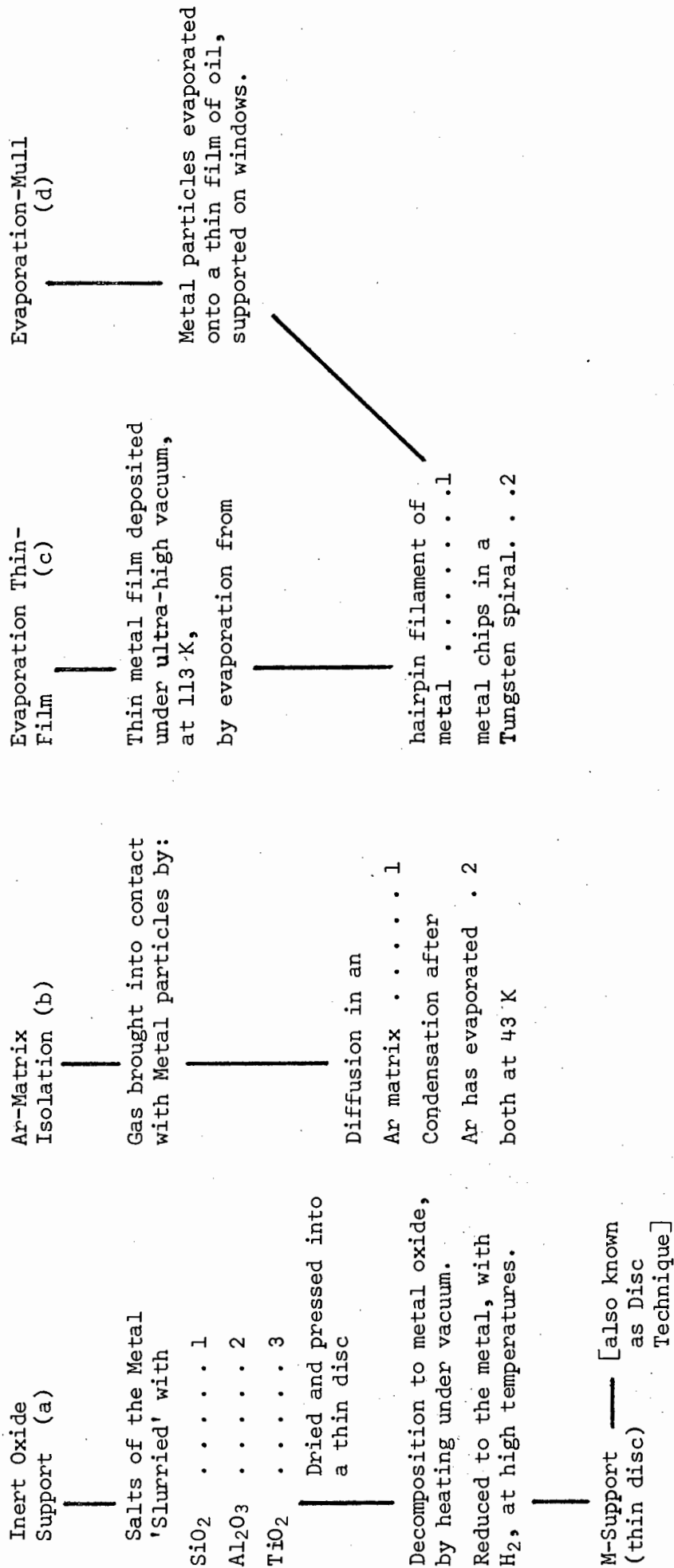
Infrared spectra of adsorbed CO are similar to those given by metal carbonyls and absorption bands (arising from the CO stretching frequency) are found in the region 2300 to 1700 cm^{-1} . In the adsorbed state the metal to carbon bond has approximately single bond character while the carbon to oxygen bond has character between double and triple bond. Very few investigations have reported on absorption bands attributable to the metal to carbon bond. For CO on platinum a band, due to the C-Pt bond, was observed at 477 cm^{-1} ⁶⁸. Blyholder reported M-C stretching absorptions at 435 and 580 cm^{-1} for CO on nickel⁶⁹ and iron⁸² respectively.

The frequency of the CO bands is dependent on several factors, e.g., the type of CO species adsorbed, and its attachment to the metal; the nature of the metal and its support; and ligand-ligand interactions. For ligand-ligand interactions, the direction of the CO frequency shift indicates the direction of electron transfer on the chemisorption of a co-adsorbate.

In the following sections of this review only those findings most relevant to this work will be discussed. For a more comprehensive study, the reader is referred to several reviews⁷¹⁻⁷⁹, and two textbooks^{48,55}.

SAMPLE PREPARATION TECHNIQUES

for Gas Adsorption Studies on Metals.

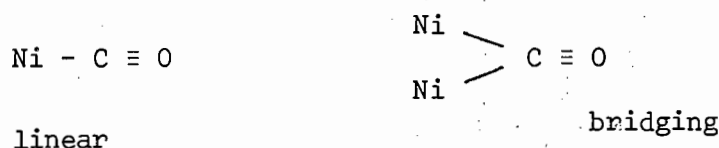


INFRARED

2.2 SPECTRA OF CARBON MONOXIDE AND OTHER GASES ADSORBED ONTO NICKEL.

A comprehensive review on infrared studies pertaining to the CO/Ni-SiO₂ system was given by Ferreira²⁷, which covered the period prior to 1970. Therefore it will be sufficient here to mention the salient points only before proceeding on to more recent work.

Infrared bands of CO chemisorbed on Ni/SiO₂ catalysts were first reported by Eischens *et al*⁸⁰. The spectrum suggested that two types of CO species were adsorbed onto the surface. Further work⁸¹ provided evidence to support this theory, and by comparing the results with spectra of metal carbonyls the following conclusions were made: CO absorption spectra could be divided into two regions with the dividing line in the vicinity of 2000 cm⁻¹. Linear, or terminal, CO species gave rise to bands found above 2000 cm⁻¹; whereas bands found below this frequency were assigned to bridging species. These complexes were thought to have the structures given below:



It soon became evident that under certain conditions linear CO groups can give bands below 2000 cm⁻¹. This would occur where the molecule is strongly coordinated to the metal, i.e. when the electron density on the metal is high, either as a result of a formal negative charge or through the presence of a promotor having

electron donor properties. In this instance the carbon to oxygen bond strength is reduced which, in turn, decreases the stretching frequency. Increased d-e. density increases the M-C σ bond which reduces the C-O bond order. The M-C-O bonding is discussed more fully in Section 5.1.

Blyholder^{69,82,83} preferred the assignment of bands at lower frequencies to linear CO coordinated to edge or corner sites on the metal. He rationalised the diverse results then available by using a simple model of linear carbonyl groups with varying degrees of π -bonding. These were dependent on the availability of d electrons for π -bonding, which would be influenced by the metal atom's nearest neighbours and ligand-ligand interactions. This view was criticised by Yates who supported Eischens in using band frequency for distinguishing between linear and bridged species. It must be understood, however, that Eischens' view was flexible as shown when he assigned a band at 1960 cm^{-1} to linear CO adsorbed on iron⁸⁵.

Clearly more evidence was required to provide a solution to what had become a controversial issue. Guerra⁸⁶, using electron microscopy techniques did not support Blyholder's theory since no appreciable crystallinity was shown by several metals then investigated. Furthermore, LEED studies⁸⁷ supported the model of "bridged" CO on Pd, and Ferreira and Leisegang²⁸ observed that at high coverage the "linear" bands grew at the expense of the "bridged" bands for CO on Ni, an observation made by Baddour *et al*⁸⁸ in their studies of supported Pd after break-in. Recently Soma-Noto and Sachtler^{89,90,84} showed that, for Pd/Ag and Ni/Cu alloy systems, the "ensemble effect" was very marked but the electronic

"ligand effect" was of minor importance.

The two effects can be described thus:

(a) The geometric "ensemble effect"^{177,178}. An adsorbing molecule can form chemical bonds with either one, two, or more surface atoms. Each of these chemisorption complexes will lead to different reaction products. Diluting the adsorbing metal atoms with inert atoms will then change the selectivities in a predictable manner since the relative concentration of ensembles with a smaller number of atoms capable of forming chemisorption bonds will increase upon alloying with an inactive metal.

(b) The electronic "ligand effect"¹⁷⁹. Even for a chemisorption bond between one metal and an adsorbed atom, the chemical nature of the neighbours of the adsorbing metal atom will be important. Catalytic selectivity is often determined by the relative chance of an adsorbed intermediate either to react further or to be desorbed. Therefore weakening of the adsorption bond by alloying can, in principle, change selectivity.

Consequently, if Eischens' assignment is correct, then with increasing dilution of Pd with Ag the concentration of the bridged complex would decrease more rapidly than that of the linear complex as the former is dependent on a pair of adjacent Pd atoms. If, however, the electronic configuration of the adsorbed atom caused the large band frequency shift to higher frequencies, then alloying Pd with Ag would be expected to produce a successively increasing shift with an increase in Ag content. The results showed that on alloying Pd with Ag this gave rise to a pronounced change in relative band intensities

but the band frequencies remained unchanged. The intensities of the low frequency bands decreased with increasing Ag content in alloys. This clearly supported Eischens assignment, and it must be concluded that bands found below 2000 cm^{-1} are attributable to bridging complexes. Hobart⁹¹ reached similar conclusions from the infrared spectra of CO adsorbed on Cu/Ni alloys. Ansorge *et al*⁹² showed that with magnetic and infrared techniques for CO adsorbed on Ni/SiO₂ catalysts the ratio of the two configurations, linear to bridged, changed with temperature. This was based on the fact that the Ni/CO ratio increased from 1,2 to 1,8 between the temperature range -78 to 20°C. Similar conclusions were reached by Barber *et al*⁹³ using secondary ion mass spectrometry for CO on Cu and Ni. At high temperatures the bridged species was the more stable of the two structures. On alloying Ni with Cu Dalmon⁹⁴ reported that the bond number between CO and the metal decreased, and for geometric reasons the "bridged" species decreased. Observed frequency shifts on alloying were ascribed to electronic effects, thus confirming earlier reports⁹⁵.

Eischens *et al*⁸¹ considered carbon monoxide frequency positions and relative intensities to be a function of the surface coverage, θ , and on decreasing θ bridged CO was more firmly held than linear. Other workers⁹⁶ have also explained these results in terms of induced dipole-dipole interactions between chemisorbed molecules. The effect of the metal concentration was investigated by Yates and Garland⁹⁷ for the CO - Ni/SiO₂ system. The variety of bands observed at frequencies $>2000\text{ cm}^{-1}$ were attributed to single linear groups adsorbed onto different crystalline, semi-crystalline, and amorphous

metal sites. This view gained much support^{27,48,55,83}, and factors such as competition between ligands for metal d electrons and dipole-dipole interactions between adjacent ligands have taken a back seat. The possibility that more than one CO molecule could be chemisorbed onto a single metal site had not been excluded^{27,81,98}, but one band only was assigned to this phenomenon, e.g. for CO on Ni²⁷ evidence suggested that the band at 2058 cm^{-1} , close to that found for gaseous nickel tetracarbonyl, was due to two or more ligands per single metal site. The tricarbonyl was found to absorb at nearly the same frequency⁹⁹.

The admission of H₂⁸¹ not only broadened the CO bands but also shifted them to lower frequencies. Blyholder and Neff¹⁰⁰ reported two bands on admission of H₂ and CO onto Ni catalysts. These were found at 2060 and 1900 cm^{-1} , and were assigned to chemisorbed CO. These bands remained on evacuation at room temperatures, but disappeared on heating to 240°C . No evidence, however, could be given to show that adsorbed CO had reacted with H₂ at that temperature. Usually evacuation affects the infrared spectra of CO adsorbed on metals^{97,101}, causing the bands to shift to lower frequencies with a slight decrease in intensity. This effect indicates the removal from the surface of less stable complexes.

The role of the support on the surface properties of Ni catalysts was examined by O'Neill and Yates⁹⁸. The CO spectra using SiO₂ as a support were found to be similar to those reported earlier^{81,102}, however Al₂O₃ and TiO₂ supports induced large variations in the relative proportions of species present and in the carbon to metal bond strength.

Peri¹⁰³ subjected Ni/SiO₂ catalysts to increasingly severe reduction with hydrogen. Consequently the spectra allowed the identification of CO adsorbed on the oxidised and reduced portions of the nickel surface. Incomplete sample reduction created different adsorption sites and, as the presence of oxygen altered the energy of adsorption sites on adjacent nickel atoms, so the CO spectrum became more complicated. The observed change in the CO spectra on further investigations¹⁰⁴ (which involved the preadsorption of HCl), was interpreted as an inter-conversion of sites. Peri¹⁰³ also concluded that the nickel surface was heterogeneous, and from the spectrum of adsorbed NH₃ on Ni/SiO₂ bands were attributed to coordinately bonded species to surface Lewis acid sites. Earlier reports¹⁰⁵ had also concluded that the surface was acidic. A novel interpretation of the spectra of adsorbed CO was proposed by Gardner and Petrucci⁴⁵. They suggested that a relationship exists between the vibrational frequencies of gaseous molecules and ions and the number of valence electrons. Bands found near 2200 cm⁻¹ were thus attributed to CO ions ranging up to CO²⁺, which were presumably generated by metal ions on the surface. Alternatively, Peri¹⁰⁴ thought that they may have been due to weak σ complexes with surface metal ions. Recently evidence¹⁰⁶ was provided to support the idea of ionic CO adsorbed species. The absorption spectra of CO on NiIII oxide of different stoichiometric composition indicated the existence of CO⁺ and CO⁻ on oxidised and reduced surfaces respectively.

Ferreira and Leisegang²⁸ reinvestigated the adsorption of CO on silica supported nickel and cobalt catalysts. Six bands (A to F) were observed for each metal, with the low frequency bands, A, being assigned to bridged carbonyl species. High frequency bands at 2060

to 2090 cm^{-1} (D) and 2035 to 2050 cm^{-1} (B) were assigned to single linear groups. The latter was associated with sites of low coordination number, and these shifted to higher frequencies with an increase in CO coverage in accord with the molecular orbital model proposed by Blyholder⁸³. At very high coverage band C was observed at 2058 cm^{-1} , close to that given by gaseous $\text{Ni}(\text{CO})_4$, and was attributed to two or more ligands per single site. Finally, bands E and F, found at frequencies $>2100\text{ cm}^{-1}$, were given on incompletely reduced samples.

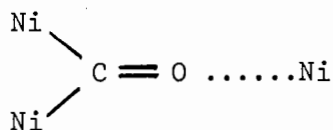
The interaction of CO and H_2 on potassium promoted and unpromoted nickel catalysts was also studied^{27,28}. By varying the H_2 : CO ratio different reactions were observed to take place on the surface. At high ratios CH_4 was given as the chief product, whereas at low ratios CO_2 was predominant. The reaction mechanism for CH_4 production was considered to involve bridged CO species only, and to proceed via a carbide or by oxygenated alcoholic-type surface intermediates. This is in accordance with the mechanism proposed by Emmett¹⁰⁷. It was also shown that gaseous $\text{Ni}(\text{CO})_4$ was formed when CO was left in contact with the nickel surface over long periods, but the reaction did not occur providing the catalyst was at room temperature prior to the admission of CO. Later Derbeneva *et al*¹⁰⁸ provided evidence which revealed the formation of $\text{Ni}(\text{CO})_x$ compounds on a nickel catalyst surface, where $x \leq 4$. Also gaseous $\text{Ni}(\text{CO})_4$ was given by CO contained in an otherwise empty stainless steel infrared cell when at room temperature and pressures ≥ 50 Torr¹⁰⁹.

Thermal desorption studies were reported for CO adsorbed

onto Ni/SiO₂ surfaces by Marx *et al*¹¹⁰ and the results compared with those given by infrared methods. In particular, the influence of preparative methods on the adsorbent characteristics was investigated. Surface models were devised by considering the correlations between desorption peaks, calculated thermodynamic and kinetic reaction data, and spectroscopically determined band positions.

The study of gases chemisorbed onto thin metal films, (see Chart 1), has become a very popular method of analysis. Either reflectance techniques on evaporated films, or transmission through specially prepared porous films are used. Early investigations by Pickering and Eckstrom¹¹¹, involved the use of reflectance spectra of CO on Ni and Rh. For Ni, the spectrum revealed a strong doublet at 2061 and 2050 cm⁻¹ with a weak band at 2031 cm⁻¹. All these bands were attributed to linearly held CO and they readily disappeared on evacuation. In contrast, adsorbed species found on Rh were more firmly held. Gardner and Petrucci⁴² observed one band only at 2060 cm⁻¹ for CO on evaporated Ni films which was again assigned to the presence of linear groups. Later Eckstrom¹¹² found, in addition to the 2060 cm⁻¹ band, many others within the frequency range 1200 to 750 cm⁻¹, but the nature of the adsorbed species responsible for them was not determined. Adsorption of CO on Ni films prepared by the evaporation-mull technique⁶⁹ gave strong bands at 2080 and 1940 cm⁻¹ together with a broad band at 435 cm⁻¹. The last could be attributed either to the Ni-C bond stretching vibration, (analogous to Ni-C in Ni(CO)₄), or being broad may encompass both the Ni-C-O bond and Ni-C stretch in accordance with earlier data¹¹³.

The above work together with that by Sardisco¹¹⁴ led to an attempt to explain the diverse results by modifying the technique of preparing evaporated nickel films¹¹⁵. Unfortunately, the investigation was not wholly successful as the authors could only conclude that strong bands of variable intensity could be found in the region 2080 to 1900 cm^{-1} . This was in agreement with previous workers. However, a new band dependent on sample preparation was given at 1620 cm^{-1} . This was ascribed to a bridged carbonyl structure of the type :



The low frequency could be explained in terms of additional bonding or association between the oxygen and a third nickel atom, because the structure was analogous to ketones adsorbed on Lewis acid sites on alumina. The high frequency bands were associated with species adsorbed onto different crystalline sites which was in agreement with Yates and Garland⁹⁷. The addition of oxygen caused these bands to disappear, but bands were observed at 1530 and 1363 cm^{-1} , characteristic of surface carbonates⁶⁹.

Other workers reinvestigated the adsorption of CO on nickel films¹¹⁶⁻¹¹⁹. Bradshaw and Pritchard¹¹⁷ deposited films under ultra high vacuum which gave spectra similar to those shown by supported nickel. Particle size effects played an important role, and small particles enhanced absorption at both low and high frequencies. Anomalous transmission peaks were thought to be produced by adsorbed species on small particles which possessed a particularly high coefficient of extinction. These effects, however, were expected to

occur only with thin films. Bradshaw and Pritchard¹²⁰ extended their studies of adsorption at low temperatures to other metals. Absorption bands only appeared at high CO coverage which suggested that strongly bound molecules may be in states which are infrared inactive. However, it was subsequently reported by Bradshaw and Vierle¹²¹ that as CO was adsorbed onto nickel films the electrical resistance changed with the spectra. It was interesting to see that the spectrum of CO on nickel prepared by the argon matrix isolation technique and reported by Blyholder *et al*¹¹⁸ closely resembled that for CO on silica supported nickel, and oil-matrix supported nickel. Clearly the electronic states accessible at room temperature are also accessible when at 44 K, i.e., C-type sites with surface atoms having coordination numbers of 6 and 7.

Less attention has been given to other diatomic adsorbates such as H₂, N₂, NO and O₂. The most relevant studies carried out on the adsorption of hydrogen will be discussed in this review, as they will have some bearing on the work covered here. Spectra were obtained by Kavtaradze and Sokolova¹²² of H₂ adsorbed onto alumina-supported iron, nickel, and other metals. Weak absorption bands were found in the region 1850 to 1940 cm⁻¹, which were duly assigned to vibrations of the M-H bond. Earlier workers¹²³, however, provided no infrared evidence of hydrogen adsorbed onto silica-supported nickel. Probably the metal particle size was unsuitable in this instance in view of the demonstration¹²⁴ showing that for N₂ the metal particle size had to lie between 15 and 70 Å before spectra could be recorded. Lapujoulade and Neil¹²⁵ used flash desorption techniques for their studies of H₂ chemisorbed onto Ni (110) and revealed that for low

surface populations, ($<10^{13}$ atoms/cm²), adsorption occurred as a one binding state having an adsorption enthalpy of 20,3 Kcal/mole. As the population increased a second, more tightly bound, state was observed. Casey¹²⁶ also studied the adsorption of H₂ and its interaction with CO on polycrystalline nickel using thermal desorption techniques. Three states were found in the desorption spectrum for H₂. It was proposed that the α and β_1 states corresponded to desorption from intrinsic states which had been predicted theoretically. The maximum combined coverage for these states was found to be 2×10^{14} atoms/cm². Also adsorption coefficients and bond energies were calculated¹²⁷ for the adsorption of H₂ on nickel films. Similar results were reported by Shirono *et al*¹²⁸ for H₂ adsorption on palladium catalysts. By calorimetric measurements the heat of adsorption decreased with an increase in the amount of hydrogen adsorbed. Again three states of H_{ads} were observed, these being strongly adsorbed, (H_s), dissolved hydrogen, (H_d), and weakly adsorbed, (H_w). On evacuation the H_s state hardly desorbed, but the other two desorbed readily. A very interesting observation showed that CO poisoned exclusively the sites of H_s. Furthermore, Primet and Sheppard¹²⁹ found that, for a Ni-SiO₂ catalyst, the infrared spectra of chemisorbed CO was sensitive to the presence or otherwise of H coadsorbed onto the metal surface. A 'hydrogen-covered' surface gave a ν CO band near 2070 cm⁻¹, whereas for a 'bare' or 'hydrogen-free' surface a band was exhibited near 2040 cm⁻¹. Using this criterion it was then shown that a 'hydrogen-covered' surface lost much of its hydrogen by evacuation at 50°C. Microgravimetric measurements¹³⁰ revealed that only 6% of supported nickel atoms can bind a hydrogen atom, whereas 21 and 71% of atoms were

available for Pt and Rh respectively.

Multireflection infrared spectra¹³¹ of CO at low pressures on nickel films gave two broad bands with maxima at 2060 and 1920 cm^{-1} . Three processes were considered to take place on the surface, all being dependent on the CO pressure. At pressures $\leq 10^{-6}$ Torr a dissociative adsorption was thought to occur in which C and O adatoms were formed. Between 10^{-6} and 10^{-2} Torr pressures adsorption would then be of the form Ni-C-O, and $\geq 10^{-2}$ Torr the slow formation of gaseous $\text{Ni}(\text{CO})_4$ was predicted. In contrast, very interesting evidence was provided by Joyner and Roberts¹³² on the nature of adsorbed CO on nickel by X-ray and ultraviolet electron spectroscopy. At 295 K CO was adsorbed in a molecular form, but on heating to 430 K changes in the spectra were interpreted as reflecting thermally induced dissociation of adsorbed CO. It is now understandable why it is difficult to obtain nickel free traces of carbon and oxygen, since their formation is relatively easy from CO_{ads} at about 400 K. Similar results were obtained for iron¹³³. Very little molecular adsorption of CO was evident on heating at 350 K. These results were confirmed later⁹³ for nickel, when it was shown that surface carbides were formed on the metal which involved a dissociation mechanism.

Further studies¹³⁴ revealed that the oxygen (1s) binding energy in the non-dissociative adsorption of CO on metals decreased as the heat of adsorption increased. Also, when the heat of adsorption was the same on different metals the O (1s) binding energy was the same. This suggests that π bonding, (back donation), is the major contribution to the M-CO bond, with the σ contribution being less significant.

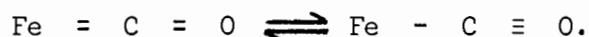
Correlation of the binding energy with the heat of adsorption suggests that, at 295 K, dissociative adsorption of CO occurs when $\Delta H_{\text{ads}} \gtrsim 300 \text{ KJ mol}^{-1}$. Further discussion on the above is given in Section 5.1.

Reduced nickel catalysts are extremely susceptible to oxygen chemisorption. For silica supported nickel¹³⁵ all the nickel atoms were assessible, and the observed ratio of 1 : 1 for O : Ni was independent of the nickel content and of the oxygen adsorption temperature. Previous workers^{115,69} had reported that oxygen readily displaced CO from the surface at room temperatures, which in turn reduces the metal's "activity" with respect to CO adsorption. Therefore, precautions were taken to ensure that the metal catalysts studied in this work remained "oxygen-free".

Other adsorbents investigated on nickel catalysts using infrared have been NO¹³⁶, NH₃¹³⁵, and MeOH¹⁰⁰.

2.3 INFRARED SPECTRA OF CARBON MONOXIDE AND OTHER GASES
ADSORBED ONTO IRON.

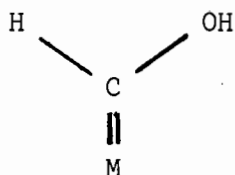
Infrared spectra recorded by Eischens and Pliskin¹³⁹ of adsorbed CO on silica supported iron catalysts when at room temperatures and low CO pressures showed one band only at 1960 cm^{-1} . With high pressures a shoulder at 2019 cm^{-1} was observed. This latter absorption was attributed either to iron carbonyl formation or to weakly held linear CO groups. By comparing spectra given by iron carbonyls the low frequency band at 1960 cm^{-1} was also assigned to linear CO, and having the structures :



The authors found that iron catalysts were very difficult to reduce at temperatures below 350°C . Furthermore, at about 500°C there appeared to be a reaction with the carrier. Therefore catalysts were first reduced for 16 hr. while gradually increasing the temperature to 380°C , and then reduction was continued at this temperature for a further 2 hr.

The Fe-CO system, (similar to that found for the Ni-CO system^{115,69}), was very sensitive to small traces of oxygen. This caused the band at 1960 cm^{-1} to disappear and be replaced by another at 2128 cm^{-1} . With the addition of hydrogen, however, no change was given in the spectrum contrary to that observed for Pt-CO and other metal-CO systems in which band shifts to lower frequencies were the norm. Generally speaking hydrogen chemisorption is enhanced by preadsorbed CO on metals and this phenomenon has been attributed to

the formation of complexes of the type:



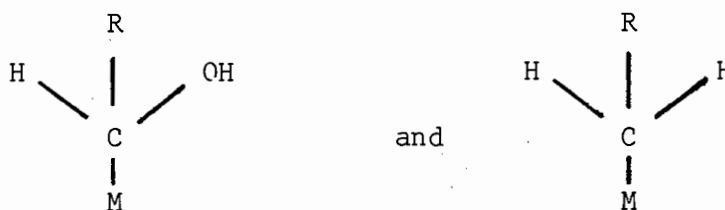
These complexes were postulated as intermediates in the Fischer-Tropsch synthesis, although no evidence was provided to support this.

Other workers^{140,82} observed a band at 2019 cm^{-1} with a shoulder at 1998 cm^{-1} for CO adsorbed on iron. Both bands were regarded as arising from linear structures, of the form $\text{Fe} = \text{C} = \text{O}$, adsorbed onto different crystallographic sites. Here a reversal in intensities was given to that previously shown¹³⁹. This was considered to be due to slight differences in preparative methods which in turn would affect the relative numbers of the two adsorption sites available. The fact that when at room temperatures the peak size, (CO coverage), was independent of pressure, whereas at 180°C it became a function of pressure provided evidence to support the existence of two different crystallographic sites. Again reduction times and temperatures were carefully controlled to produce an 'active' surface⁸².

The addition of foreign gases to adsorbed CO often resulted in the displacement of the adsorbate from the metal surface due to preferential adsorption of the additive gas. Displacement effects by oxygen have been observed in all cases^{139,140}, and the appearance of a band at much higher frequencies clearly represents CO_{ads} on an oxidised surface. Occasionally foreign gases do not displace CO but merely cause a shift of the carbonyl frequency either to higher or

lower values. In these cases changes in the spectrum were interpreted⁸³ in terms of decreased or increased electron-donor capacity of the metal towards adsorbed CO arising from adsorption of a foreign gas on adjacent metal sites. On heating¹⁴⁰ the iron catalyst, in the presence of CO and O₂ or on addition of CO₂, the characteristic carbonate structures⁶⁹ were given, as shown by the appearance of a band at 1560 cm⁻¹.

The interaction of CO and H₂ on silica supported iron gave negative results when at room temperatures, but at 180°C three bands in the C-H stretching region appeared in addition to the carbonyl bands. These vibrations were assigned to free methane^{139,141}. Also a band found at 2943 cm⁻¹ was attributed to saturated hydrocarbons existing in a chemisorbed state. No chemisorbed or free species containing the group (=C-H) was detected. Thus the infrared evidence was in accord with intermediates of the type:



Prior to this work several mechanisms had been postulated for the interaction of hydrogen and carbon monoxide on iron. For example, those proceeding via carbide intermediates¹⁴², or oxygenated alcoholic type compounds^{23,143}.

The interaction of H₂ and CO is of considerable interest in relation to the Fischer-Tropsch synthesis, and was investigated by Kölbel *et al*¹⁴⁴ for an iron-magnesium oxide mixed catalyst. The

infrared spectrum was extremely complicated, providing evidence for carbonate and carboxylate species as well as adsorbed CO. After exposure to the gas mixture at temperatures of 453 K, bands appeared at 2840 and 2720 cm^{-1} . These were assigned to aldehyde groups. Interactions occurred with the support, and CO on pure MgO^{145} produced absorptions characteristic of carbonate groups. Consequently the carbonyl stretching vibration of the aldehyde group was obscured. Furthermore, a complex spectrum was given¹⁴⁶ for CO alone with a mixed catalyst, and all absorptions were assigned to carbonyl groups attached to the iron surface. These absorptions were not influenced by recrystallisation or by hydrogen pretreatment. Another absorption found at 1825 cm^{-1} , which shifted to higher frequencies on the addition of hydrogen, was thought to be due to dissociative adsorption of CO_2 on iron.

Ferreira²⁷ failed to produce "active" iron catalysts despite alterations made in the sample content and method of preparation. Two reasons were put forward to explain this "inactivity", (i) compound formation could have occurred between the metal and its support; and (ii) the thermodynamics of reactions of iron, nickel, and cobalt predict¹⁰⁷ that iron oxide is extremely difficult to reduce at high temperatures relative to nickel and cobalt oxides.

Infrared studies of adsorbed species on iron catalysts prepared by other methods have been numerous and a few are worth mention here. The most popular method has been the evaporation thin-film technique. Spectra of CO on thin iron films were reported by Bradshaw and Pritchard¹²⁰ to be similar to that given on supported

iron, although bands only appeared at high CO coverage and so were considered to be due in part only to chemisorbed CO. Others¹¹⁶ observed a band at 1950 cm^{-1} for CO on Fe films when at 170 K, which on warming to room temperatures shifted to 1900 cm^{-1} and possessed a low frequency tail. A similar result was given with cobalt. On admission of oxygen the 1900 cm^{-1} band disappeared; once again a result analogous to that given on supported iron^{139,140}.

The absorption bands were generally broad in appearance, in contrast with the much sharper bands shown on supported iron¹³⁹. This was predicted by Smith and Eckstrom¹⁴⁸. Band sharpness was considered to be related to the crystalline size on which the ligands adsorb. Pashley¹⁴⁹ considered that very thin films have an island-like structure, or formation, consisting largely of discrete nuclei which aggregate as the film thickness increases. It seems likely that an aggregation sintering process may well be responsible for the disappearance of spectral bands with thicker films. On the other hand, the average size of crystallites of a supported catalyst is usually smaller than for evaporated films. This is shown by electron microscopy and volumetric adsorption data. Therefore spectra of supported metals, e.g. iron, show similar features to those given by evaporated films, but these are overshadowed by the more intense contributions from smaller particles.

Baker *et al*¹¹⁶ investigated the effect of warming to room temperatures and found the film structure became slightly altered. It was argued that the accompanied loss of the high frequency absorption may have been due either to desorption of some CO or conversion to a less

strongly absorbing state. Sintering had probably been the chief influence which removed adsorption sites having special geometry. Spectra of CO on sintered iron¹⁵⁰ gave bands at 1910 and 2020 cm^{-1} which were indicative of two chemisorbed forms on densely packed faces. They were unaffected by the addition of hydrogen, but disappeared with oxygen. Preadsorption of hydrogen also had no effect on the spectrum for Fe/MgO catalysts¹⁴⁶ as mentioned earlier. Blyholder¹⁵¹ provided interesting data for CO on iron prepared by the argon matrix isolation technique. Low temperature studies were considered to be very important for observing primary gas-solid processes as secondary processes would be suppressed. Evidence pointed to the existence of distinct low temperature adsorption sites, referred to as type 'C' chemisorption. Previous observations¹⁵² were made for H₂ and N₂ adsorbed onto Fe, Ni, and other metals. Type 'C' chemisorption was thought to be both atomic and molecular. Existence of a low temperature chemisorbed state for CO on tungsten, referred to as "virgin CO", had been inferred earlier¹⁵³ from flash filament, field emittance, and electron impact desorption studies. Now the same evidence was provided by infrared for CO on iron¹⁵¹.

Experiments¹⁵⁴ involving chemisorbed CO and Lewis bases on metal films, (including iron and nickel), suggested that for metal complexes there is an electronic balance between the different species simultaneously chemisorbed onto a metallic surface. This was considered one of the best justifications in support of the concept of "surface complexes". However, the results did not resolve the different interpretations of Eischens^{80,81} and Blyholder^{69,82,83} with regard to bridged CO complexes.

A complete picture of the nature of iron catalysts cannot be obtained from infrared data alone and results obtained using other techniques provide valuable information, for example, on the reduction of supported iron catalysts using Mössbauer spectroscopy¹⁵⁵. X-ray and vacuum u.v. photoelectron spectroscopic methods¹³³ showed that kinetic control of CO dissociation on iron was operating since molecular adsorption occurred at low temperatures and dissociation adsorption became increasingly important above 290 K. The concept of charged species offered an interesting approach. Kovalev *et al*¹⁵⁶ identified different charged forms of H and CO, and their interaction on iron during alcohol synthesis were determined from electronic work function data. Below catalytic temperatures (-30 to + 23°C) the forms H^- and CO^+ existed, whereas at catalytic temperatures (110 to 180°C) H^+ and CO^- predominated. Catalytic activity for chain propagation during the interaction of H_2 and CO on Fe(111) surfaces was deduced by Kölbel and Tillmetz¹⁵⁷ from the geometrical and electronic structure of the complex. Complexes of the Anderson type containing oxygen were found to be stable on both iron and cobalt, whereas for nickel the complex was thought to be of the methylene type.

Very recently adsorption forms of CO were studied¹⁵⁸ on ferric oxide of different reduction states. Chemisorbed CO forms differed in the nature of the bond between CO and the surface and in the deformation of the electronic structure of CO. Silica supported ferric oxide was subjected to increasingly severe reduction with hydrogen. An infrared absorption band was observed at 2180 cm^{-1} for CO on Fe_2O_3 , indicating that the CO bond was strengthened in comparison

with the bond for free CO. However, for CO on FeO and Fe, bands at 2070 and 2020 cm^{-1} respectively clearly showed that the CO bond was weakened in comparison with the free CO molecule.

2.4 INFRARED SPECTRA OF CARBON MONOXIDE AND OTHER GASES
ADSORBED ONTO COBALT.

Infrared spectra recorded by Gardner and Petrucci⁴² of carbon monoxide on silica supported cobalt showed three bands at 2179, 2160 and 2091 cm^{-1} . From this, and spectra of CO on other metals, a relationship was postulated between the ligand's frequency and the number of valence electrons associated with it. Furthermore, the various CO species, CO^{n+} , differed from one another by having different integral numbers of valence electrons. These conclusions have been covered in more detail in Section 1.3.

Basila¹⁵⁹ observed infrared bands for CO on cobalt in the frequency ranges 2179 - 2140 cm^{-1} and 2091 - 2070 cm^{-1} . Occasionally bands were found at 1950 and 1820 cm^{-1} . No structure assignments were given to the species responsible for these absorptions. The only other spectra recorded prior to Ferreira's²⁷ work were for $\text{C}_x\text{H}_y\text{O}$ compounds adsorbed onto cobalt films¹⁶⁰ using the evaporation-mull technique.

A more comprehensive study²⁷ was made on the adsorption of CO on potassium promoted and unpromoted silica supported cobalt catalysts. The results were as follows:

(1) Infrared absorption bands were observed for CO on potassium promoted and unpromoted cobalt oxide at 2155 and 2170 cm^{-1} , and 2178 cm^{-1} respectively. These absorptions were assigned to chemisorbed CO species.

(2) Cobalt was found to be more difficult to reduce than nickel; hence the degree of reduction was measured by the diminution of the band at 2178 cm^{-1} .

(3) Infrared absorptions for CO on unpromoted cobalt were observed at 2025, 2070, 2095, 2130 and 2180 cm^{-1} which were assigned as bands A to F respectively.

(4) The intensities of bands B and D were directly related to CO pressure, whereas A was found to be inversely proportional to pressure. Band B showed the largest increase in intensity with pressure, but band A was the most persistent on decreasing the pressure.

(5) Bands E and F disappeared rapidly on evacuation.

(6) Prolonged treatment with CO appeared to have a more beneficial effect on the activity of available sites, especially B sites, than did hydrogen reduction.

(7) Potassium promoted cobalt catalysts exhibited CO absorptions at slightly lower frequencies. These absorptions decreased further with an increase in the K : Co ratio.

The general conclusions reached on the interpretation of the spectra for nickel^{27,28} also applied to cobalt.

Other investigations made use of the evaporation thin film technique. An infrared band was observed by Baker *et al*¹¹⁶ at 1990 cm^{-1} for CO on cobalt when at temperatures of 170 K. The band possessed a low frequency tail which extended to below 1800 cm^{-1} . Earlier reports¹⁶² had also shown very broad CO bands on both iron and cobalt. The spectrum did not change in appearance on evacuation, but on warming to room

temperatures the maximum shifted to 1970 cm^{-1} . As with iron, it was concluded that this loss of absorption on warming may have been due to (1) desorption of some CO; (2) conversion to a less strongly absorbing state; or (3) sintering. Spectra reported¹²⁰ for CO on thin films deposited at 113 K under ultra high vacuum were similar to silica supported cobalt catalysts. However, the band at 2040 cm^{-1} was only given at high coverages. This band also shifted to lower frequencies on both warming and evacuation (compare the results¹¹⁶ given above). It is most interesting to note that re-adsorption of CO did not bring back the high frequency band.

The interaction of the Lewis bases, Me_3N and EtNC , caused the 1980 cm^{-1} band for CO on cobalt to shift to lower frequencies. This was observed by Queau and Poilblanc¹⁵⁴ who explained the shift in terms of the Lewis bases being chemisorbed onto free sites, which then augment the electronic charge on the metal by increasing the π bond between the metal and the CO ligand. This in turn decreases the CO bond strength and thus decreases the vibrational frequency.

A molecular orbital model proposed by Blyholder and Marvin¹⁶¹ for the π -electron system of adsorbed CO on a cluster of metal atoms successfully accounts for the shift in position of the two principle bands as the metal is varied across the series, vanadium-copper. This important fact will be discussed more fully in Chapter 5. Other studies^{138,147} will also require further discussion as they are highly relevant to this work. In brief, they concern (i) the adsorption of hydrogen and oxygen on cobalt and nickel as determined by calorimetric and magnetic measurements¹³⁸, and (ii) the adsorption of CO on Co-Mg mixed catalysts using infrared techniques¹⁴⁷.

O B J E C T I V E S.

Most researchers using infrared techniques in catalysis studies have been concerned only with observing the adsorbed complexes on metal surfaces. From the absorption spectra they postulated reactions of these complexes that were most likely to occur when subjecting a system to certain conditions, such as evacuation, co-adsorption, or changes in temperature. The evidence obtained has provided valuable information on the nature and properties of these adsorbed complexes, but, by limiting their investigations to state B (see page 2), the transition to state C has been left open to conjecture. Comprehensive data about state B has been obtained for many catalysts and adsorbates. This on its own was inadequate, and other methods of analysis were often necessary to substantiate any proposed theories. The chief problem has been the disagreement between the different sets of results obtained by varying the method of sample preparation, making generalisations difficult. Unless the use of infrared is extended or modified to include the analysis of more than state B, it seems inevitable that experimental details will always play an important role; and each system studied will possess its own degree of independence.

The 'model' systems investigated in this work have been based on a 'real' one; the industrial synthesis of hydrocarbons known as the Fischer-Tropsch process in which the two reactants, carbon monoxide and hydrogen, are brought into contact with an iron catalyst. With the exception of Ferreira²⁷, very little work using infrared techniques

has been done on this process. Consequently several parameters have not been touched on at all. For example, the effect of (1) a steady increase in temperature on the absorption spectra; and (2) varying the order of addition of reactants on the catalytic activity. Also the problem of how and why catalytic activity changes with respect to final products formed remains partially unsolved.

The objectives of this research can now be listed below:-

- (a) To investigate the catalytic process involving the formation of hydrocarbons using infrared spectroscopy. The study to be confined to the three 'model' systems:

(i) $(\text{CO} + \text{H}_2) - \text{Ni}$

(ii) $(\text{CO} + \text{H}_2) - \text{Co}$

(iii) $(\text{CO} + \text{H}_2) - \text{Fe}$

Nickel and cobalt were chosen because of their known 'activity' with respect to hydrocarbon formation^{107,23}, and for the relative ease with which they form "complexes" with CO. Both will be regarded as "test" catalysts. The iron will act as the "true" model catalyst based on the more complex ones used industrially.

- (b) To determine the structure of adsorbed surface species and observe their reactions on the metal surface, using thin transparent circular discs as samples. Also to monitor the reactants and products in the gas phase using bulk (powdered) samples. This procedure would provide information on two states in the scheme, viz., the chemisorption complex (state B) and the final products (state D). Therefore, correlations can be sought between the two sets of results with a view to obtaining a description of the catalytic reaction (state C).

- (c) To report on the effect of varying the two parameters given below for all the systems described in (a) and (b) above:
- (i) the effect of the regularly varying temperature on the adsorption and reaction of carbon monoxide, alone and with hydrogen present;
 - (ii) to observe changes in catalytic activity on varying the order of addition of reactants to the catalysts.

CHAPTER 3

EXPERIMENTAL METHODS AND PROCEDURE

In order to achieve the objectives it was necessary to carry out a systematic but more complex experimental procedure than has usually been adopted for metals supported by inert oxides. Furthermore, additional and modified apparatus was required. Hence this chapter describes in full the apparatus and procedures used for the three systems which were investigated.

3.1 APPARATUS.

3.1.1 The Infrared Spectrometer:

A Perkin-Elmer model 180 infrared spectrometer was used. This is a double-beam grating instrument. It was required to measure carbon monoxide and its reaction products, with or without hydrogen present, both in the gas phase and when adsorbed onto the surfaces of "Cab-O-Sil" silica supported metal catalysts.

In one mode of operation spectra were scanned, and in the other given species were monitored in time and/or with temperature at a constant wavenumber using the CONST. CM^{-1} control. The selected frequency ranges and individual wavenumbers will be described in Section 3.4. The slit width was usually set to correspond to a resolution of 2.0 cm^{-1} when at the highest frequency of the scan. A higher resolution was not necessary because no quantitative measurements were done on any of the observed absorptions.

3.1.2 The *in situ* cell:

It was necessary to construct an infrared cell which would hold the silica supported metal discs in a vertical position in the infrared beam. There have been numerous cell designs^{27,163,98,164,140} and these were first examined before engaging on a design; the construction of which would make for efficient and convenient experimentation. Therefore, this section reports the design of a simple variable temperature infrared *in situ* cell¹⁶⁵, which meets the same specifications as that reported by Igarashi *et al*¹⁶³, and which has been used successfully in this laboratory for the entire programme. The complete body of the cell does not contain any parts that require adjustment. Thus its simplicity of design allows for convenient handling and easy access to the sample. Also its small size makes it non-specific to any model of infrared spectrometer. Decomposition of the supported metal salts and their reduction to the metal using hydrogen at high temperatures was accomplished in the cell in the normal way, followed by adsorption studies on the prepared catalysts *in situ*.

In the cell's construction four features were of considerable importance: (i) the position and efficiency of the heating assembly; (ii) a convenient sample holder capable of holding a thin disc in a vertical position relative to the horizontal infrared beam; (iii) precise monitoring of the sample temperature; and (iv) an adequate cooling system, in order to prevent cracking of the windows whilst heating the sample and to protect the vacuum seal.

The design of the cell is given in Figure 1. The entire cell, with the exception of the heating assembly and sample holder, is made

of Pyrex, blow-moulded into a single unit. This consists of the main body of the cell, 1, the water-cooling system, 2, a thermocouple well, 3, and the gas inlet and outlet tubes, 4. The latter are fitted with high vacuum stopcocks, 5, in order to isolate the cell when required, and ball joints, 6, for attachment to the vacuum line.

The ends of the cell are ground in order to accommodate the windows. The most efficient seal was obtained with Edwards 'Hard Grade' high vacuum grease when it was applied sparingly and then warmed before the positioning of the windows. This grease requires no thickening additives such as silica gel, and will also hold the windows securely to the cell at atmospheric pressure without additional support. A hard vacuum (10^{-6} Torr) is readily reached and maintained. The position of the thermocouple well is illustrated by Figures 1 and 2. It is large enough to accommodate an iron-constantan thermocouple and it hardly, if at all, interferes with the infrared beam. Thus the temperature of the cell centre, including the sample, may be determined accurately.

The lagged heating element, 7, is situated outside the cell as shown in Figure 1. This was considered more suitable than inside¹⁶³ not only because of its accessibility in the event of failure, but also because no extraneous material is introduced to the cell. Direct contact of the wire onto the glass is prevented by a layer of thin asbestos paper. This distributes the heat evenly and holds the wire in position during winding. 50 plus turns of nickel-chromium (65/15) element wire (length ~ 9.5 m; 0.23mm diameter and $26\Omega \text{ m}^{-1}$) was found suitable. An input voltage of 150 from a variable auto transformer

FIGURE 1. Infrared *in situ* cell.

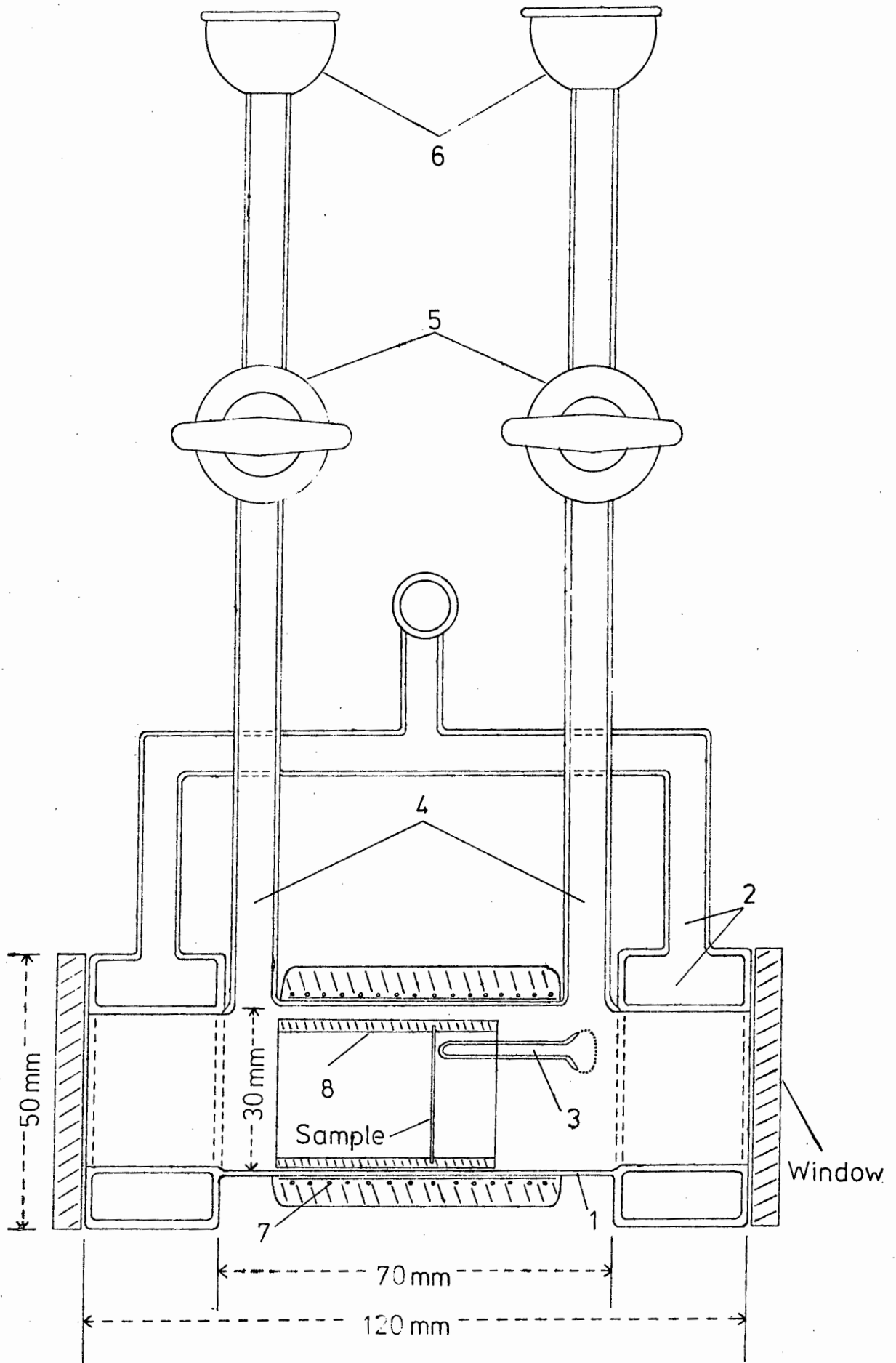


FIGURE 2. Infrared *in situ* cell, end-on view.

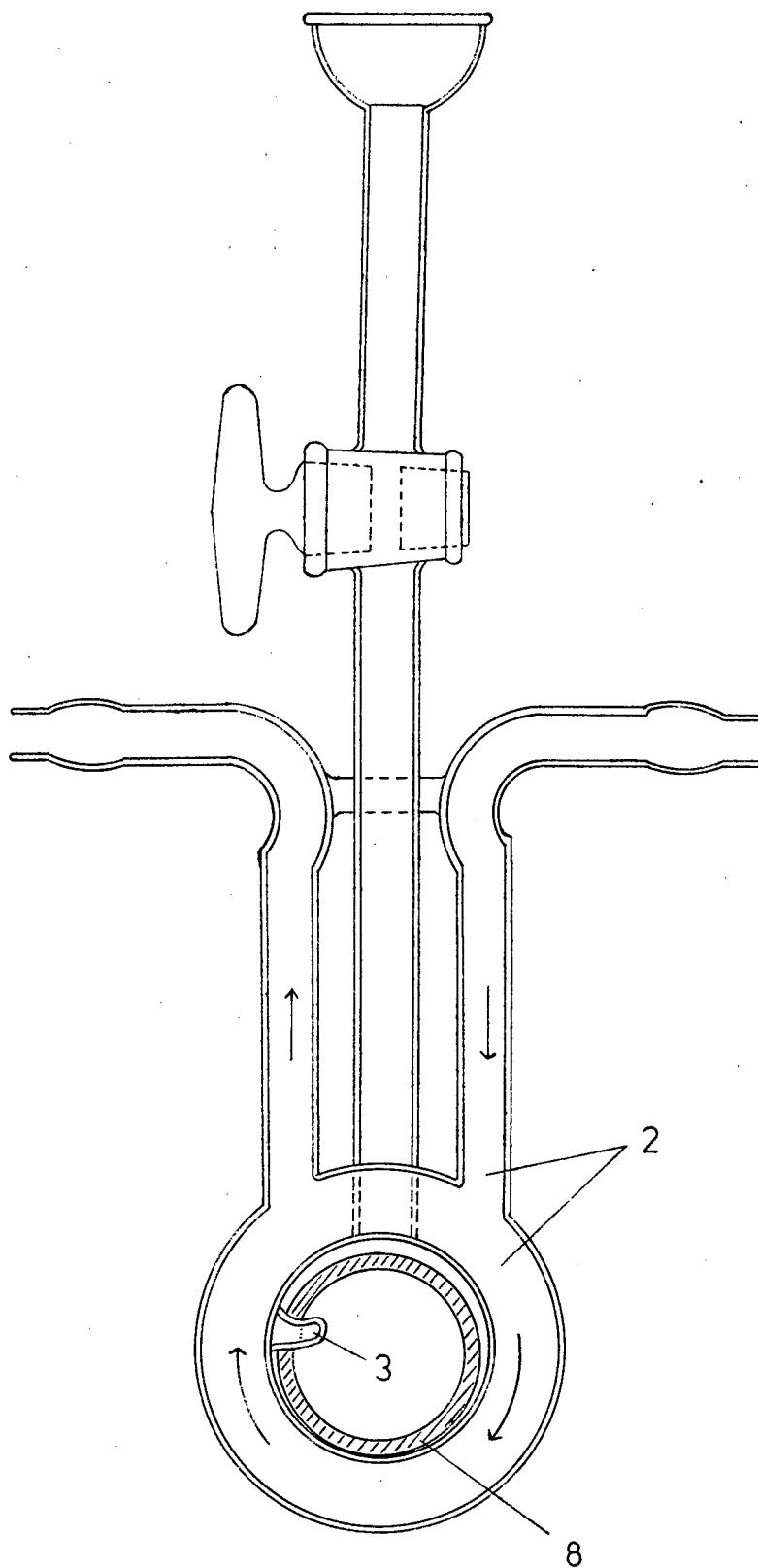
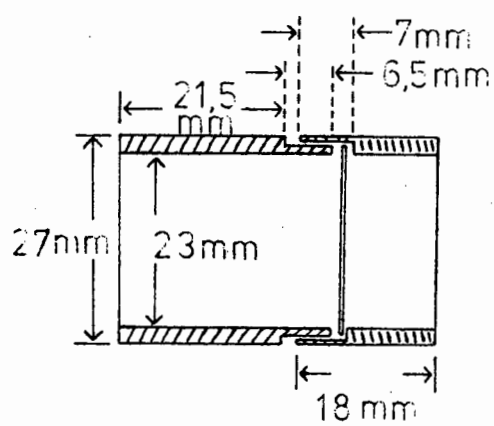


FIGURE 3. Sample holder with sample disc in position.



giving 100 W power raised the cell temperature to 450°C in $\frac{1}{2}$ hr. The heating element was lagged with plaster of Paris followed by asbestos string and tape.

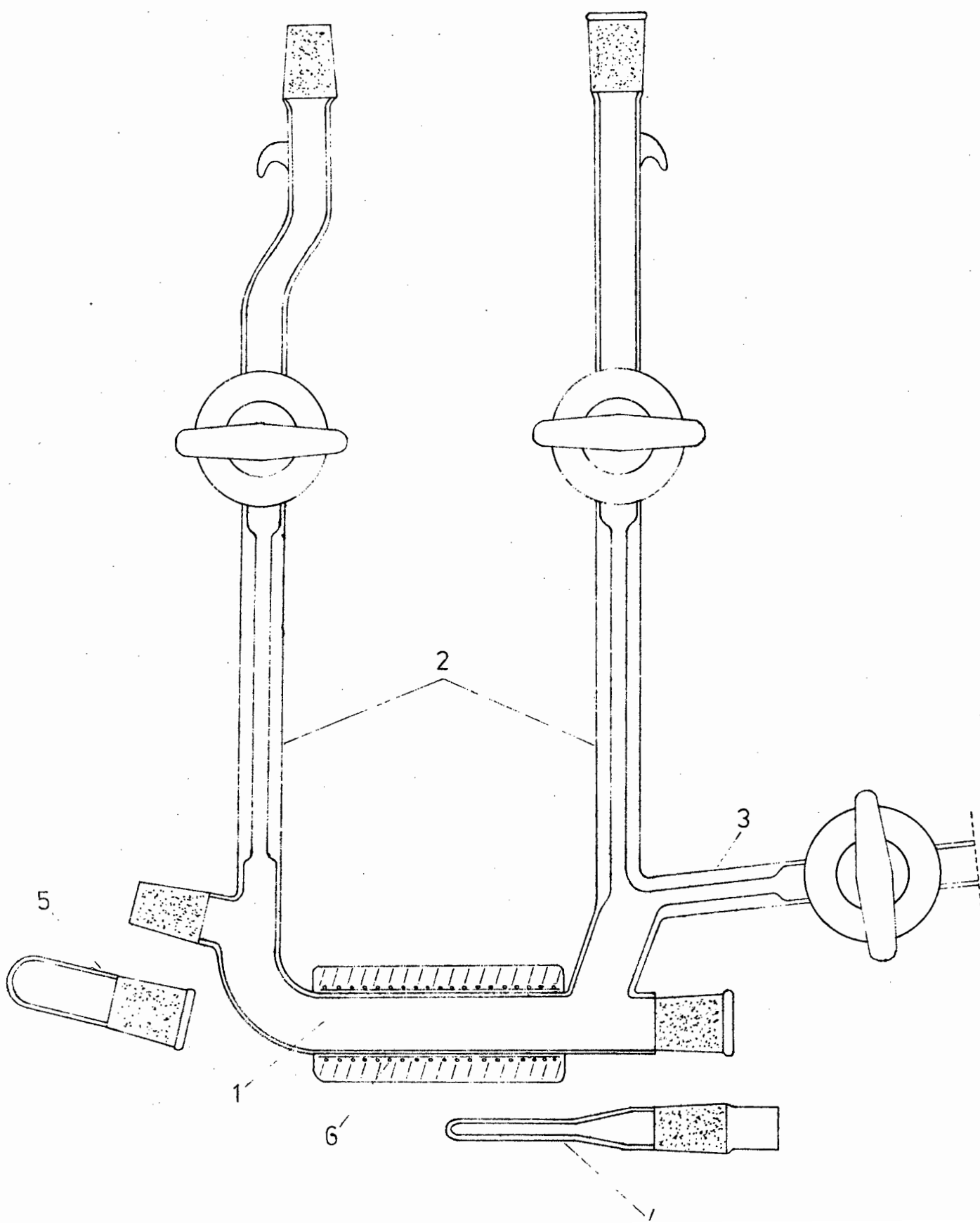
The sample holder, Figure 3, was originally made of brass. However, at elevated temperatures under reducing conditions, the zinc vaporised and deposited as a thin film on the cooler surfaces of the cell and windows. A high quality stainless steel was then used and found to be unaffected at temperatures $\leq 450^{\circ}\text{C}$ while subjected to carbon monoxide, hydrogen, nitrate fumes, etc. The sample holder consists of two cylinders machined to fit, and securely hold, a thin circular sample of diameter 25 mm. This holder when placed inside the cell rests against the side of the thermocouple well. In this position the tip of the well is ≤ 1 mm from the sample disc.

3.1.3 The Reactor:

In order to follow the composition of reactant and product gases as a function of time, or as a function of time and temperature, a small Pyrex reactor was constructed to accommodate about 0.7 g of powdered material. The reactor was connected to a gas line and to a standard 10 cm path length infrared gas cell fitted with calcium fluoride windows. The infrared cell was housed in the sample beam of the spectrometer.

The reactor is shown in Figure 4. The main body, 1, was enclosed in a furnace, 6, of similar construction to that for the *in situ* cell, such that the temperature could also be raised to

FIGURE 4. The reactor.



450°C in $\frac{1}{2}$ hr. Gas inlet and outlet tubes, 2 and 3, all fitted with stopcocks, were for use during the sample reduction and for connecting to the infrared cell respectively. The position of the thermocouple well, 4, is clearly shown, and enables the temperature of the cell centre including the sample to be determined accurately. Finally, the socket cap, 5, was fitted to facilitate cleaning of the reactor after use.

3.1.4 The Differential-Pulley System:

For some of the reactor and *in situ* experiments it was required that the temperature be raised smoothly (over the range 20 to 400°C), in order to monitor accurately the appearance or disappearance of a given species or to observe spectral changes more closely. This was achieved by using a differential-pulley system which connected the autotransformer to a small motor. The system proved extremely efficient and allowed the temperature of both reactor and *in situ* cell to be raised to 400°C over a period of about three hours. Figure 5 shows a typical plot of time with temperature for each of the two furnaces, 1. the *in situ* cell, and 2. the reactor. It was necessary to draw separate plots for each experiment because not only were the curves parabolic, but also very slight differences occurred, attributable to indeterminate errors, although the shape of these curves remained unchanged. Nevertheless, over the range of most interest, 150 to 400°C, the plots were found to be almost linear. The heating procedure described here will be referred to in the text as the 'thermal programme'.

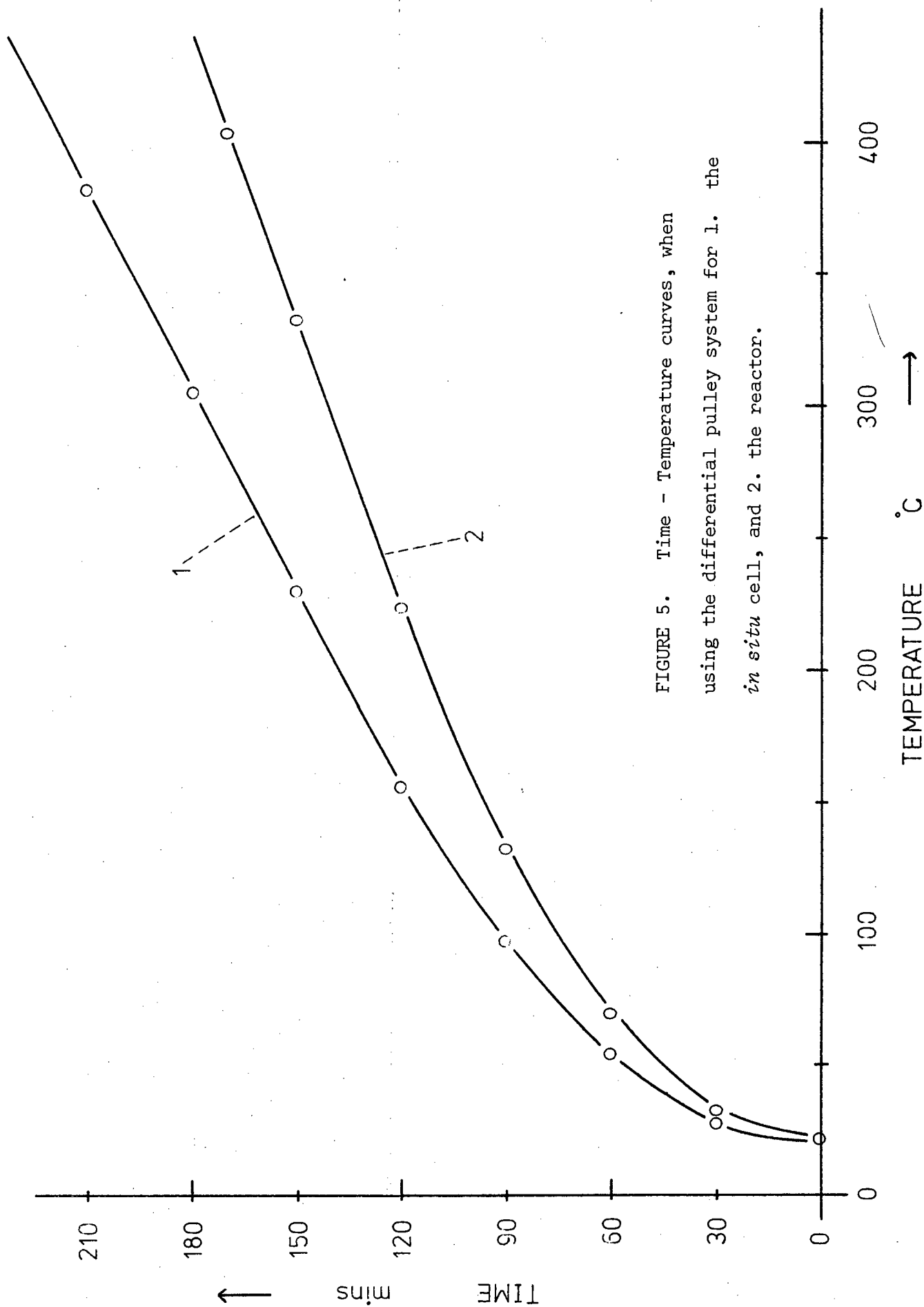


FIGURE 5. Time - Temperature curves, when using the differential pulley system for 1. the *in situ* cell, and 2. the reactor.

3.1.5 The Die:

A die was used to press powders into thin circular sample discs (25 mm diameter), of either a metal salt mixed with silica or that of silica alone. The die used was the one constructed by Ferreira²⁷ which incorporates the bevelled mouth at the bottom of the cylinder, and the flat backing plate. The bevelled mouth was reduced slightly in an attempt to improve on the quality of the discs and to increase their diameter. Also the conditions for pressing (time and pressures) were altered, again to improve on the quality. Further details are given in Section 3.3.2.

3.1.6 The Vacuum Line:

A schematic diagram of the vacuum line employed is given to simplify the description of the experimental procedures, which were often very intricate. The line, shown in Figure 6, has been divided, for simplicity, into Sections A to E which represent given volumes, and this notation will be referred to later. The ratios of volumes B to E relative to volume A are given in Table 1.

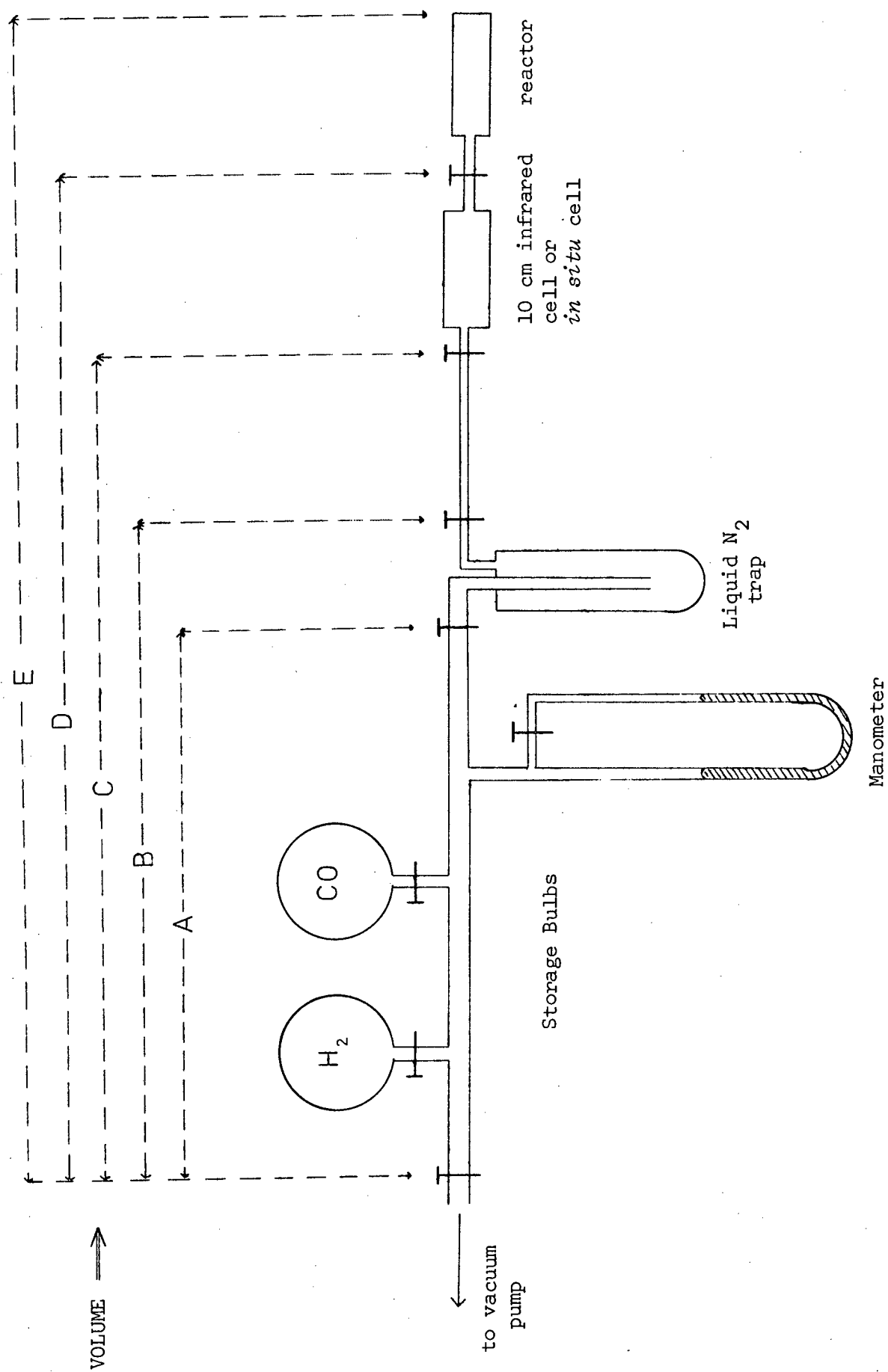
TABLE 1.

Relative Volumes	Ratio of Volumes
A : B	1 : 1,84
A : C	1 : 2,22
A : D _i	1 : 2,33
A : D _r	1 : 2,38
A : E	1 : 2,42

Where volume :
 (D_i - C) represents the *in situ* cell.
 (D_r - C) represents the standard 10 cm path length
 infrared cell.
 (E - D) represents the reactor.

[See Figure 6].

FIGURE 6. The vacuum line : schematic diagram.



3.2 GAS PURIFICATION:

The hydrogen, obtained from a cylinder, was purified¹⁴⁰ by first passing it through a trap cooled in liquid nitrogen which removed the water vapour present. The gas was then passed over copper turnings heated to a temperature of 360°C to remove oxygen; followed by an activated charcoal trap also cooled in liquid nitrogen. The latter removed any other unwanted gases or vapours from the hydrogen stream.

Carbon monoxide, also obtained from a cylinder, was purified¹⁴⁰ by passing it through a trap cooled in liquid nitrogen, and then through an activated charcoal trap also cooled in the same manner. The former trap removed the impurity iron carbonyl, and the latter any other impurities.

Both gases were stored, after purification, in glass bulbs pre-evacuated to 10^{-6} Torr. Alternatively, a stream of purified hydrogen was passed over a catalyst sample for 'reduction' purposes. The charcoal trap was re-activated after each 'reduction' by heating to temperatures of $> 300^{\circ}\text{C}$, under vacuum, for about three hours.

3.2.1

Unless otherwise stated pure carbon monoxide and hydrogen were admitted to the sample cells at room temperatures in the pressure ranges :

- (i) 10 to 15 Torr and 65 to 85 Torr respectively for the reactor experiments; and
- (ii) 1 to 2 Torr and 10 to 15 Torr respectively for the *in situ* cell experiments.

The method of introduction of these gases into the reactor and *in situ* cell has been described in Appendix 1.

3.3 ADSORBENT PREPARATION:

3.3.1 Nickel, Iron, and Cobalt Catalysts for use in the Reactor:

Samples used in the reactor experiments were prepared by mixing silica ("Cab-O-Sil") with a solution of a salt of the metal until a slurry was obtained. The mixture was dried for a few hours within the temperature range 100 to 120°C, and then ground into a fine powder using a mortar and pestle. Between 0,4 and 0,7 g of the powder was placed in the main body of the reactor and kept in position with glass wool. The salt was decomposed to the oxides *in situ* by heating at high temperatures for 3 to 5 hours whilst under vacuum, and then reduced to the metal in flowing hydrogen for longer periods, still maintaining a high temperature. Purified hydrogen was used during this latter procedure. To prevent mercury poisoning of the catalyst a liquid nitrogen trap was placed between the sample cell and the manometer. Also a flow meter was installed at the end of the gas line to ensure that the air did not diffuse back to the sample.

Various catalyst samples were prepared. Full details of the sample composition and preparation are given in Table 2.

TABLE 2.

Catalyst Type	Weight % of Metal	Salt	Solvent (mls) per 10 g material (salt plus SiO ₂)	Decomposition/Reduction Temperatures, °C	Reduction Time, hr.
Ni I	5% Ni	Ni(NO ₃) ₂ • 6 H ₂ O	Water (30 mls)	270 - 330	10 - 18
Fe I	5% Fe	Fe(NO ₃) ₃ • 9 H ₂ O	Water (30 mls)	390 - 425	10 - 16
Fe II	5% Fe	Fe(NO ₃) ₃ • 9 H ₂ O	Water (30 mls)	400 - 440	12
Fe III	0,1% Cu	Cu(NO ₃) ₂ • 3 H ₂ O	Ethyl alcohol, (Absolute) (90 mls)	410 - 435	12
	5% Fe	FeOH • (CH ₃ COO) ₂			
Co I	5% Co	Co(NO ₃) ₂ • 6 H ₂ O	Acetone/Water (50 ml/1ml)	385 - 410	11 - 12

Higher reduction temperatures were necessary for the iron and cobalt catalysts as thermodynamically both metals are more difficult to reduce from their oxides than is nickel¹⁰⁷. To facilitate the reduction of iron a small quantity of copper was added, as shown for catalyst type FeII.

3.3.2 Nickel, Iron, and Cobalt Catalysts for use in the *in situ* Cell:

Samples of silica supported metals used in the *in situ* cell were prepared as thin circular discs of diameter 25 mm and approximate thickness 0,25 mm. It was found that on pressing discs directly from the bulk powders, (described in Section 3.3.1) they tended to crumble and had a mottled appearance indicative of inhomogeneity. The bevelled mouth of the die was reduced in an attempt to improve on the quality of the discs. Also, conditions for pressing, times and pressures, were varied. However, all attempts to overcome these two problems proved unsatisfactory.

The only discs which could be prepared from the bulk powder with relative ease were those of iron acetate on silica. The powder was prepared from a mixture of the two compounds slurried with alcohol, and contained 2,5 wt. % iron; type FeIV, Table 3. By slurrying with either acetone or alcohol the powders had a more feathery fluffy-like consistency than those slurried with water. This markedly improved the binding effect during pressing, but did not overcome the problem of the mottled appearance. Furthermore, discs prepared this way were almost completely opaque to infrared radiation.

Therefore a new method was tried in which pressed silica discs were simply dipped for a few seconds into a solution of a metal salt, (designed to yield 5-6 wt. % of the metal), and allowed to dry in a desiccator. This method, referred to as the "dip" method, produced stable discs, i.e., they did not crumble or crack. They also had a homogeneous appearance. All discs were then decomposed, reduced, and degassed *in situ* in a similar way to that described for the reactor catalysts, see 3.3.1.

The various catalysts studied, their composition and conditions of preparation are given in Table 3.

The metal content for those discs prepared by the "dip" method was determined simply by weighing each disc before and after "dipping" into a salt solution, and also when dry. This afforded the weight ratio, silica to metal salt. The method provided a reasonable estimate of the metal content, having an error of $\pm 1\%$ by weight of metal which was considered satisfactory for this work.

TABLE 3.

Catalyst Type	'Solution' Salt/ Solvent	Concentration of salt in 'Solution' w/v %	Weight % of Metal	Decomposition/ Reduction Temperatures, C.	Reduction Time, hr.
N 1	Ni(NO ₃) ₂ ·6H ₂ O/ water	50%	5,5 - 6,5	270 - 320	10 - 22
N 2	Ni(NO ₃) ₂ ·6H ₂ O/ water	25%	3,0 - 3,5	270 - 320	11 - 22
F 1	FeOH·(CH ₃ COO) ₂ Absolute alcohol	40%	4,0 - 4,5	390 - 420	6
F 2	Fe(NO ₃) ₃ ·9H ₂ O Cu(NO ₃) ₂ ·3H ₂ O water	45% 0,27%	4,5 - 5,0(Fe)	390 - 465	6 - 24
F 3	Fe(NO ₃) ₃ ·9H ₂ O Cu(NO ₃) ₂ ·3H ₂ O water	22,5% 0,135%	2,5 - 3,0(Fe)	390 - 410	7
C 1	Co(NO ₃) ₂ ·6H ₂ O Acetone/Water 50 mls/8 mls	50%	5,5 - 6,0	385 - 430	12 - 22
Fe IV	FeOH·(CH ₃ COO) ₂ Absolute alcohol (90 mls)	(2½ wt.% of Fe)		400 - 450	6 - 24

3.4 PROCEDURE

3.4.1 Procedure - reactor experiments:

Several procedures were adopted in which the order of addition of reactants was of prime importance. These are discussed in detail below, and the notation given for each is used when presenting the results in Chapter 4. For example, the notation CO-H₂-ΔH means that the catalyst was subjected to carbon monoxide, hydrogen, and heating in that order, and conforming to the procedure set down in Section 3.4.(1.1). In procedures 1.1 to 1.7 inclusive the reactor contained an aliquot of prepared catalyst sample.

(1.1) CO - H₂ - ΔH:

A background spectrum over the frequency range 4000 to 1000 cm⁻¹ was recorded with the reactor and 10 cm infrared cell pre-evacuated to 10⁻⁶ Torr and at room temperatures. Carbon monoxide was then admitted and the system was allowed to reach equilibrium over a period of 1 hr. During this time either the appearance of the band assigned to free Ni(CO)₄ was observed by monitoring at a constant frequency, at 2063,6 cm⁻¹; or the complete spectrum (4000 to 1000 cm⁻¹) was re-recorded. Hydrogen was then added to give a CO/H₂ mixture, with the H₂ : CO ratio ≥ 5 : 1. After allowing the system to stand a further ½ hr. the reactor was then heated slowly using the 'thermal programme', (see Section 3.1.4). During heating the appearance of one of the following gases, Ni(CO)₄, CH₄, and CO₂ was observed by monitoring at a constant frequency of 2063,6; 3017,5; and 2334,2 cm⁻¹ respectively. The frequency of

3017,5 cm^{-1} corresponded to the $\nu_3\text{Q}$ branch of methane; and that of 2334,2 cm^{-1} to the P_{18} rotational line of the ν_3 asymmetric mode of CO_2 . Finally, the complete spectrum (4000 to 1000 cm^{-1}) was recorded when the reactor had reached a temperature of 400°C.

(1.2) $\text{CO}/\text{H}_2 - \Delta\text{H}$:

For this and subsequent procedures two actions were always carried out, namely (i) the $\text{H}_2 : \text{CO}$ ratio was regulated to give a value of $\geq 5 : 1$; and (ii) a background spectrum (4000 to 1000 cm^{-1}) was first recorded under conditions similar to those described in procedure (1.1).

This experiment involved the admission of a CO/H_2 mixture to the reactor and infrared cell. The system was allowed to reach equilibrium over a period of 1 hr., during which time either the $\text{Ni}(\text{CO})_4$ band was monitored or a spectrum was scanned. The reactor was then heated slowly as before and the methane Q branch monitored at a frequency of 3017,5 cm^{-1} . The full spectrum was recorded again when the reactor had reached 400°C.

(1.3) $\text{H}_2 - \text{CO} - \Delta\text{H}$:

Here hydrogen was admitted first and the system allowed to reach equilibrium over a period of $\frac{1}{2}$ hr. Carbon monoxide was then added, giving a CO/H_2 mixture, and the system allowed to stand for a further 1 hr. At this stage, either the $\text{Ni}(\text{CO})_4$ band was monitored or a spectrum was scanned in the usual way. The reactor was then heated using the 'thermal programme' and only the methane Q branch

was monitored. Once again a full spectrum was taken when the reactor had reached 400°C .

(1.4) CO - ΔH :

This time only carbon monoxide was admitted and either the $\text{Ni}(\text{CO})_4$ band monitored or the spectrum was scanned during the 1 hr. standing period. The reactor was then heated in the usual manner, and the presence of CO_2 was investigated by monitoring at a frequency of $2334,2\text{ cm}^{-1}$. A full spectrum was recorded, as before, after the heating programme.

(1.5) CO - evacuate - H_2 - ΔH :

For this experiment the same procedure applied in (1.1) was adopted with the inclusion of an additional stage, that of evacuation. Thus, after the admission of CO and before the addition of H_2 the entire system was evacuated at room temperatures for a period of 10 min. Whilst heating, only the methane Q branch was monitored.

(1.6) CO/ H_2 - cool.

With the system evacuated to 10^{-6} Torr and the reactor at a temperature of 430°C , a CO/ H_2 mixture was admitted. The system was then allowed to reach equilibrium at that temperature over a period of 1 hr. after which the reactor was cooled slowly to about 210°C . During the entire procedure only the methane Q branch was monitored.

(1.7) CO/ H_2 - fixed temperature:

This procedure was applied to cobalt catalysts only. With the reactor and infrared cell pre-evacuated to 10^{-6} Torr, the reactor

was heated to a fixed (specific) temperature. A CO/H₂ mixture was then admitted to this system. The methane Q branch was then monitored continuously for a period of 2 hr. whilst still maintaining the reactor at a constant temperature. After monitoring, the methane fundamental band was recorded over the frequency range 3200 to 2800 cm⁻¹. This procedure was repeated for various temperatures.

(1.8) Ni(CO)₄ - blank 1:

This experiment involved the heating of Ni(CO)₄ together with H₂ and CO but in the absence of catalyst. For practical purposes the 10 cm infrared cell was replaced by the *in situ* cell, which in turn was connected to the reactor, as the former was not equipped with a heating assembly. Nickel tetracarbonyl was produced in the reactor in the usual way by allowing CO to come into contact with the nickel catalyst at room temperatures, but in the absence of hydrogen. When sufficient Ni(CO)₄ had been produced, the *in situ* cell (containing the gases Ni(CO)₄ and CO) was isolated from the reactor by closing the stopcock between them. Hydrogen was then added to the contents of the cell, and heating commenced using the 'thermal programme'. The Ni(CO)₄ band, at 2063,6 cm⁻¹, was monitored throughout the experiment.

(1.9) CO/H₂ - blank 2:

Here a CO/H₂ mixture was contained in the reactor and 10 cm infrared cell, but in the absence of catalyst, while the reactor was heated in the usual way. Spectra were recorded over the frequency range 4000 to 1000 cm⁻¹ when the reactor was at room temperatures and at 400°C.

A 'blank', consisting of an evacuated 10 cm infrared gas cell fitted with CaF_2 windows, was placed in the reference beam of the spectrometer during the recording of spectra for all the experiments described above. This established the more sensitive differential technique and produced a flat 100% Transmittance line.

3.4.2 Procedure - *in situ* cell experiments:

The technique applied to the reactor catalysts, whereby the order of addition of reactants was changed, was also used for the *in situ* sample discs. Three sets of experiments were carried out, and these together with some other procedures are described below. A 'blank' silica disc, held in an evacuated 10 cm infrared gas cell, was placed in the reference beam of the spectrometer in order to flatten the 100% Transmittance line over the range of most interest.

(2.1)

The various procedures of altering the order of addition of reactant gases, e.g. $\text{CO-H}_2-\Delta\text{H}$, $\text{CO/H}_2-\Delta\text{H}$, $\text{H}_2-\text{CO}-\Delta\text{H}$, and $\text{CO}-\Delta\text{H}$ were carried out in a similar manner to that described in Section 3.4.1 excepting that the lower gas pressures applicable to the *in situ* experiments were used. At the end of each stage, and also at half hourly intervals while the cell was being heated, spectra were scanned over the frequency range 2300 to 1700 cm^{-1} . This frequency range was chosen because it adequately covered any possible absorptions which could be assigned to the carbonyl stretching frequency of adsorbed CO species. The same time intervals were allowed for the system to attain equilibrium after the admission of reactant gases, and the *in situ* cell was heated slowly using the 'thermal programme'. At the start of each experiment a

'background' spectrum was recorded, over the same frequency range, when the *in situ* cell was at room temperatures and evacuated to a pressure of 10^{-6} Torr. 'Background' spectra were also recorded at half hourly intervals when the catalysts were heated slowly in the absence of reactant gases. These latter spectra served as 'blanks'.

(2.2)

Here the same procedures were adopted as in (2.1) but an evacuation period was included. Thus each system was evacuated for 10 min. when at room temperatures, after the admission of CO but prior to heating the catalyst. Therefore they can be re-written as follows:

- (i) CO - evacuate - H_2 - ΔH
- (ii) CO/ H_2 - evacuate - H_2 - ΔH
- (iii) H_2 - CO - evacuate - H_2 - ΔH
- (iv) CO - evacuate - ΔH .

In some instances, as shown, a further aliquot of hydrogen was added after the evacuation period. This allowed the system under investigation to comprise essentially of adsorbed CO in an atmosphere of hydrogen. Generally, spectra were scanned after each stage of a procedure over the frequency range 2300 to 1700 cm^{-1} with the systems still at room temperatures; and a given species was monitored at a constant wavenumber during the heating programme.

For nickel catalysts the adsorbed species which were monitored were termed A, B, and C with maxima at frequencies of 1900, 2030, and 2056 cm^{-1} respectively. Species B was monitored for

all procedures, whereas only procedures (i) and (iv) were applied to species A and C. It was not necessary to carry out all the above-mentioned experiments for the iron and cobalt catalysts. For cobalt, procedure (ii) was omitted. While heating the cell, an adsorbed species on cobalt, termed species B, was observed during every experiment by monitoring at a frequency of 2020 cm^{-1} . Only for procedure (iv) was a species, termed C, monitored at 2181 cm^{-1} . Unfortunately only procedure (iv) could be applied to the iron catalysts because of their relative inactivity. However, during the heating programme adsorbed species, termed A and B, were monitored at frequencies of 1980 and 2169 cm^{-1} respectively.

(2.3)

The effect of a heating/cooling procedure was investigated (chiefly for nickel catalysts) in which only carbon monoxide was admitted to the system at room temperatures. The system was then heated slowly in the usual way using the 'thermal programme' until a temperature of 400°C was reached, and then cooled slowly back to room temperatures. This experiment was repeated with the addition that after allowing the system to stand overnight it was evacuated for 1 hr. at room temperatures followed by reheating to 400°C . Throughout both experiments spectra were scanned continuously over the frequency range 2300 to 1700 cm^{-1} .

A similar experiment was carried out wherein the CO was only admitted when the catalyst was at a temperature of 400°C . The system was then cooled slowly as before. Approximately 1 Torr CO pressure was found to be sufficient when studying nickel catalysts, but higher

pressures were required for cobalt. On one occasion, however, the heating/cooling cycle was applied to nickel using a pressure of 12 Torr.

A spectrum was recorded when the system had been evacuated for 1 hr. at room temperatures after the admission of CO on an otherwise 'cleaned' nickel surface. This provided a comparison to show the effect of prolonged evacuation under different conditions.

Miscellaneous experiments such as varying the CO pressure and 'check' spectra for the silica disc reference will be covered separately in the following Chapter.

3.4.3 Experiments on the Rate of Carbon Monoxide Diffusion:

In the course of the reactor experiments an interesting phenomenon was revealed.

(i) On mixing the two reactant gases, for procedures $\text{CO} - \text{H}_2 - \Delta\text{H}$ and $\text{CO}/\text{H}_2 - \Delta\text{H}$, the presence of hydrogen (which was usually added after CO) caused an immediate increase in intensity of the CO fundamental at a frequency of 2143 cm^{-1} . This was contrary to the expected decrease as, on mixing, the CO should then occupy a larger volume.

(ii) Frequently, when applying the procedure $\text{H}_2 - \text{CO} - \Delta\text{H}$, no CO absorption band at 2143 cm^{-1} was observed at all. This was then followed by the fact that no methane was detected on heating the catalyst. Here the step which involved mixing of the two gases comprised of opening the stopcock between volumes A and (E-A), which

contained CO and H₂ respectively.

Clearly the method used for admitting the reactant gases into the reactor and infrared gas cell was incorrect. Therefore a few experiments, conducted in the absence of catalyst, were necessary in order to solve these problems.

Initially it was suspected that the CO was either being adsorbed onto the glass walls of the vacuum line when permitted to occupy volume E from a previous volume of (E-B), or was condensing in the liquid nitrogen trap, (volume (B-A)), when the volume occupied was changed from that of A to E. Some CO condensation must in fact take place because of the close proximity of the boiling points of the two liquids, N₂ and CO, which are -195,8 and -191,5°C respectively. However, the liquifaction of CO would, at -195,8°C, be dependent on the pressure and a state of equilibrium would exist. Nevertheless, although condensation would be low due to the low CO pressures used, the technique was altered such that, before mixing, CO first occupied volume B, and the H₂ volume (E-B) for the procedure H₂ - CO - ΔH. However, both problems still remained. CO adsorption on the glass walls of the vacuum line was eliminated as a possible explanation because the proportion of adsorbed CO to free CO would be extremely low when using relatively high pressures demanded by the reactor experiments.

Another explanation is that the rate of diffusion of CO into a volume, otherwise occupied by another gas, is decreased. The set of experiments, described in Appendix 1, proved this to be the case and the following conclusions were made:-

1. The rate of diffusion of CO from a volume V_1 into a volume V_2 , (where $V_2 > V_1$), was found to be (a) very rapid when the volume $(V_2 - V_1)$ was pre-evacuated, and (b) very slow when $(V_2 - V_1)$ was otherwise occupied by another gas, e.g. H_2 or air.
2. The CO diffusion rate was surprisingly slow under the conditions given in 1. (b) above. Experiment A.1.2 showed that mixing of H_2 and CO was still incomplete even after 5 hr. standing at room temperatures.
3. On mixing CO with H_2 or air, when CO previously occupied volume (D-C) and the other gas had occupied volume C, an immediate increase in intensity of the CO fundamental at 2143 cm^{-1} was observed, providing the CO pressure did not exceed that of the other gas prior to mixing. The observed increase in intensity was analogous to a 'pressure broadening' effect.

With this information the experimental procedure $H_2 - CO - \Delta H$ was modified to afford more meaningful results simply by allowing more time for the two gases to mix and by increasing the CO pressure in volume B prior to mixing. Thus, during mixing, the CO fundamental, within the frequency range $2200\text{ to }2020\text{ cm}^{-1}$, was observed over a period of time until sufficient CO had diffused into volume E-B. No alteration in procedure was required for the other experiments because the H_2 pressure was always maintained to give an $H_2 : CO$ ratio of at least 5 : 1. It must be remembered that the entire work was designed to yield only qualitative, not quantitative, results.

CHAPTER 4

R E S U L T S

4.1 THE REACTIONS OF CO AND H₂ ON SILICA SUPPORTED NICKEL CATALYSTS.

The results obtained from the interaction of carbon monoxide and hydrogen on silica supported nickel catalysts will be presented in the same format, for both reactor and *in situ* cell experiments, as that given in the Procedure, Section 3.4. For example, the notation CO - H₂ - ΔH means that the results correspond to the procedure, set down in 3.4 (1.1) in which the catalyst was treated with CO followed by H₂ and then heated.

4.1.1 Reactor experiments - Nickel:

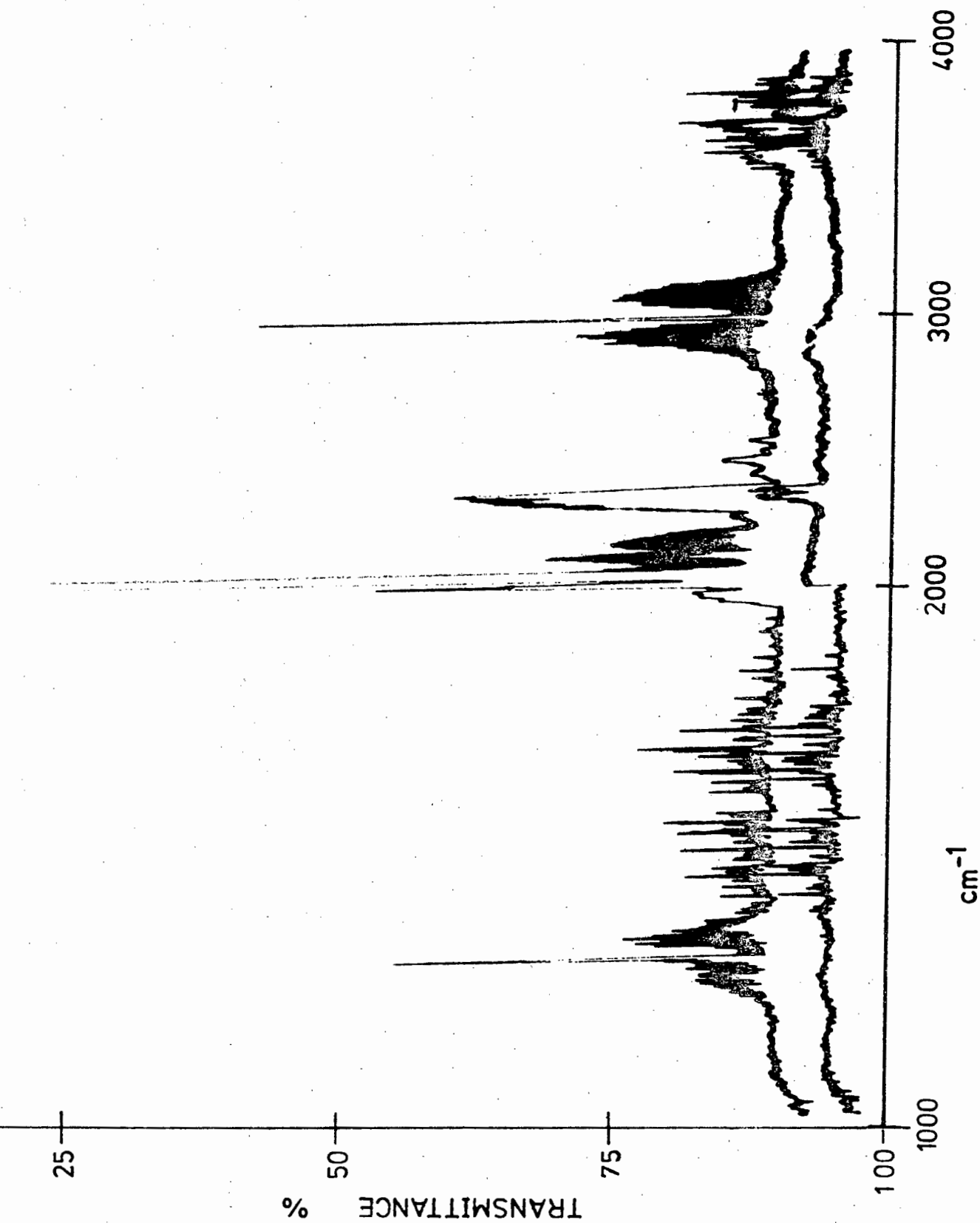
The following results were obtained using catalyst type NiI, which contained 5 wt. % Ni on SiO₂ and was prepared from the nitrate.

(1.1) CO - H₂ - ΔH:

The complete spectrum recorded after the reactor had reached a temperature of 400°C is shown in Figure 7.

The strong sharp band at a frequency of 2063,6 cm⁻¹ together with the weak band at 2024 cm⁻¹ clearly indicate the presence of gaseous Ni(CO)₄ and Ni(C¹²O)₃(C¹³O) respectively. The latter band

FIGURE 7. Spectrum of products at 400°C from CO followed by H₂ adsorbed on Ni/SiO₂, with background offset.

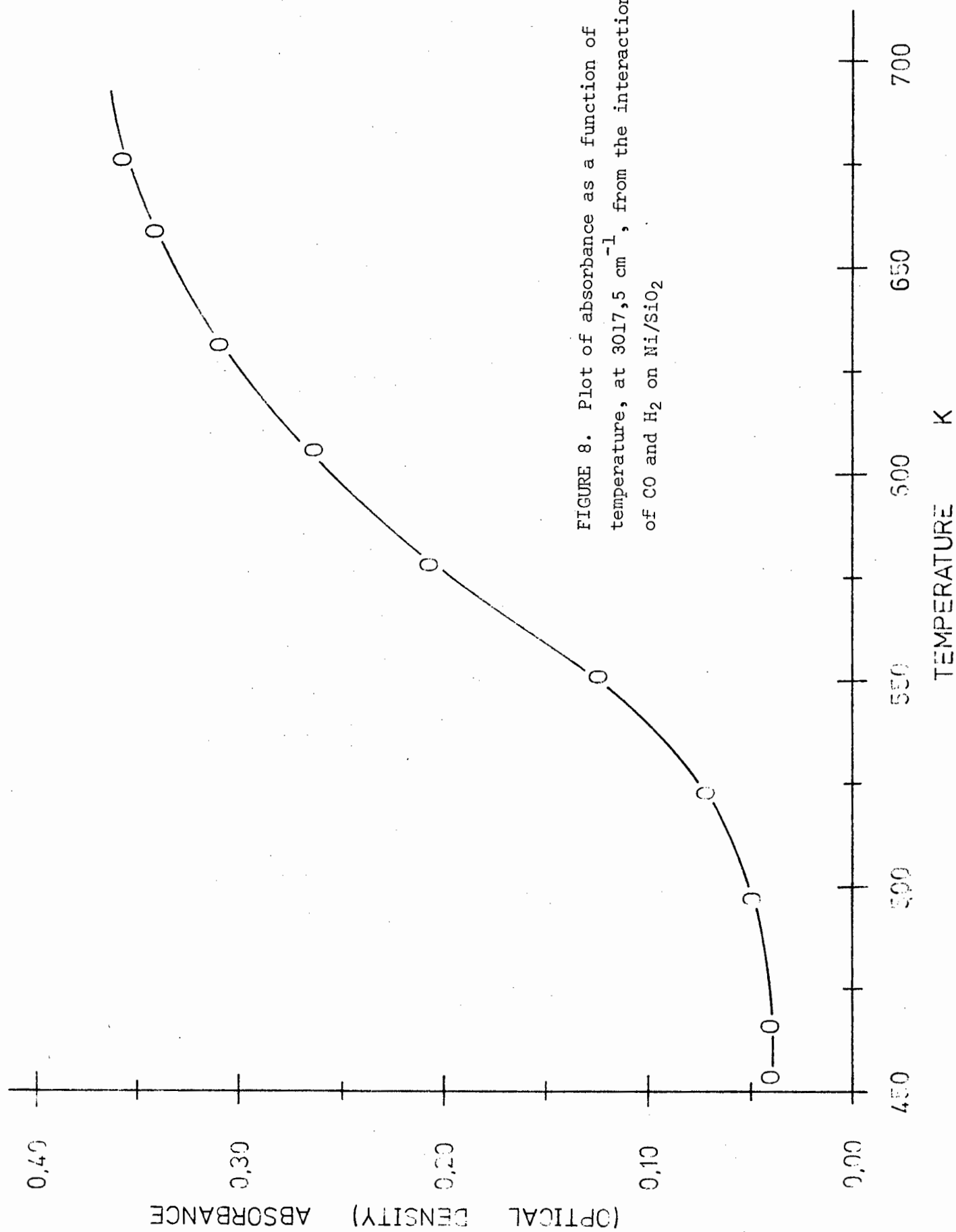


was assigned to the isotopic carbonyl species¹⁶⁶. Nickel carbonyl formation was observed by the steady decrease in transmittance with time at a frequency of $2063,6\text{ cm}^{-1}$ when the catalyst was allowed to stand in the presence of CO alone at room temperatures. Its formation was very rapid, usually being detectable within 5 min. of admitting CO to the system. This result can be compared with that of Ludlum and Eischens¹⁰⁹ on the formation of nickel carbonyl by the action of CO in stainless steel infrared cells.

Therefore, since these bands occur in the same region as those given by chemisorbed CO on nickel, they must be taken into consideration when interpreting the spectra of CO adsorbed species, Section 4.1.2.

The presence of methane was shown by its ν_3 and ν_4 bands at frequencies of $3017,5$ and 1305 cm^{-1} respectively¹⁶⁷. Both bands exhibited the rotational fine structure characteristic of small molecules.

Figure 8 shows the change in absorbance with temperature on monitoring the appearance of methane at $3017,5\text{ cm}^{-1}$. Clearly no methane was formed below temperatures of $190\pm 5^\circ\text{C}$, (463 K), and a steady increase in absorbance was observed thereafter. Although no quantitative measurements were recorded, the amount of methane produced in the reaction was considerable; a good measure of the catalyst's activity with respect to hydrocarbon formation. However, no other hydrocarbon, either saturated or unsaturated, could be detected by infrared methods for this and subsequent experiments on nickel catalysts.



Another product observed for this system, when at high temperatures, was carbon dioxide. This was shown by the increase in intensity of the ν_3 fundamental at 2350 cm^{-1} over the background spectrum, Figure 7. An attempt was made to observe the appearance of CO_2 , as the temperature was gradually increased, by monitoring at a constant frequency of $2334,2\text{ cm}^{-1}$. Unfortunately a poor result was obtained, partly due to a very low signal to noise ratio. Nevertheless, a steady decrease in transmittance was observed over the temperature range 100 to 400°C . None, or very little, $\text{H}_2\text{O}_{\text{vap.}}$ was detected as a by-product in this reaction as shown by Figure 7.

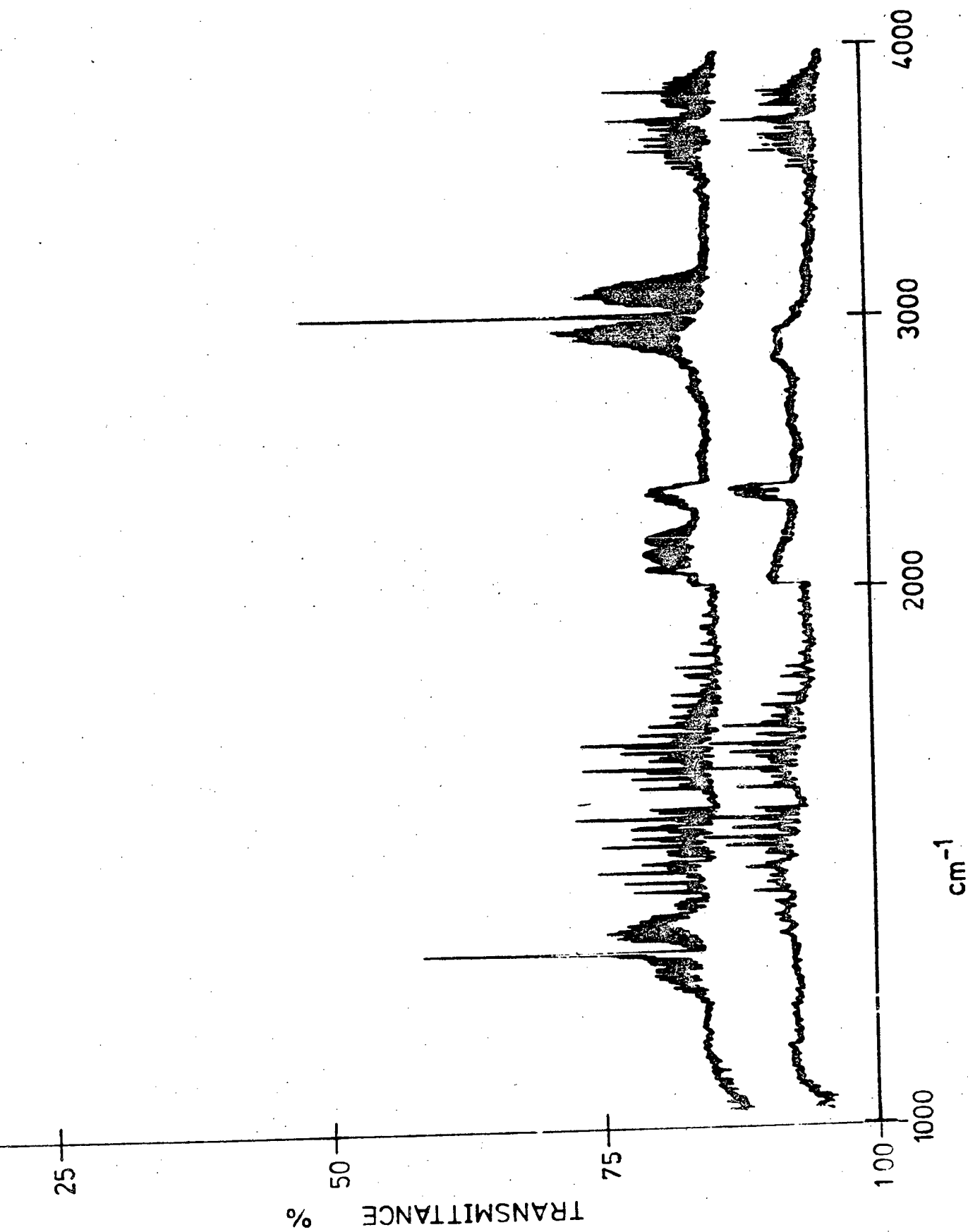
(1.2) $\text{CO}/\text{H}_2 - \Delta\text{H}$:

The spectrum recorded when the reactor had reached a temperature of 400°C , see Figure 9, showed that although methane was produced, none, or very little, $\text{Ni}(\text{CO})_4$ and CO_2 were detected. The absence of $\text{Ni}(\text{CO})_4$ was confirmed by monitoring at $2063,6\text{ cm}^{-1}$ whilst the system was at room temperature during the 1 hr. standing period. No decrease in transmittance was observed, contrary to that found in (1.1). Once again, monitoring at $3017,5\text{ cm}^{-1}$ on heating demonstrated that methane was formed only at temperatures above $190 \pm 5^\circ\text{C}$. Also, contrary to the results in (1.1), trace amounts of $\text{H}_2\text{O}_{\text{vap.}}$ were produced during the reaction. However, the fact that $\text{H}_2\text{O}_{\text{vap.}}$ was given as a by-product under these conditions must remain suspect, as frequently the amount present in the atmosphere fluctuated markedly, although the laboratory was humidity controlled.

(1.3) $\text{H}_2 - \text{CO} - \Delta\text{H}$:

Similar results were obtained, when the catalyst was pretreated

FIGURE 9. Spectrum of products at 400°C from a CO/H₂ mixture adsorbed on Ni/SiO₂, with background offset.



with hydrogen, to those observed for a CO/H₂ mixture. Figure 10 demonstrates this, and is marked by a definite absence of a band attributable to Ni(CO)₄. The result was confirmed by monitoring at 2063,6 cm⁻¹ as before, (1.2). No decrease in transmittance occurred. Once again methane was formed only at temperatures above 190±5°C.

(1.4) CO - ΔH:

In this experiment Ni(CO)₄ was formed, as expected, when the system containing CO was at room temperatures; and CO₂ was given off during the heating programme. These two gases were the only products of the reaction as shown by Figure 11, the recorded spectrum when the reactor had reached 400°C. Once again, the appearance of CO₂ was shown by the steady decrease in transmittance at temperatures above 100°C at a frequency of 2334,2 cm⁻¹. This confirmed the result obtained in (1.1).

(1.5) CO - evacuate - H₂ - ΔH:

During the 1 hr. standing period, after the admission of CO, Ni(CO)₄ was formed as previously found. Evacuation for 10 min. removed this and the CO from the gas phase. This left the system containing catalyst and essentially chemisorbed CO only. After the addition of hydrogen, followed by the heating programme, the complete spectrum, given by Figure 12, showed methane to be the only product. Considering this experiment was carried out on an aged/sintered sample, i.e., one which had repeatedly been subjected to temperatures above 400°C (of necessity for 'cleaning' the sample) the amount of methane formed was relatively substantial. This not only indicates

FIGURE 10. Spectrum of products at 400°C from H_2 followed by CO adsorbed on Ni/SiO_2 , with background offset.

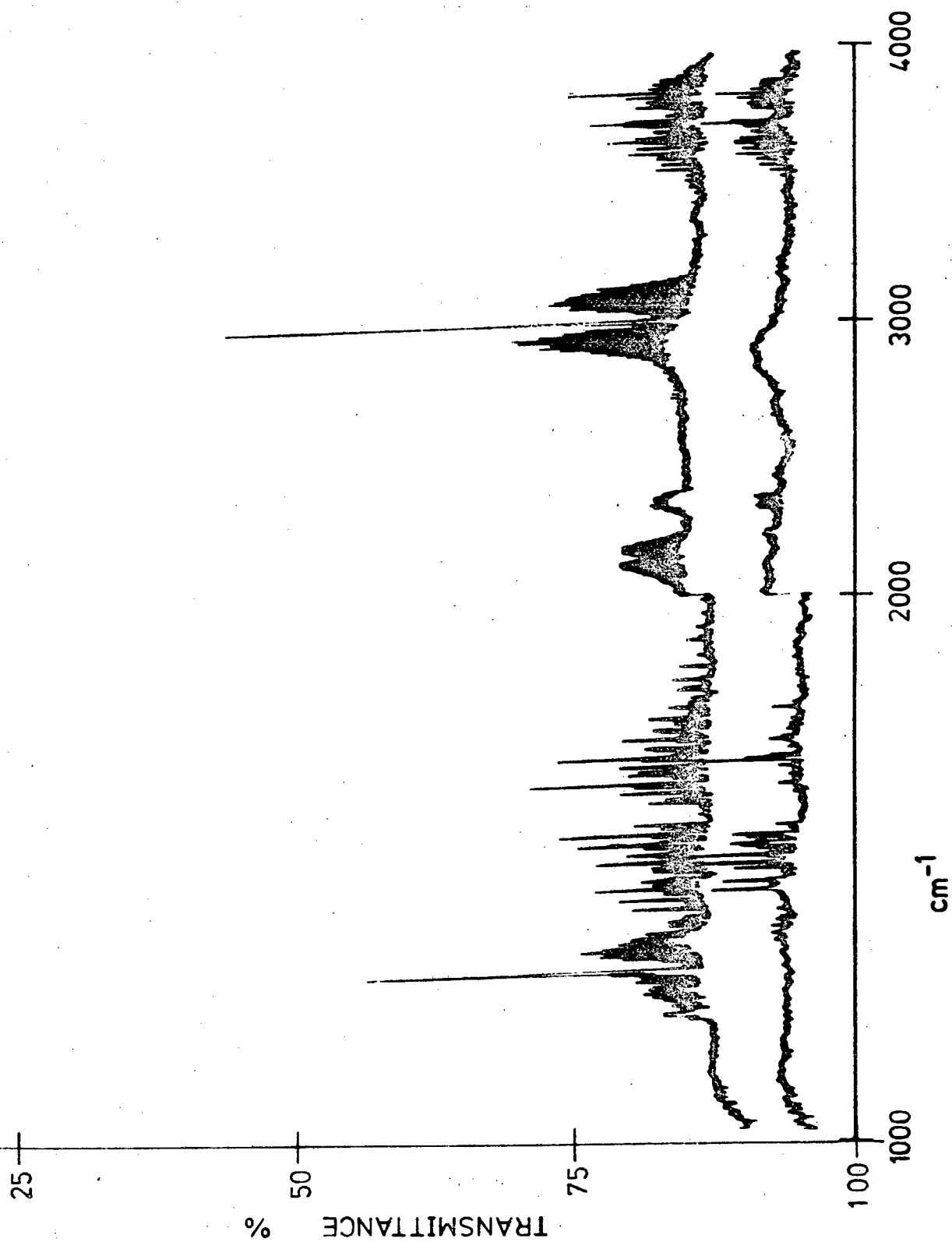


FIGURE 11. Spectrum of products at 400°C from CO adsorbed on Ni/siO₂, with background offset.

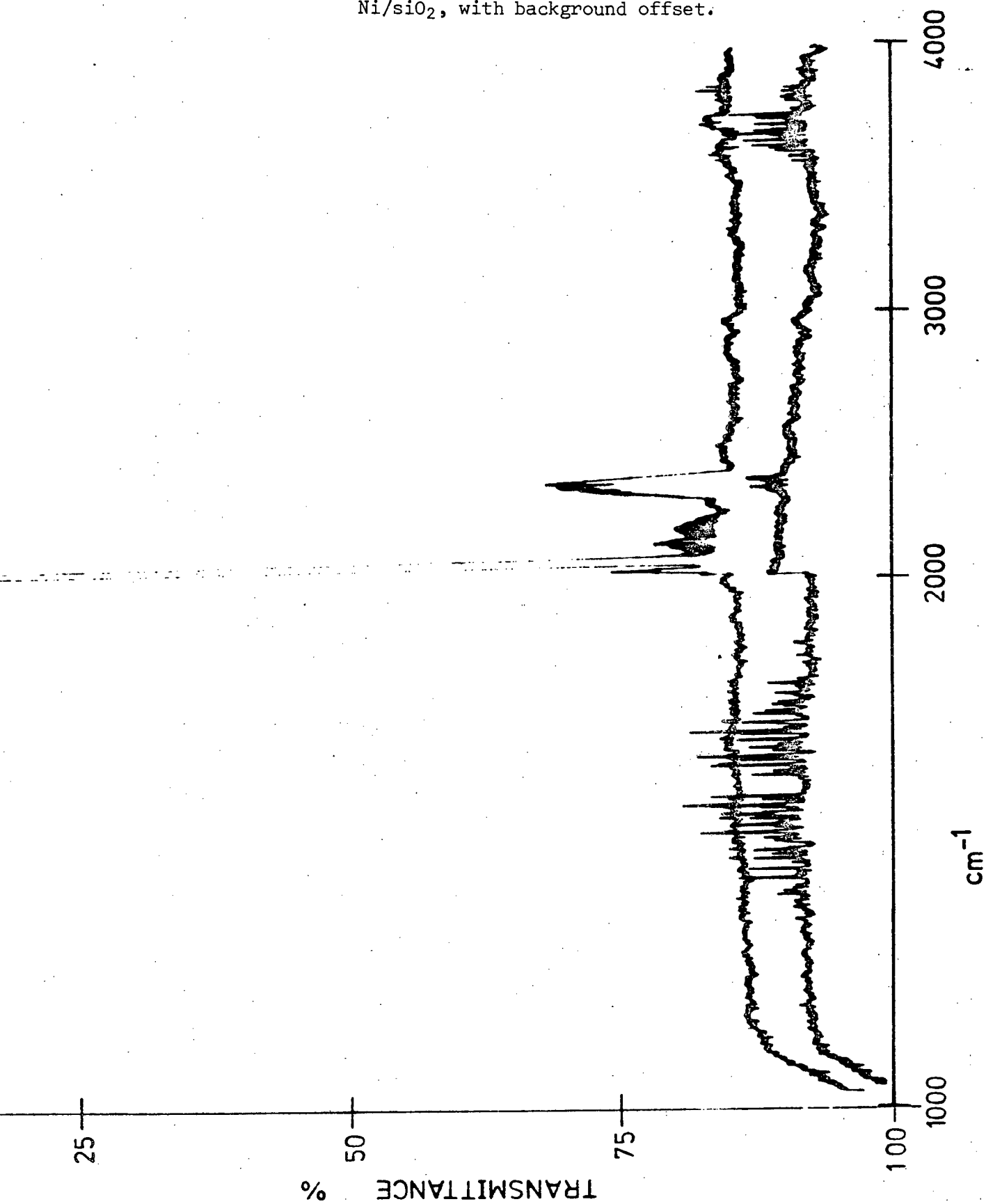
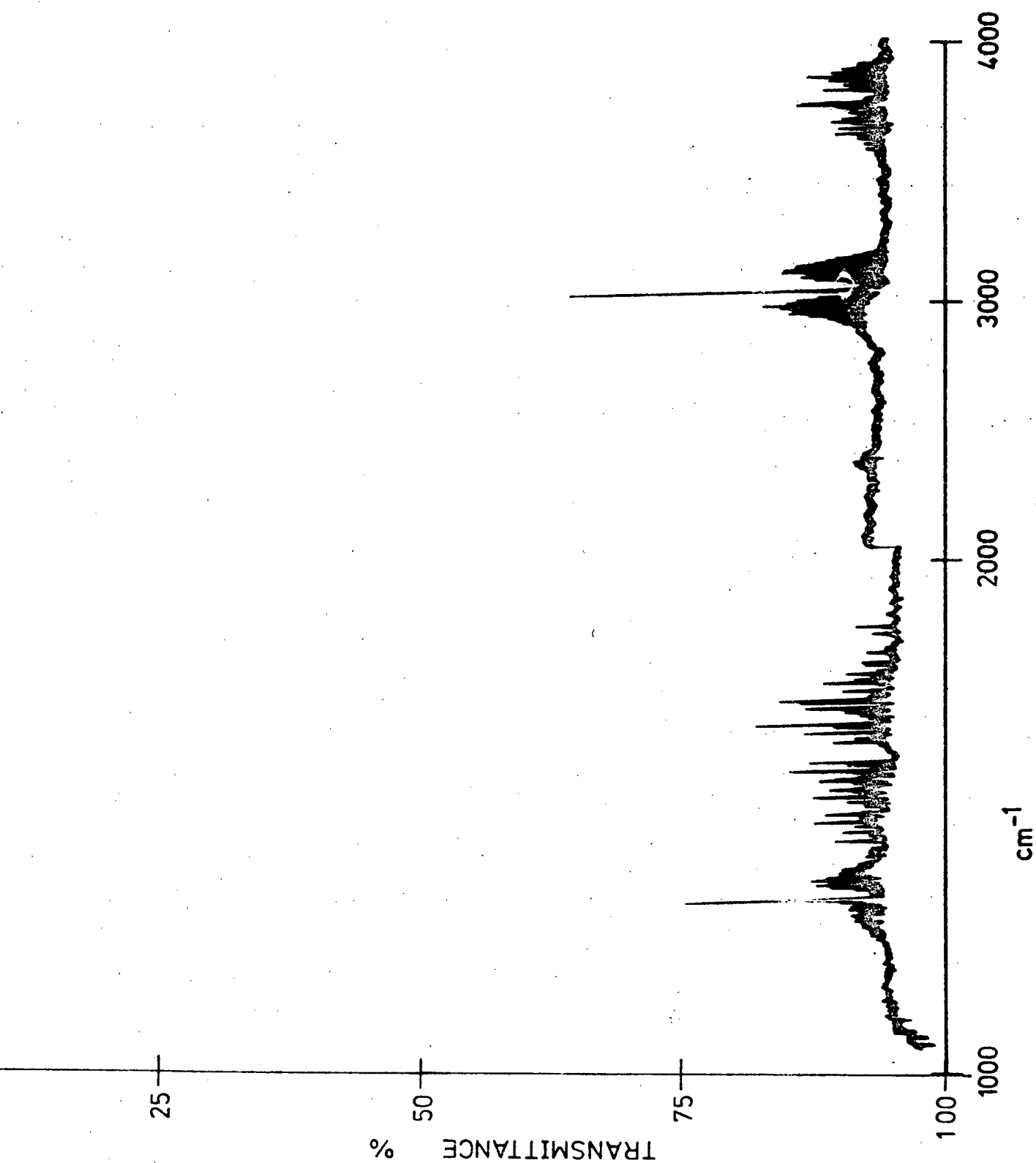


FIGURE 12. Spectrum of products at 400°C from $\text{CO}_{\text{ads.}}$ and H_2 on Ni/SiO_2 .



that Ni(CO)_4 is unlikely to be involved in the reaction mechanism, but also demonstrates very simply the sample's 'catalytic' properties. Thus the statement, "interaction with the surface complex is definitely a stage in the reaction mechanism", is verified by the above result.

(1.6) CO/H₂ - cool:

On admission of a CO/H₂ mixture to the reactor, when at 430°C, an immediate reaction occurred as shown by the production of methane. Monitoring at 3017,5 cm⁻¹ revealed that methane formation was fairly slow at this temperature, and after a period of about 1 hr. the reaction ceased and an equilibrium was reached. On cooling the system to 210°C a further aliquot of methane was given, although the total amount observed at the end of the experiment was small in comparison with earlier results. Complete spectra, recorded when the reactor was at 430°C and also at the end of the procedure, showed that CO₂ was formed as a by-product in the reaction.

Clearly the upper temperature limit for methane formation is >430°C. This suggests that even at these high temperatures CO must still become adsorbed onto the catalyst's surface.

(1.7) Ni(CO)₄ - blank 1:

The objective of heating Ni(CO)₄ with H₂ and CO, but in the absence of catalyst, was to observe the effect of high temperatures on the carbonyl and to determine its involvement, if any, in methane production. Hence the system containing only Ni(CO)₄, H₂, and CO was heated as described in Section 3.4 (1.8) whilst monitoring the

carbonyl frequency at $2063,6\text{ cm}^{-1}$. Figure 13 shows the decrease in absorbance with increase in temperature, which was attributed to the rapid decomposition of Ni(CO)_4 over the range 150 to 195°C . Comparison of spectra, taken at room temperatures and at 400°C , revealed the disappearance of the Ni(CO)_4 bands at 400°C , but an appreciable increase in the amount of free CO at this temperature. No methane was detected at any stage of the procedure.

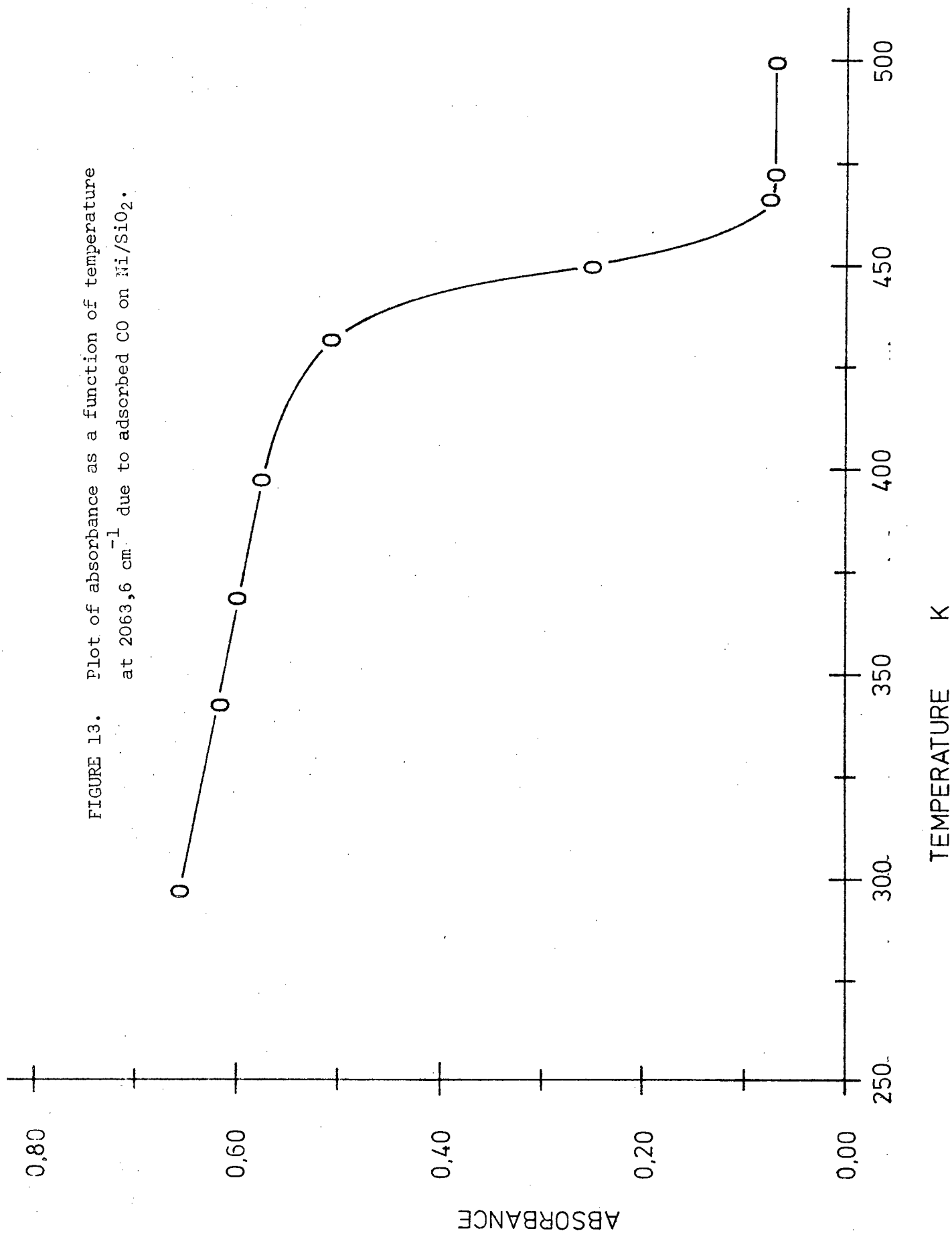
(1.8) CO/H₂ - blank 2:

Similar spectra were obtained with the reactor at room temperatures and 400°C with only a CO/H₂ mixture in the system. A small increase in intensity of the CO fundamental at 2143 cm^{-1} was observed, as expected, when at 400°C , but otherwise no other differences were given. This result demonstrated that the system was 'well behaved'.

4.1.2 In situ cell experiments - Nickel:

Unless otherwise stated, the following results were obtained using sample discs of catalyst type N1, 5,5 - 6,5 wt. % Ni, prepared from the nitrate by the 'dip' method. After reduction and degasing of these discs a 'background' spectrum was always recorded, over the frequency range $2300\text{ to }1700\text{ cm}^{-1}$, prior to the admission of reactant gases. The double-beam technique was employed by placing a 'blank' pressed silica disc, contained in a 10 cm infrared gas cell, in the reference beam of the spectrometer. The gas cell was evacuated to at least 10^{-3} Torr pressure. A 'background' spectrum usually varied between 60 and 90% Transmittance. Outside the range of interest the transmittance decreased quite rapidly.

FIGURE 13. Plot of absorbance as a function of temperature at $2063,6\text{ cm}^{-1}$ due to adsorbed CO on Ni/SiO₂.



(2.1)

A typical spectrum, given by CO chemisorbed on an Ni catalyst surface when at room temperatures, is shown by Figure 14. A very strong broad band in the frequency range 2090 to 2050 cm^{-1} was observed, having maxima at 2080 and 2055 cm^{-1} , ($\pm 2 \text{ cm}^{-1}$). The two maxima were classified as bands B and C respectively. A very broad band of medium intensity was also found, and had its maximum in the range 1925 to 1935 cm^{-1} . This latter band was classified band A. A characteristic of band A was that it always exhibited a low frequency tail, often with a weak but broad inflection point at about 1850 cm^{-1} . This inflection was attributed to vibrations of adsorbed species, similar in their structure to those giving rise to band A, see Chapter 5. These absorptions agree well with the observations of Ferreira and Leisegang²⁸.

The spectrum shown in Figure 14 was only observed when the catalyst was treated with either CO alone or alternatively CO followed by H_2 at room temperatures. It is interesting to note that on addition of H_2 at room temperatures to a Ni/SiO₂ catalyst, pretreated with CO also at room temperatures, the spectrum remained unaltered. This was contrary to the findings of others⁸¹, in which the admission of H_2 not only broadened the CO bands but also shifted them to lower frequencies.

However, at these same temperatures, on pretreatment with H_2 followed by CO, or on admission of a CO/ H_2 mixture to the catalyst, the CO absorption spectrum was altered. Under these conditions only band B was observed in the region above 2000 cm^{-1} . This appeared as a strong but narrower absorption having its maximum at a frequency of $2074 \pm 2 \text{ cm}^{-1}$. Band A occurred as before in the range 1925 to 1935 cm^{-1} .

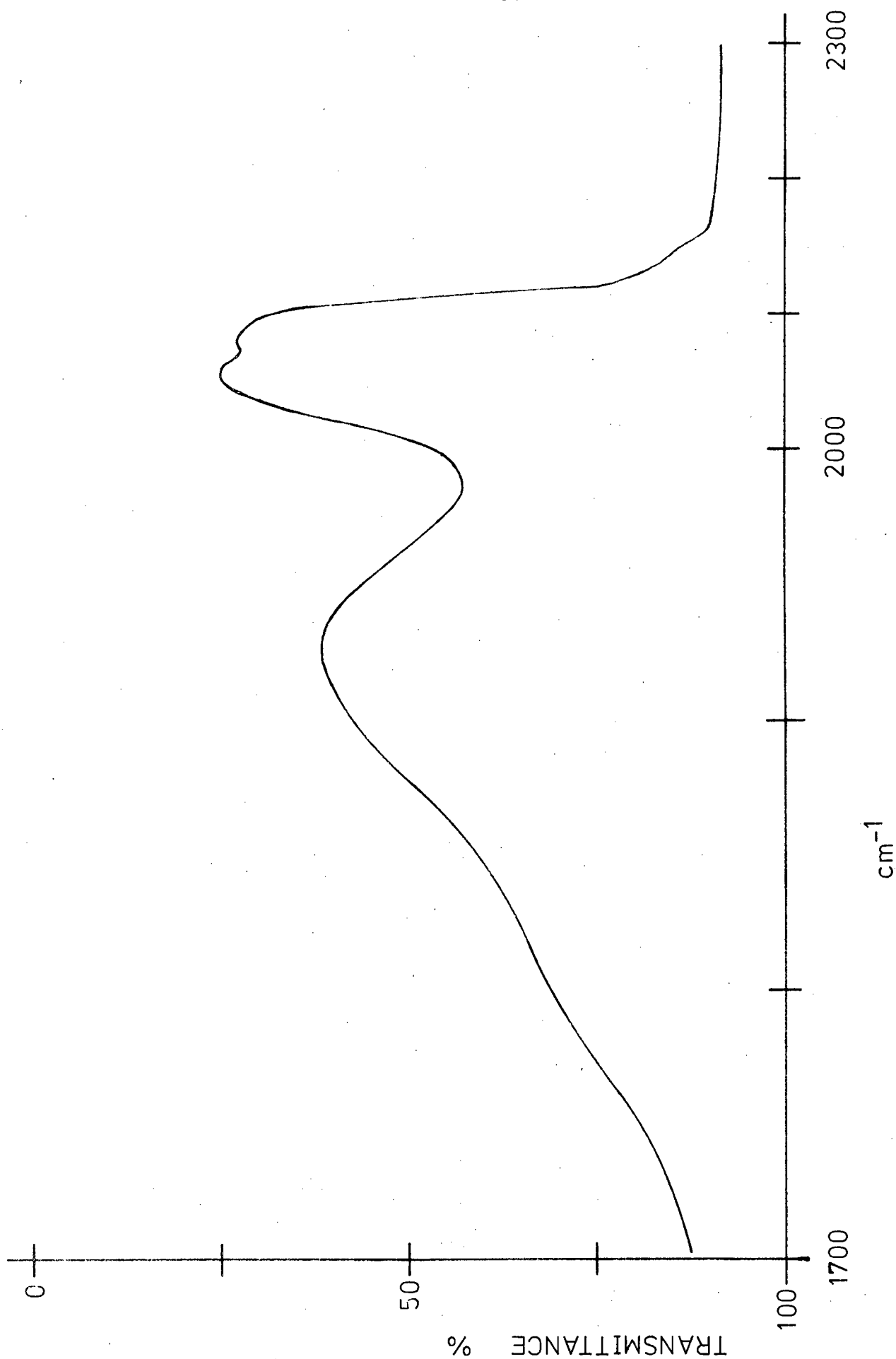


FIGURE 14. Spectrum of CO adsorbed on Ni/SiO₂ at room temperature for both CO alone and CO followed by H₂.

with no apparent change in shape. A typical spectrum demonstrating this single absorption above 2000 cm^{-1} is clearly shown in Figure 15.

On heating the catalyst, in the presence of either CO or CO and H₂, the spectrum was found to undergo a number of changes. However, before these changes are discussed, it is necessary to record the changes that occurred in the 'background' spectrum on heating the catalyst in the absence of reactant gases. The spectra recorded at half-hourly intervals showed a decrease in transmittance with increasing temperature. This was particularly marked over the frequency range 1850 to 1700 cm^{-1} . Consequently the band found at 1850 cm^{-1} became of little interest in this work for this reason, and also because of the band's own general very broad appearance. The above effect, however, was found to be temperature reversible and the original 'background' spectrum was re-obtained on allowing the system to return to room temperatures.

During the heating programme, after either CO pretreatment followed by H₂ or on admission of CO alone, only one band was observed in the region above 2000 cm^{-1} instead of two. Thus at temperatures of about 100°C the only band given in this region occurred near 2065 cm^{-1} , and was assigned as band B. On further heating, this band shifted to even lower frequencies. At the same time band B was observed to decrease in intensity, slowly at first and then more rapidly at temperatures $> 200^{\circ}\text{C}$. The band shifts and reduction in band intensities at elevated temperatures are clearly shown in Figure 16. Band B similarly shifted to lower frequencies for those procedures in which the catalyst had been pretreated with H₂ and then

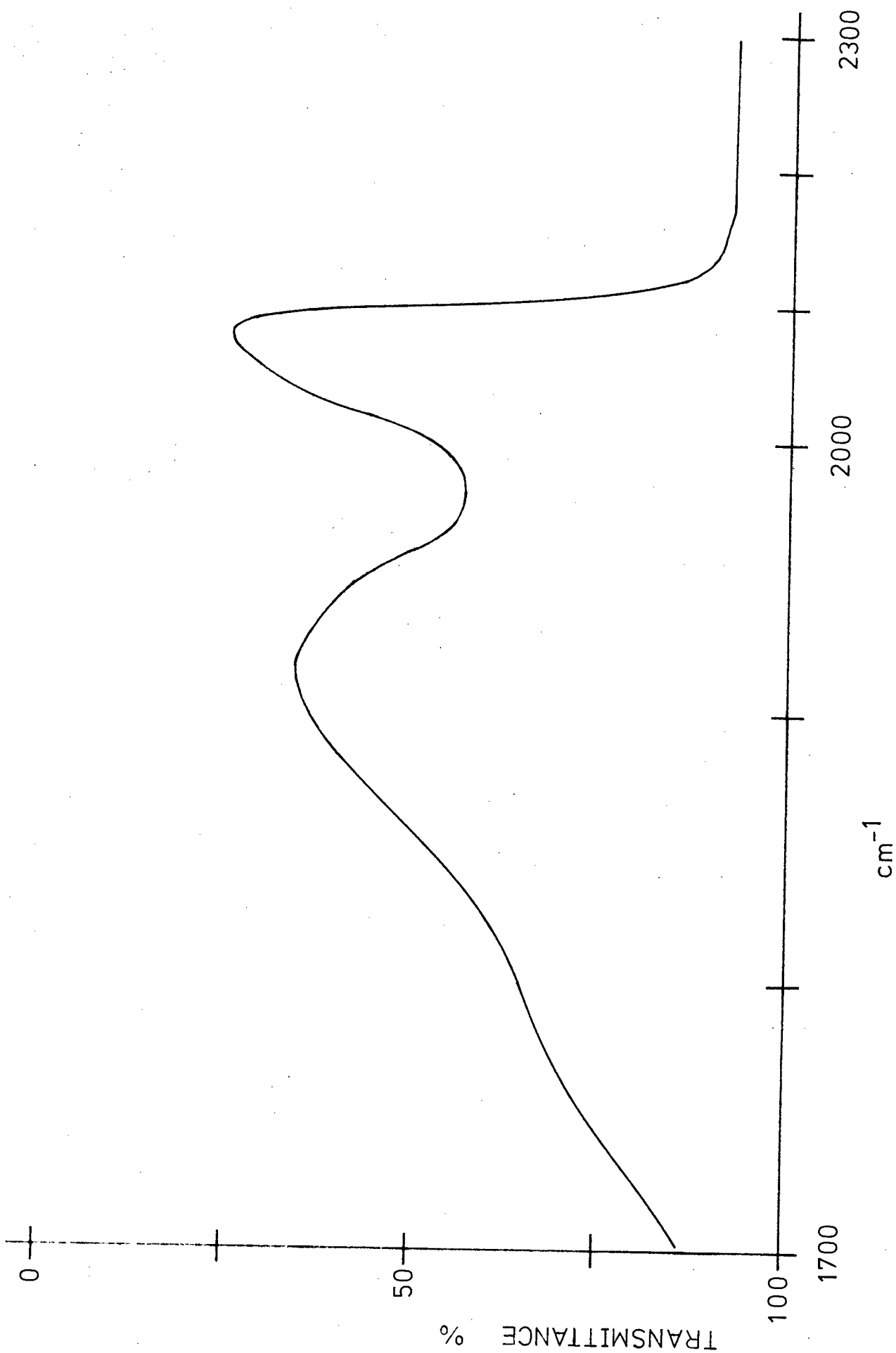
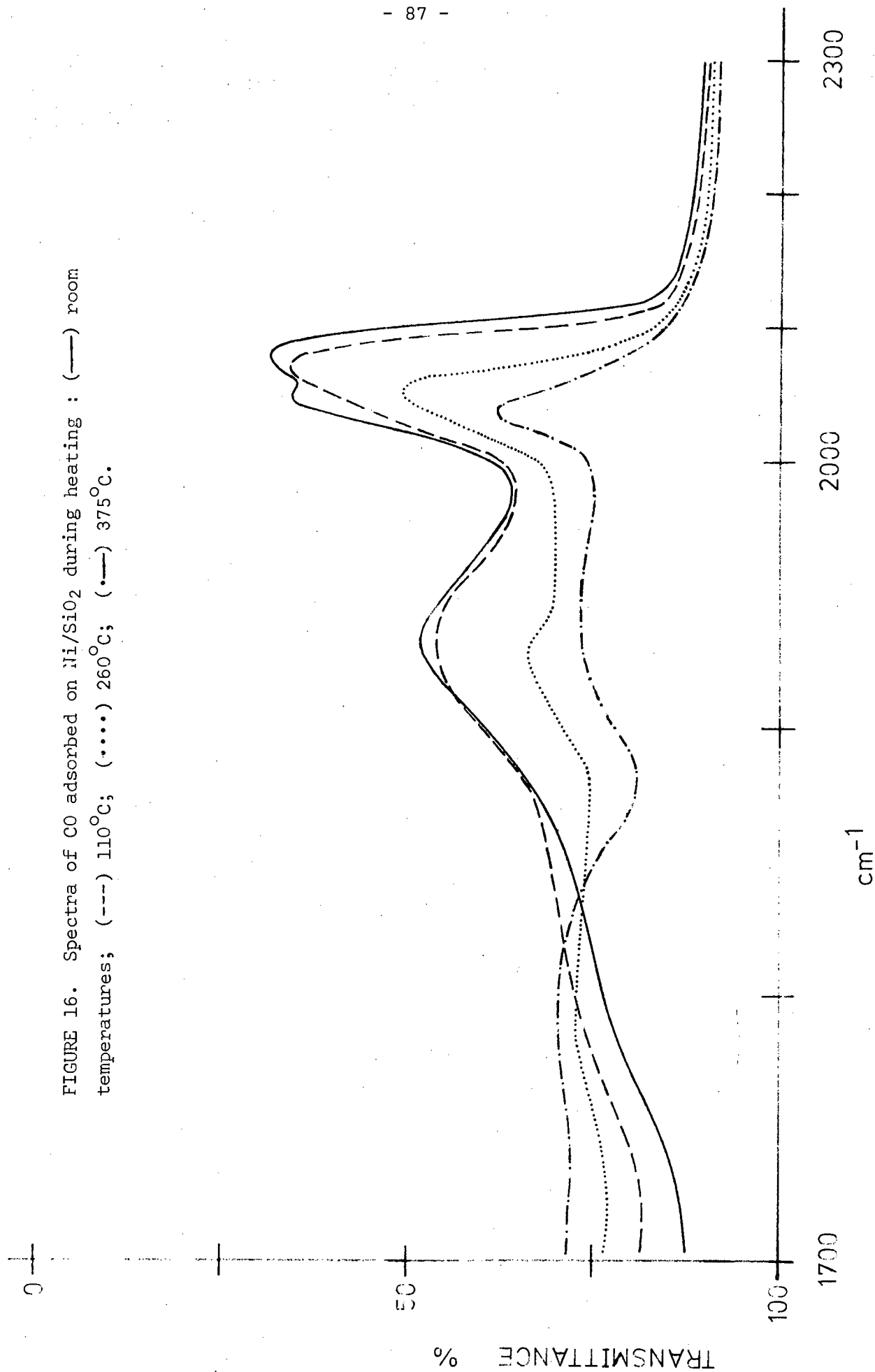


FIGURE 15. Spectrum of CO adsorbed on Ni/SiO₂ at room temperatures for both H₂ followed by CO and a CO/H₂ mixture.

FIGURE 16. Spectra of CO adsorbed on Ni/SiO₂ during heating : (—) room temperatures; (---) 110°C; (.....) 260°C; (·-·-) 375°C.



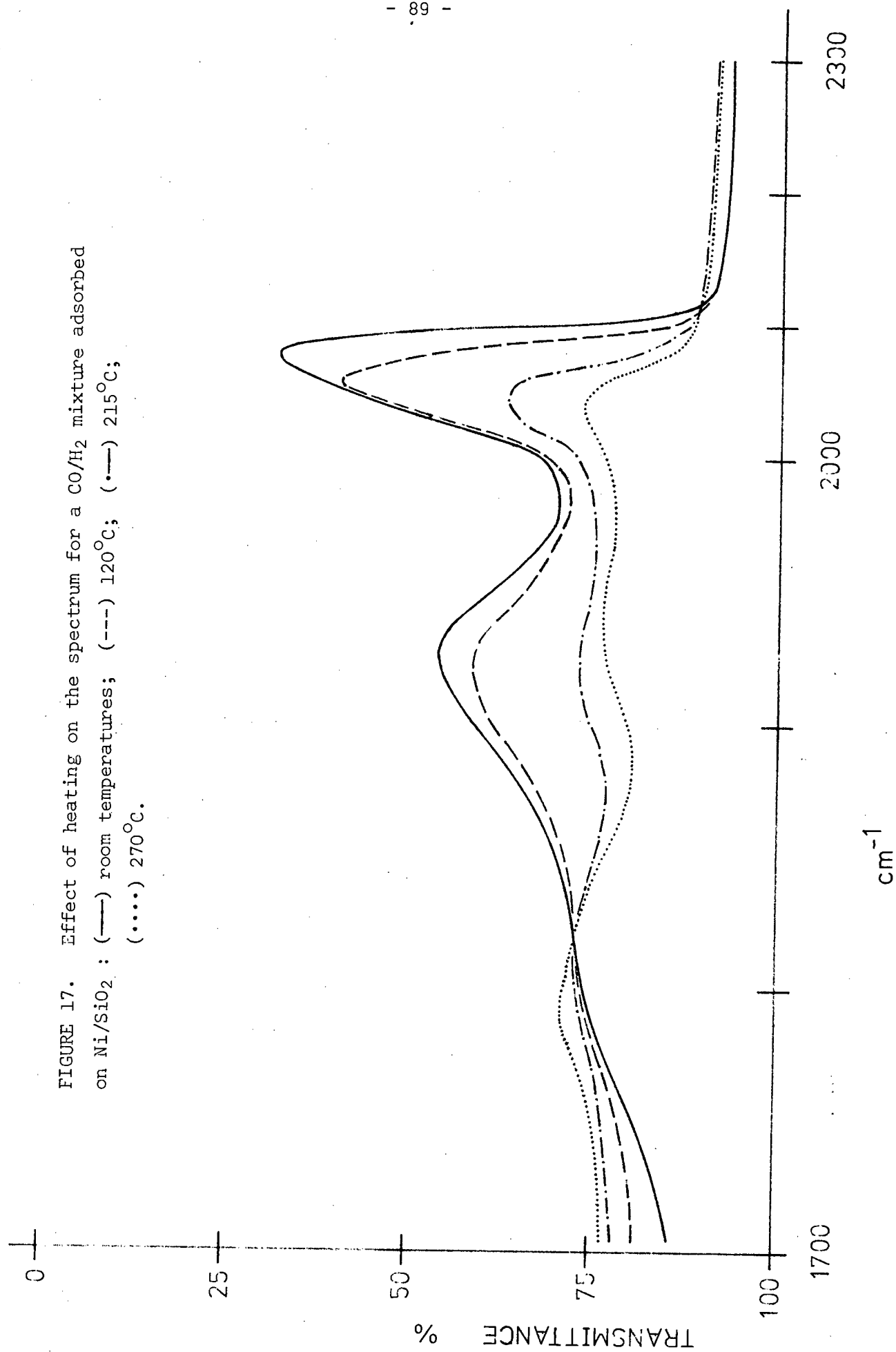
subjected to CO and, on treatment with a CO/H₂ mixture. This effect is shown in Figure 17 for a CO/H₂ mixture.

The frequency shifts observed for band B are also given in Figure 18. Here the band's maximum was simply plotted at various temperatures during the heating programme in an attempt to observe the trend to lower frequencies more closely. The scatter of results can be explained by two factors; (i) the slight variations in experimental conditions used for the separate procedures, such as variations in the H₂ : CO ratio; and (ii) the aged/sintered condition of the samples which was not taken into consideration when formulating these results. But despite the scatter, two lines can be drawn to indicate the general trends. One line corresponds to the experiment in which only CO was present, and the other to those procedures which involved both H₂ and CO. It can be seen that the frequency shift for the latter is more pronounced, an indication that a reaction had occurred between the two gases.

Band A also shifted to lower frequencies on increasing the temperature, but this shift did not appear to be as pronounced as that given by band B. Unfortunately, satisfactory measurements could not be made on band A because of the band's general very broad appearance.

(2.2)

Evacuation of each system for 10 min., at room temperatures and prior to heating the catalyst, had the following effect. With CO alone or on CO pretreatment followed by H₂, the spectrum recorded after evacuation showed only one peak above 2000 cm⁻¹ instead of two.



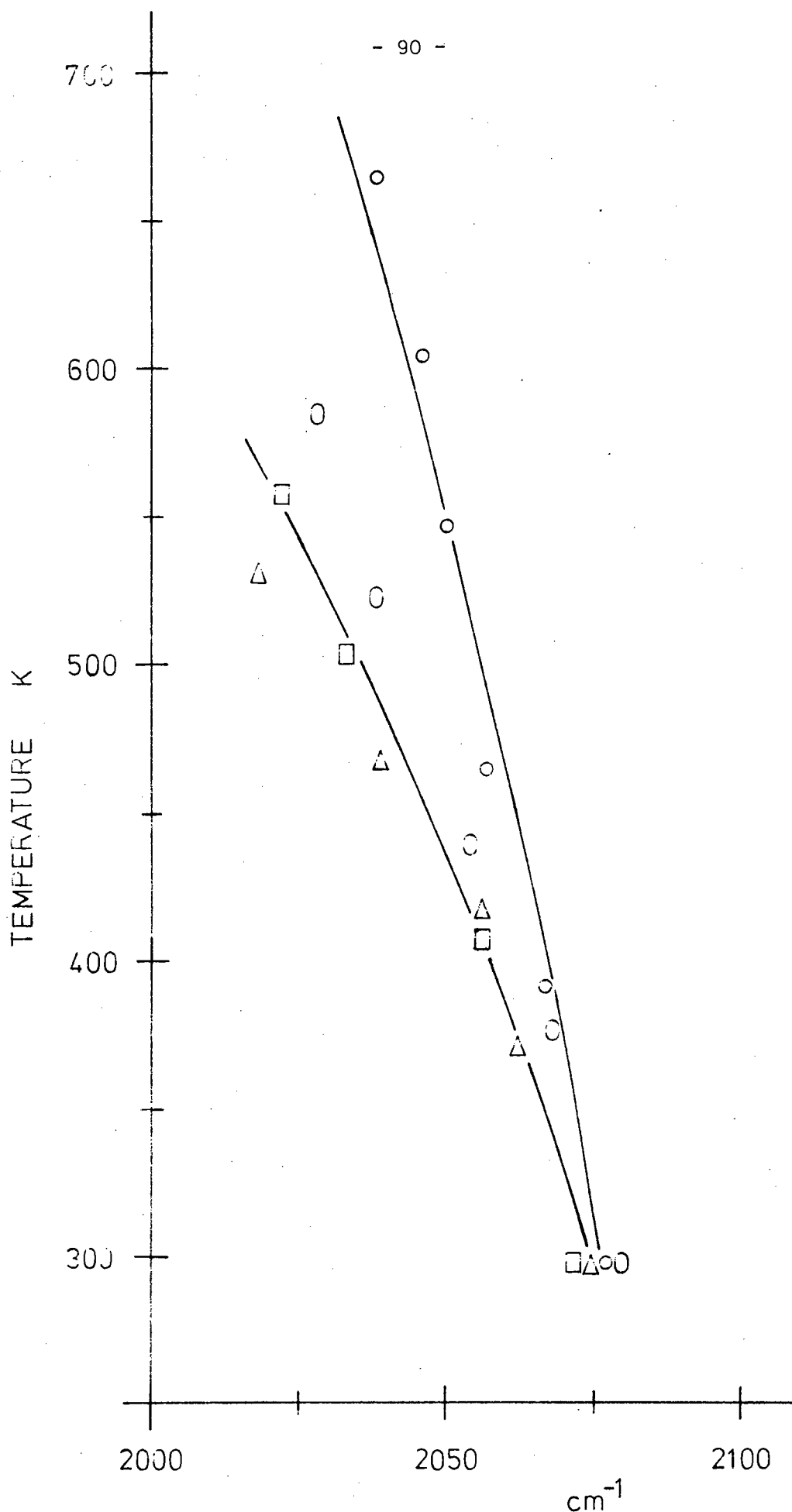
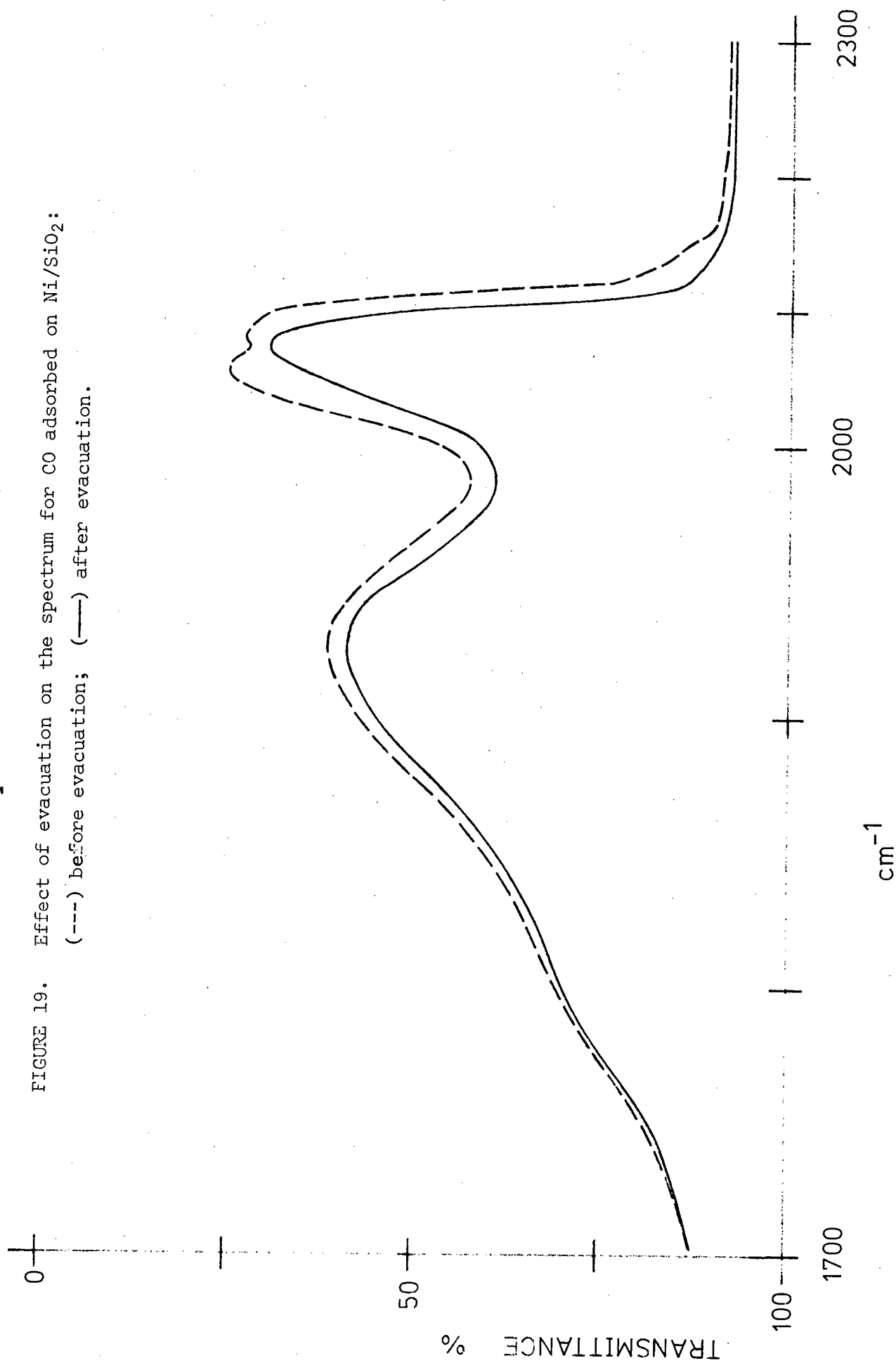


FIGURE 18. Plot of band B frequency as a function of temperature: (O) CO followed by H₂; (Δ) CO/H₂ mixture; (□) H₂ followed by CO; (o) CO alone. The lines drawn indicate the general trends, (see text).

This was accompanied by a very small decrease in band intensity. The single band had its maximum at about 2074 cm^{-1} . The spectrum after evacuation is shown in Figure 19 together with the spectrum taken prior to this step, and is of similar shape to that shown by heating to 100°C , ((2.1), Figure 16). With H_2 followed by CO , or with a CO/H_2 mixture, the spectrum recorded after evacuation showed that band B had shifted by approximately 6 cm^{-1} to lower frequencies, and also decreased slightly in intensity, Figure 20. In all cases band A also decreased in intensity, but no apparent frequency shift was observed. Evacuation at room temperatures for longer periods, e.g. $1\frac{1}{2}\text{ hr.}$, had very little further effect on the spectra regardless of the procedure.

After evacuation and the addition of a further aliquot of H_2 the heating programme was commenced. Results of monitoring at a frequency of 2030 cm^{-1} are given in Figure 21. The frequency of 2030 cm^{-1} was chosen to demonstrate the effect of temperature on band B in the methane formation temperature range, viz., 190°C -reactor experiments. This frequency was possibly a little low but the effect as shown in the Figure was very marked. Namely, a very sharp decrease in absorbance was given, which occurred at approximately 190°C (463 K), in all cases in which CO_{ads} and excess H_2 were simultaneously present, but which did not occur when only CO was present. With the latter procedure CO appeared to remain firmly held onto the catalyst surface until temperatures of 250 to 260°C (about 530 K) were reached; and thereafter up to 400°C band B decreased in intensity, but only slowly. Even at this temperature band B was still

FIGURE 19. Effect of evacuation on the spectrum for CO adsorbed on Ni/SiO₂:
(---) before evacuation; (—) after evacuation.



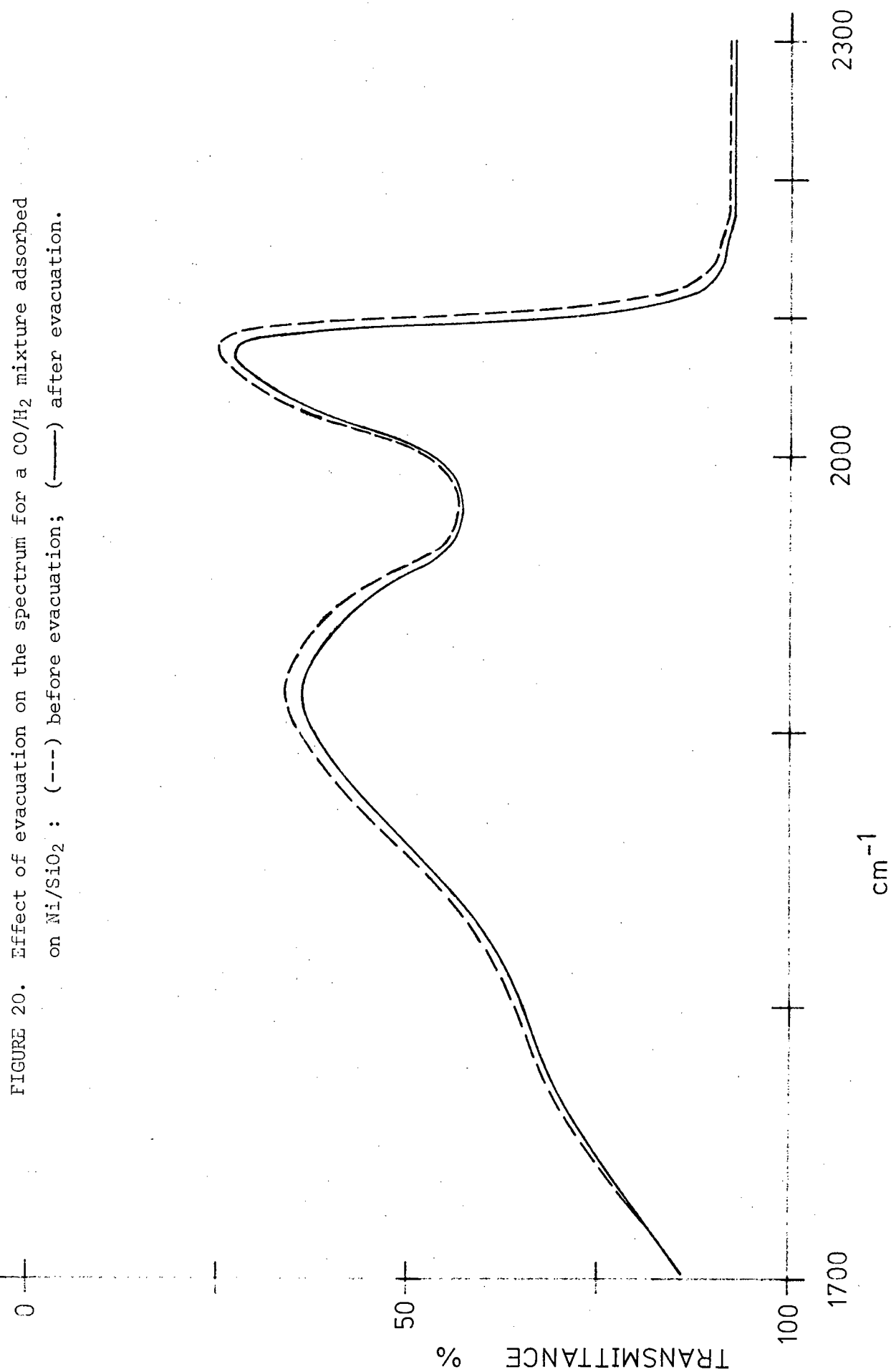
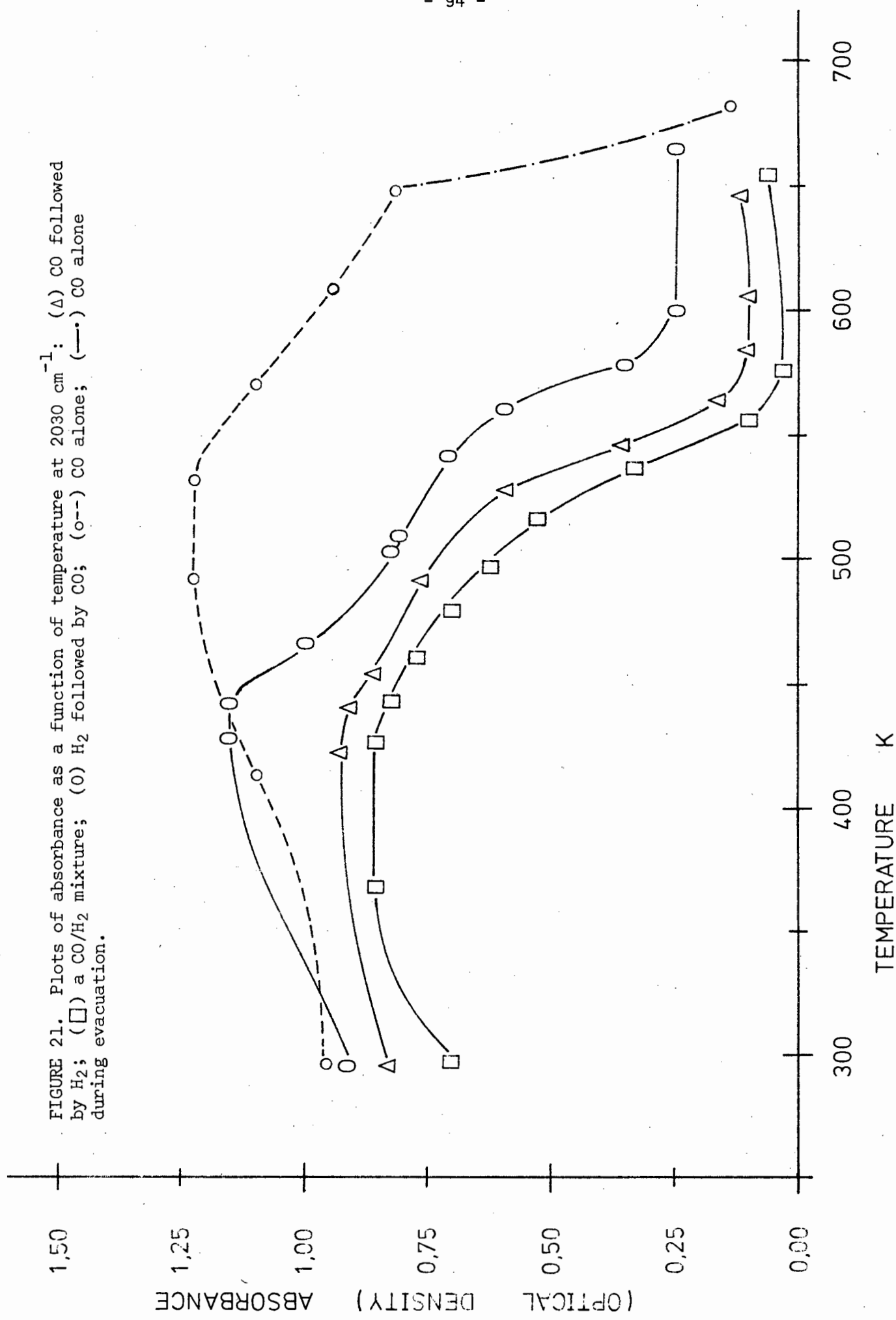


FIGURE 21. Plots of absorbance as a function of temperature at 2030 cm^{-1} : (Δ) CO followed by H_2 ; (\square) a CO/ H_2 mixture; (O) H_2 followed by CO; (o--o) CO alone; (---) CO alone during evacuation.



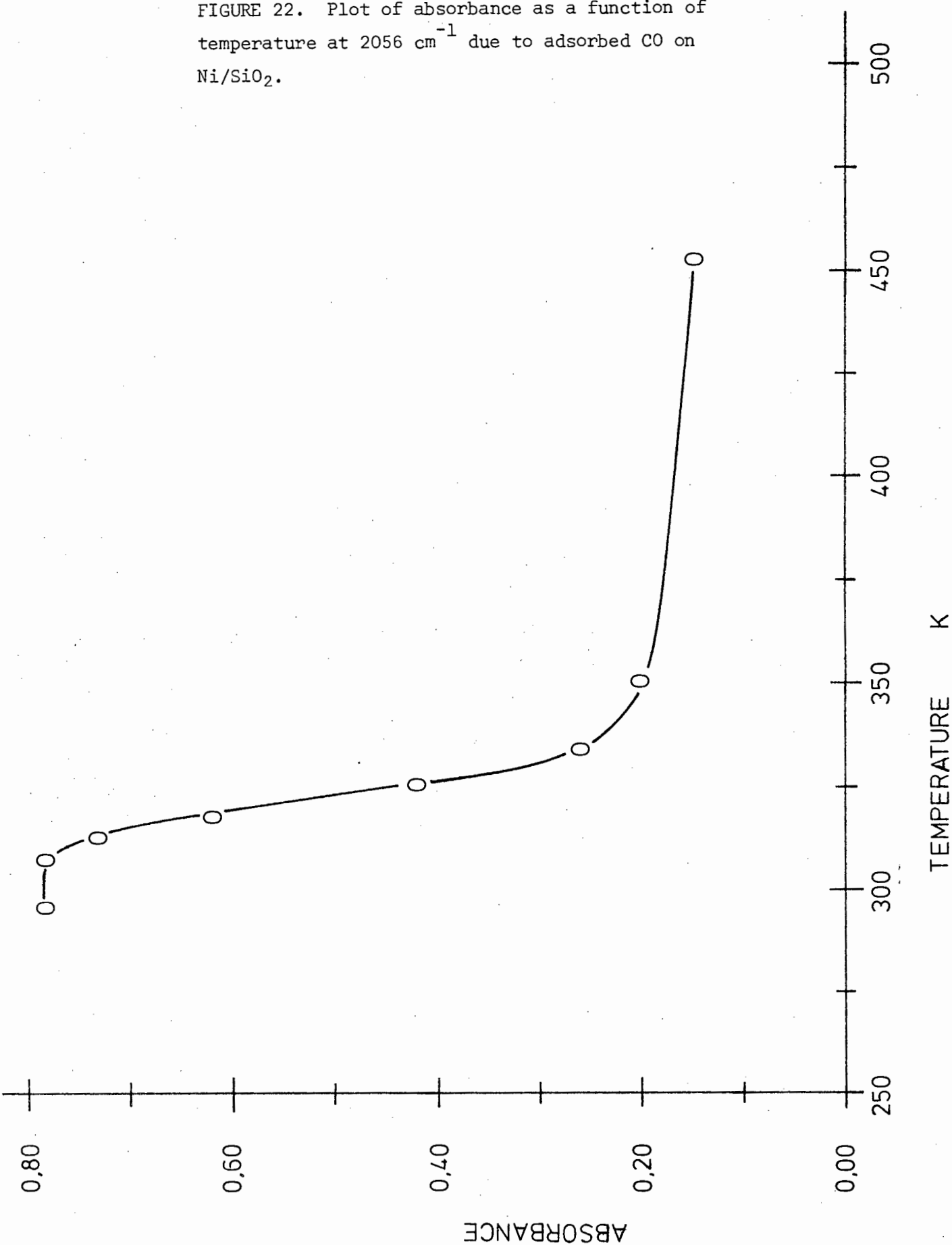
observed, and only disappeared on evacuating the system as shown in the Figure. It was concluded that the loss in intensity of band B, throughout this latter procedure, was a measure of the desorption of the CO species giving rise to B. The fact that this band was still observed quite clearly at temperatures as high as 400°C suggests that some CO was still firmly held on the metal surface. However, although this will be discussed in more detail in the next chapter, the conclusions do coincide with those made in Section 4.1 (1.6) in which it was seen that methane could still be formed at temperatures $\geq 430^{\circ}\text{C}$.

For all procedures an initial increase in absorbance was given over the range 25 to 150°C . This was attributed to the band shift to lower frequencies, an effect more predominant at these lower temperatures than the corresponding decrease in band intensity.

The effect of heating on band C, at 2056 cm^{-1} , with only CO present and without evacuating the system, is shown in Figure 22. A considerable decrease in absorbance can be seen to occur within the temperature range 35 to 80°C . The same result was obtained using discs of catalyst type N.2, of 3-3,5 wt. % Ni content.

For the procedure (CO - evacuate - ΔH), adsorbed CO giving rise to band A at 1900 cm^{-1} was firmly held onto the surface until temperatures $\geq 230^{\circ}\text{C}$ were reached. Only then was band A found to decrease in intensity. The monitoring of band A at 1900 cm^{-1} was made impossible above 300°C due to the change in 'background' with temperature (2.1) which tended to mask any further 'real' effects.

FIGURE 22. Plot of absorbance as a function of temperature at 2056 cm^{-1} due to adsorbed CO on Ni/SiO_2 .



(2.3)

The effects of a heating/cooling cycle on band B are shown in Figures 23, 24, and 25.

Firstly, Figure 23 demonstrates once again the shift to lower frequencies and decrease in band intensity with increase in temperature, on heating the catalyst in the presence of CO; compare earlier results (2.1). It is interesting to note that only one maximum was observed, with the system while at room temperatures, and not two, contrary to that found in (2.1). This can be accounted for by the following modification of the experimental procedure. The *in situ* cell, containing the sample disc, was opened to the vacuum line to admit CO for a few seconds only and not the customary $\frac{1}{2}$ hr. Then, as soon as a spectrum was recorded, the cell was heated in the usual manner. Thus, in effect, minimal time was allowed during which the CO was in contact with the catalyst at room temperatures. Clearly further discussion on this point is required, but will be covered in Chapter 5. After heating, the system was allowed to cool slowly back to room temperatures over a 3 hr. period, while spectra were again recorded at various temperatures. This cooling effect is adequately shown by the three plots in Figure 24. A frequency shift was observed to occur in the opposite direction, but this time it followed a different path. The band also increased in intensity on cooling but never attained its original height. Band B, on returning to room temperatures, had only one maximum, and not two, which occurred about 2050 cm^{-1} .

The system was then allowed to stand overnight at room temperatures. The recorded spectrum showed no change in the band's position or intensity. A further spectrum taken after an evacuation

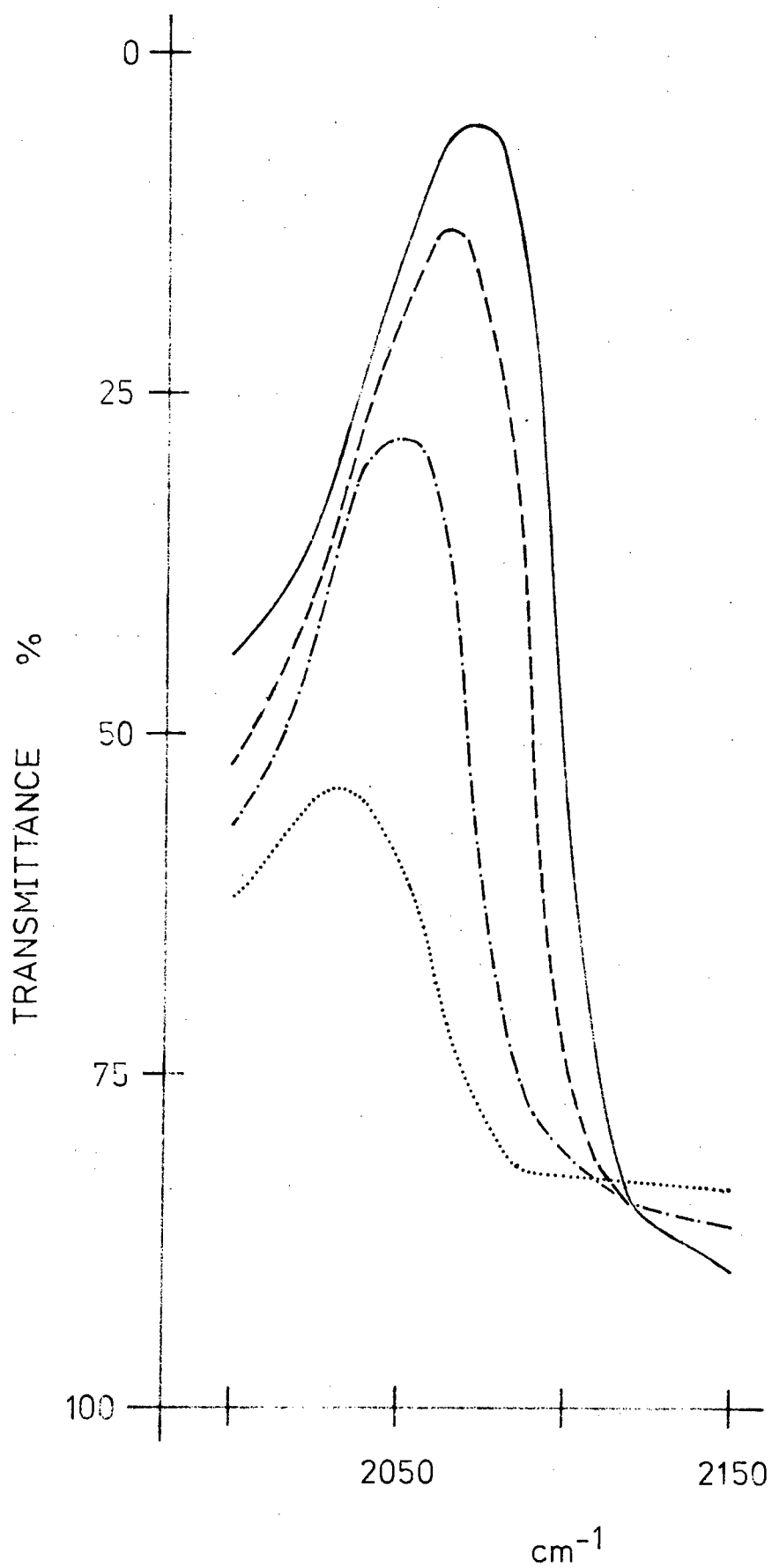


FIGURE 23. Spectra of CO adsorbed on Ni/SiO₂ during heating :
(—) room temperatures; (---) 135°C; (—·) 300°C;
(.....) 385°C.

FIGURE 24. Spectra of CO adsorbed on Ni/SiO₂ on cooling: (.....) 410°C; (---) 325°C; (—) 225°C to room temperatures.

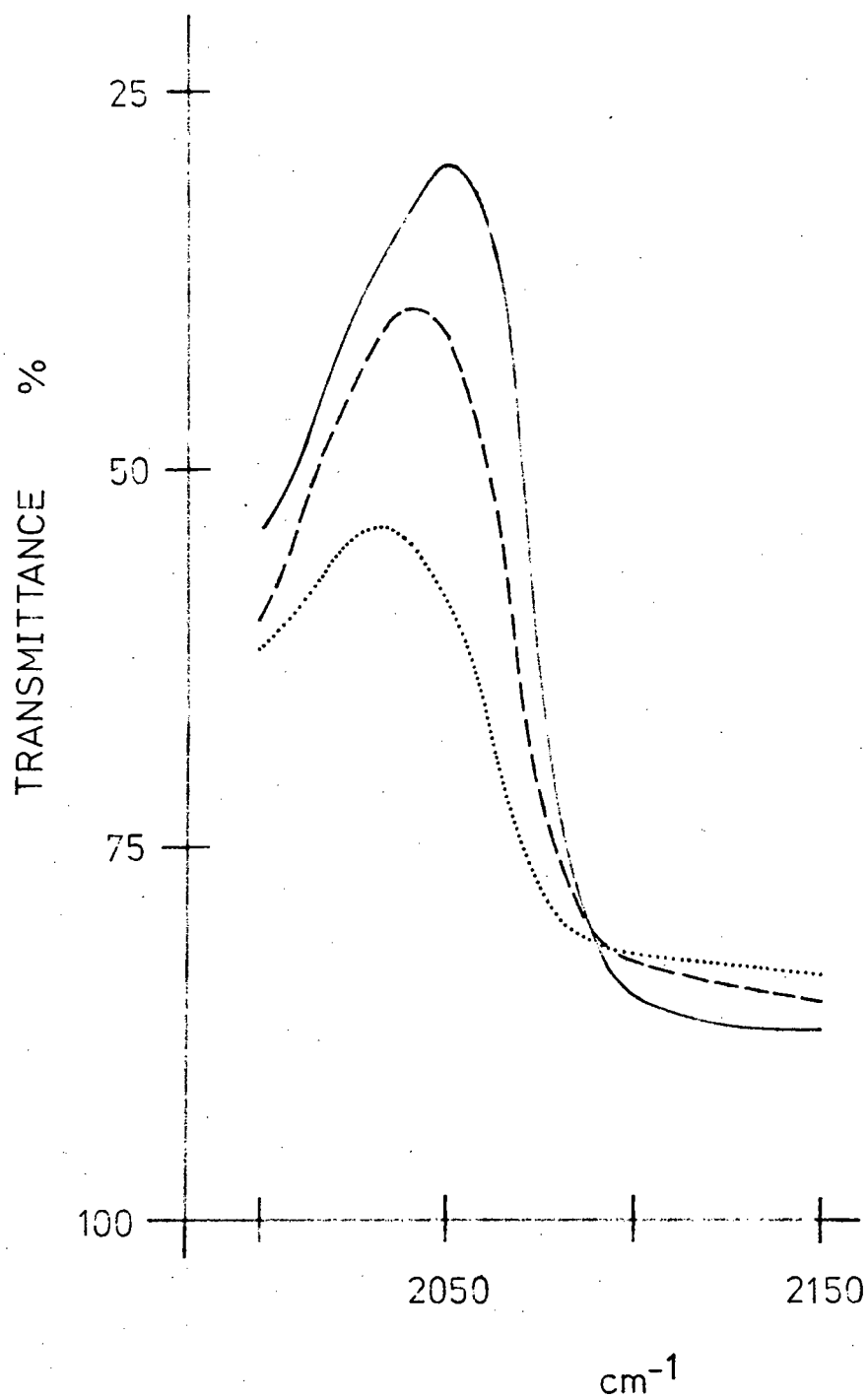
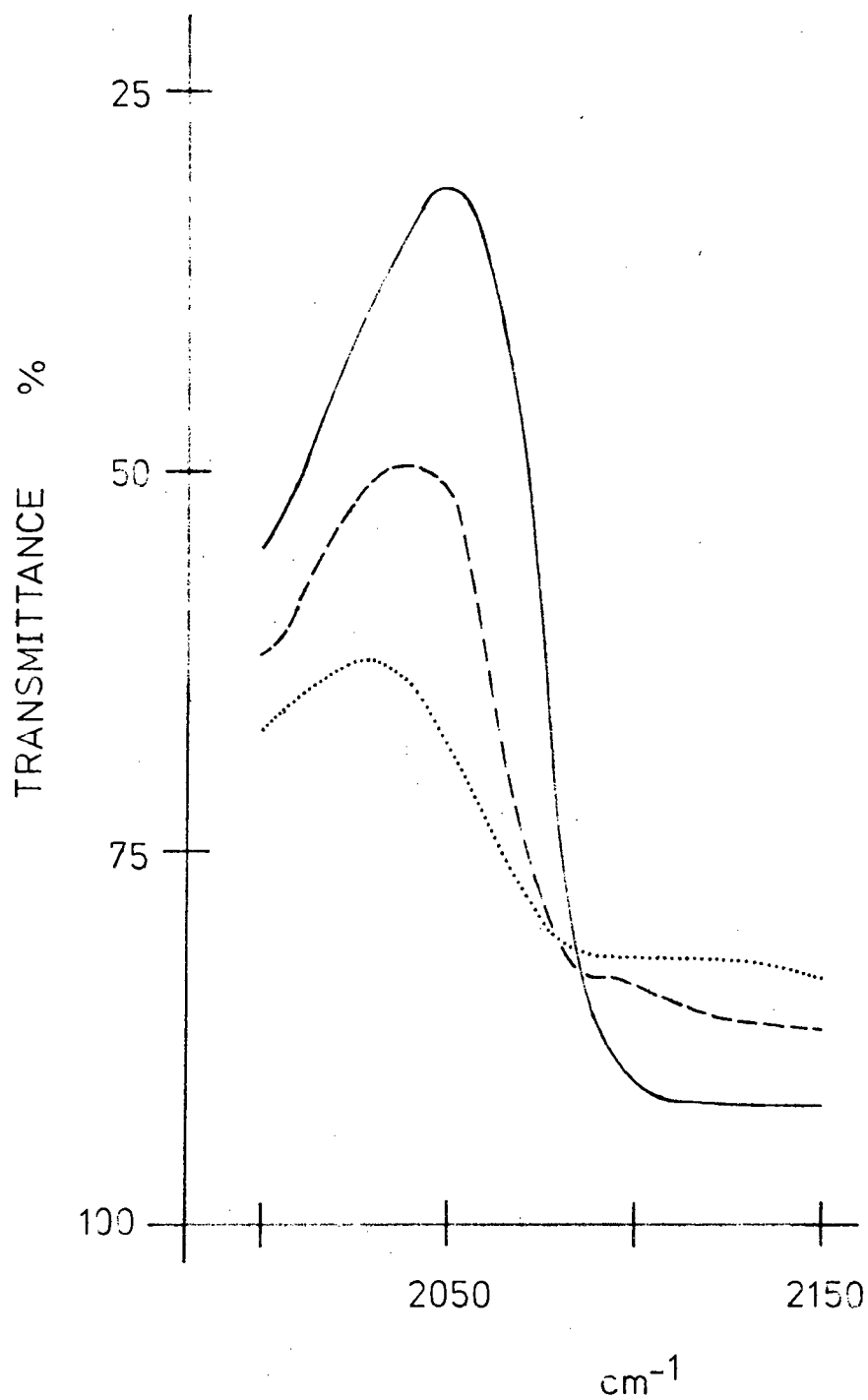


FIGURE 25. Spectra of CO adsorbed on Ni/SiO₂ on re-heating:
(—) room temperatures, evacuation for 1 hr., and up to
215°C; (---) 315°C; (.....) 400°C.



period of 1 hr. again showed that there was no change. This is represented by the strongest absorption plot in Figure 25 which compares favourably with its counterpart in Figure 24. This provides strong evidence to show that the chemisorbed species giving rise to the band at 2050 cm^{-1} was very firmly held on the surface. The above can be compared with the effect on band B of a 1 hr. evacuation period with CO chemisorbed on an otherwise 'cleaned' sample. Here a band shift to lower frequencies together with a decrease in intensity is observed. The heated/cooled system was finally re-heated, see Figure 25. The frequency shift now was found to be temperature reversible.

The heating/cooling experiment was repeated for confirmation and the frequency maximum of band B plotted at various temperatures by recording the spectrum frequently. The result is given in Figure 26. On returning to room temperatures again only one band, and not two, occurred at high frequencies, with a maximum at 2053 cm^{-1} . The plot clearly shows the different path taken by the band shift on cooling. On admitting CO to the catalyst, when at temperatures $> 400^{\circ}\text{C}$, followed by cooling, the position of band B was similar to that given by the previous cooling curve, see Figure 26. This time band B had its maximum at 2047 cm^{-1} , slightly lower than before. However, for all these experiments band B has been found within the narrow frequency range $2047\text{ to }2053\text{ cm}^{-1}$. The discrepancy could well be due to small changes in experimental conditions and the degree of sintering of the sample. On reheating the system the frequency shift was again shown to be temperature reversible, see the single line plot in Figure 26.

Finally, a very interesting result was obtained on the

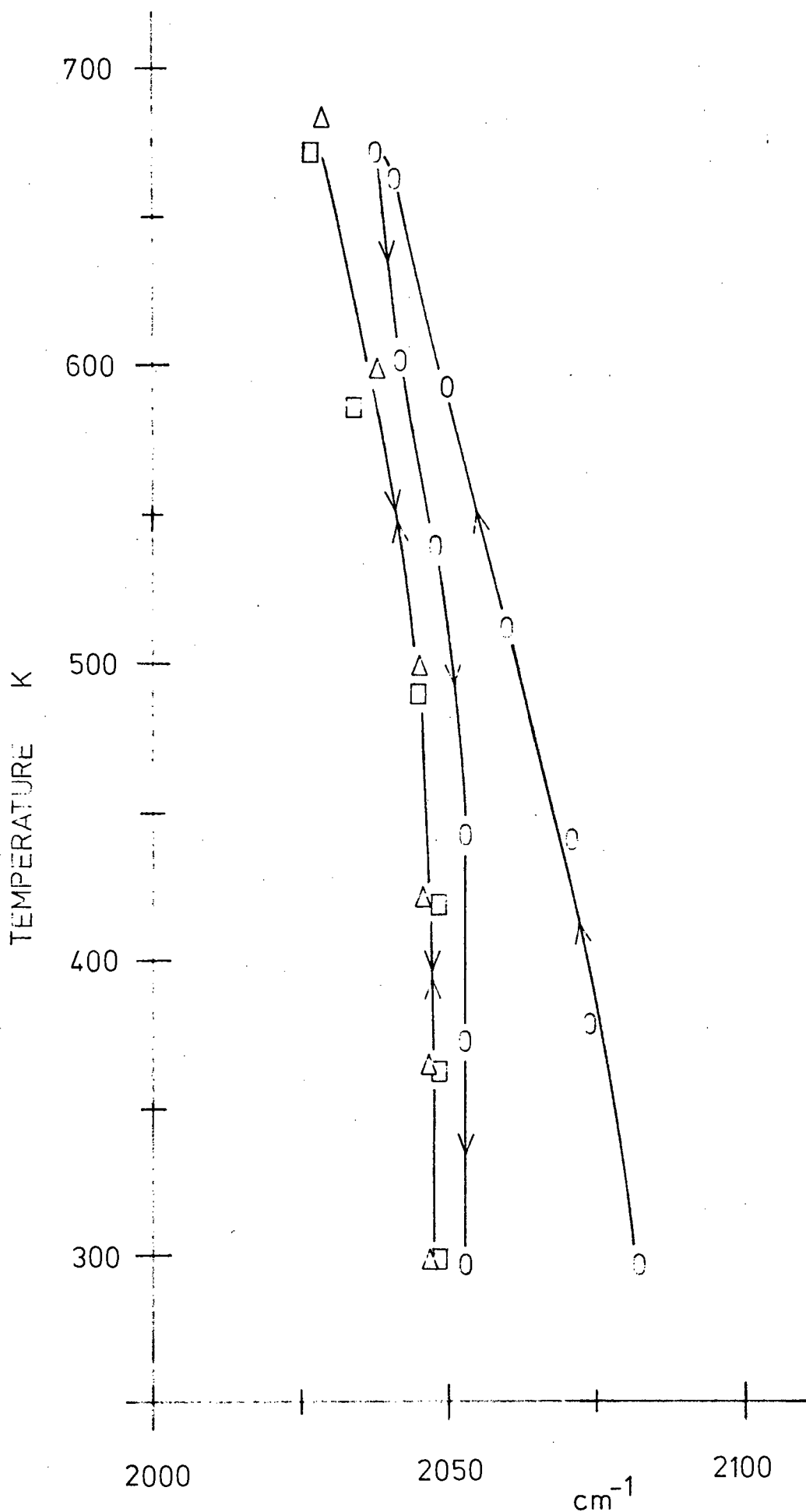


FIGURE 26. Plot of band B frequency as a function of temperature for CO adsorbed on Ni/SiO_2 : (O) during a heating/cooling cycle; (Δ) during cooling and after evacuation (\square) on reheating.

admission of 12 Torr CO, and then subjecting the catalyst to a heating/cooling cycle. Initially, the presence of CO gave rise to an extremely strong broad band which was at maximum absorbance, almost zero transmittance, over the entire frequency range 2090 to 2050 cm^{-1} . However, on heating and cooling, similar spectra were observed to those previously found, viz., band B shifted its position in the opposite direction, on cooling, but followed a different path. A final maximum was given in the range 2065 to 2070 cm^{-1} . Furthermore, the intensity of B was very much reduced by the end of the experiment, again comparable with previous spectra. The relatively high CO pressure should have been sufficient to restore the *status quo*, i.e. identical spectra were expected at both the end and the beginning of the procedure. That this was not so, suggested that a side-reaction had occurred. Consequently on recording a spectrum (after the cooling cycle) over the frequency range 2600 to 2300 cm^{-1} a medium sharp band was observed at a frequency of 2342 cm^{-1} ; and the intensity of the free CO₂ fundamental at 2345 cm^{-1} could not have been attributed solely to 'background'.

(2.4)

Another phenomenon observed was that of ageing and/or sintering of the catalyst. After repeated use, during which the catalyst was frequently subjected to temperatures in excess of 400°C (necessary for cleaning the samples, 400 to 420°C) the high wavenumber bands at 2080 and 2055 cm^{-1} , (2.1), were replaced by a set of four bands. These are shown in Figure 27. Well defined maxima were given at 2063 and 2055 cm^{-1} usually with shoulders at 2075 and 2051 cm^{-1} . This characteristic was also observed for CO adsorbed on catalysts having a lower

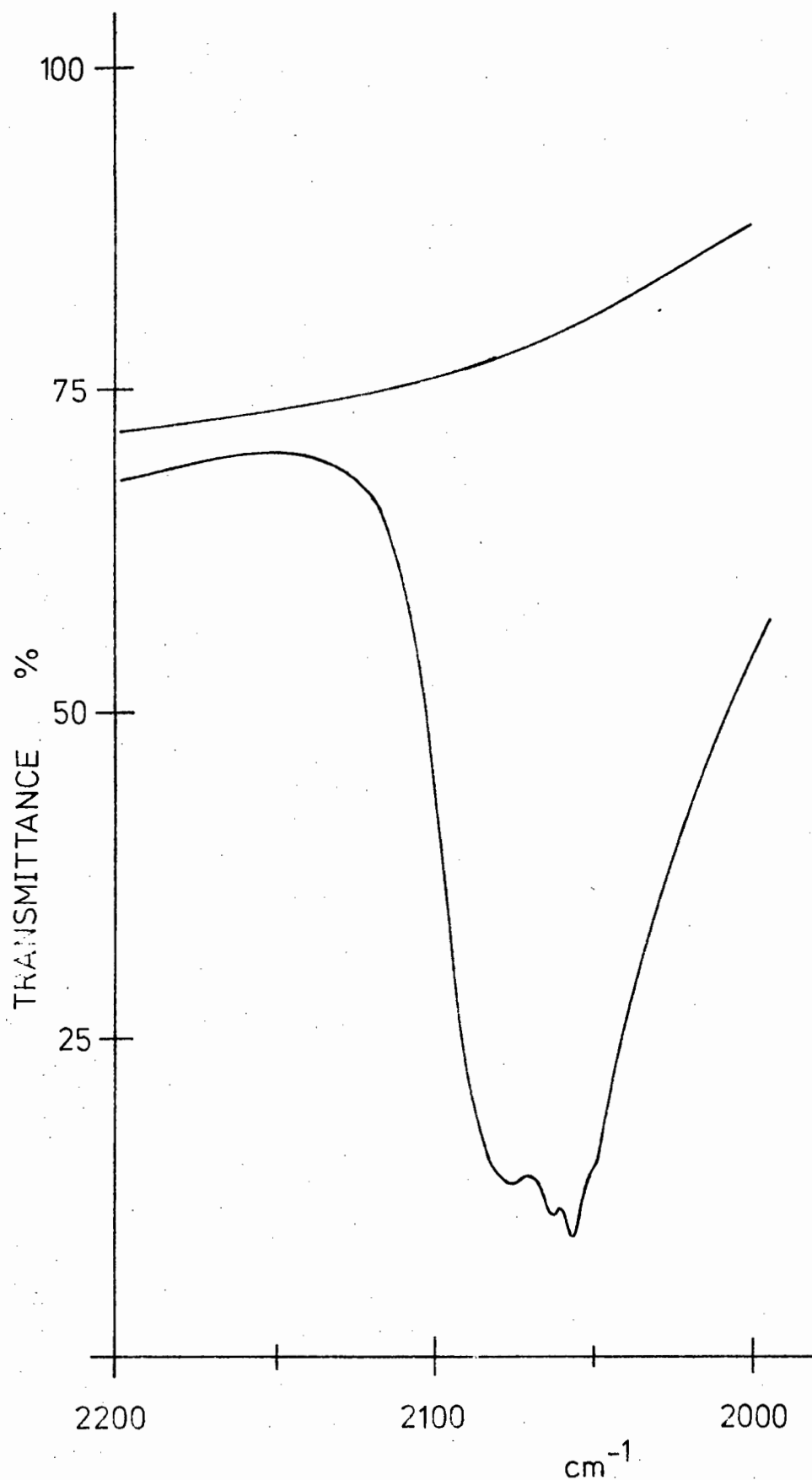


FIGURE 27. Spectrum of CO adsorbed on an aged/sintered Ni/SiO₂ disc.

nickel content, type N2 catalysts. The four bands disappeared either on evacuation for 10 min. or on heating at 120°C for 1 hr. after which one band only was given, less intense than the others, with its maximum in the region 2065 to 2062 cm^{-1} .

The greater the degree of ageing/sintering the weaker the absorptions per given pressure of CO; an indication that the sample was becoming less 'active'. Usually samples were abandoned well before they reached this stage of inactivity. A similar effect, attributable to an ageing/sintering process, is illustrated in Figure 21. Here the three full line plots refer to the same catalyst sample and, as shown, the absorbance decreased with age of sample.

(2.5)

All the above results given in sections (2.1) to (2.4) inclusive were obtained using well reduced catalysts, and usually samples were abandoned as soon as oxidation became evident. Surface oxidation, caused either by incomplete reduction of the sample during preparation or by an air leak in the vacuum line, affected the spectrum of chemisorbed CO by giving rise to two additional bands. These were classified as bands E and F and found at frequencies of 2126 and 2185 cm^{-1} , ($\pm 3 \text{ cm}^{-1}$), respectively. The CO spectrum of an oxidised sample is illustrated in Figure 28. Both absorptions were very weak, although their intensity was found to increase with increase in oxidation of the catalyst. Furthermore, bands E and F readily disappeared on evacuation. These findings compare well with those of Ferreira²⁷.

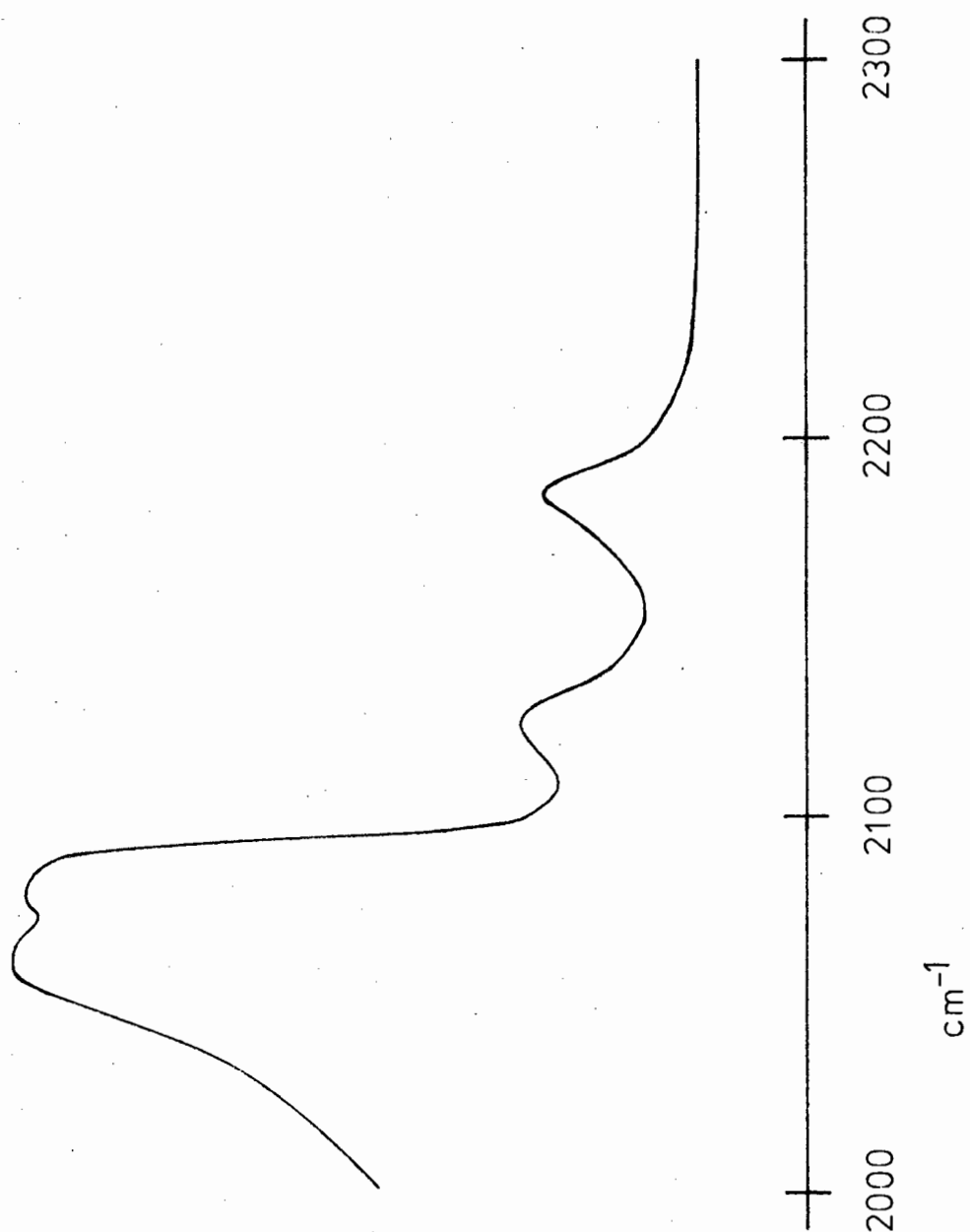


FIGURE 28. Spectrum of CO adsorbed on an oxidised Ni/SiO₂ sample disc.

(2.6)

Tests were carried out on the silica disc reference to check noise and drift levels when monitoring at a constant frequency over long periods, and also to ensure that the silica provided no interference fringes within the range of interest (2300 to 1700 cm^{-1}). The results are given in Appendix 2. It was concluded that a silica disc, of comparable thickness to the sample, when placed in an evacuated 10 cm infrared cell, provided a satisfactory reference for this work.

4.2 THE REACTIONS OF CO AND H₂ ON SILICA SUPPORTED IRON CATALYSTS.

The results obtained for the interaction of carbon monoxide and hydrogen on silica supported iron catalysts were not as substantial as those of nickel. The main reason was considered to be the ease of reducibility of the metal oxides, as thermodynamically nickel oxide is reduced at high temperatures with considerable ease over that of iron oxide¹⁰⁷. Although various parameters were explored to produce an 'active' iron catalyst (such as prolonged reduction times at higher temperatures, a reduction promoter, and use of different starting materials) conditions were controlled to simulate those used for nickel as much as possible, so that comparisons could be drawn between the results obtained for the two metals.

4.2.1 Reactor experiments - Iron:

The four procedures; CO - H₂ - ΔH, CO/H₂ - ΔH, H₂ - CO - ΔH, and CO - ΔH (Sections 3.4 (1.1) - (1.4)), were applied in turn to each of the iron catalysts, types FeI, II and III. Spectra were scanned over the frequency range 4000 to 1000 cm⁻¹ before and after the reactant gases were admitted at room temperatures, and also when the reactor had reached 400°C. During the heating programme the methane Q branch was usually monitored, at a frequency of 3017,5 cm⁻¹. The results were as follows.

The interaction of CO and H₂ on all catalyst types at elevated temperatures formed methane as the chief product. This was shown by the final spectra recorded when the reactor had reached

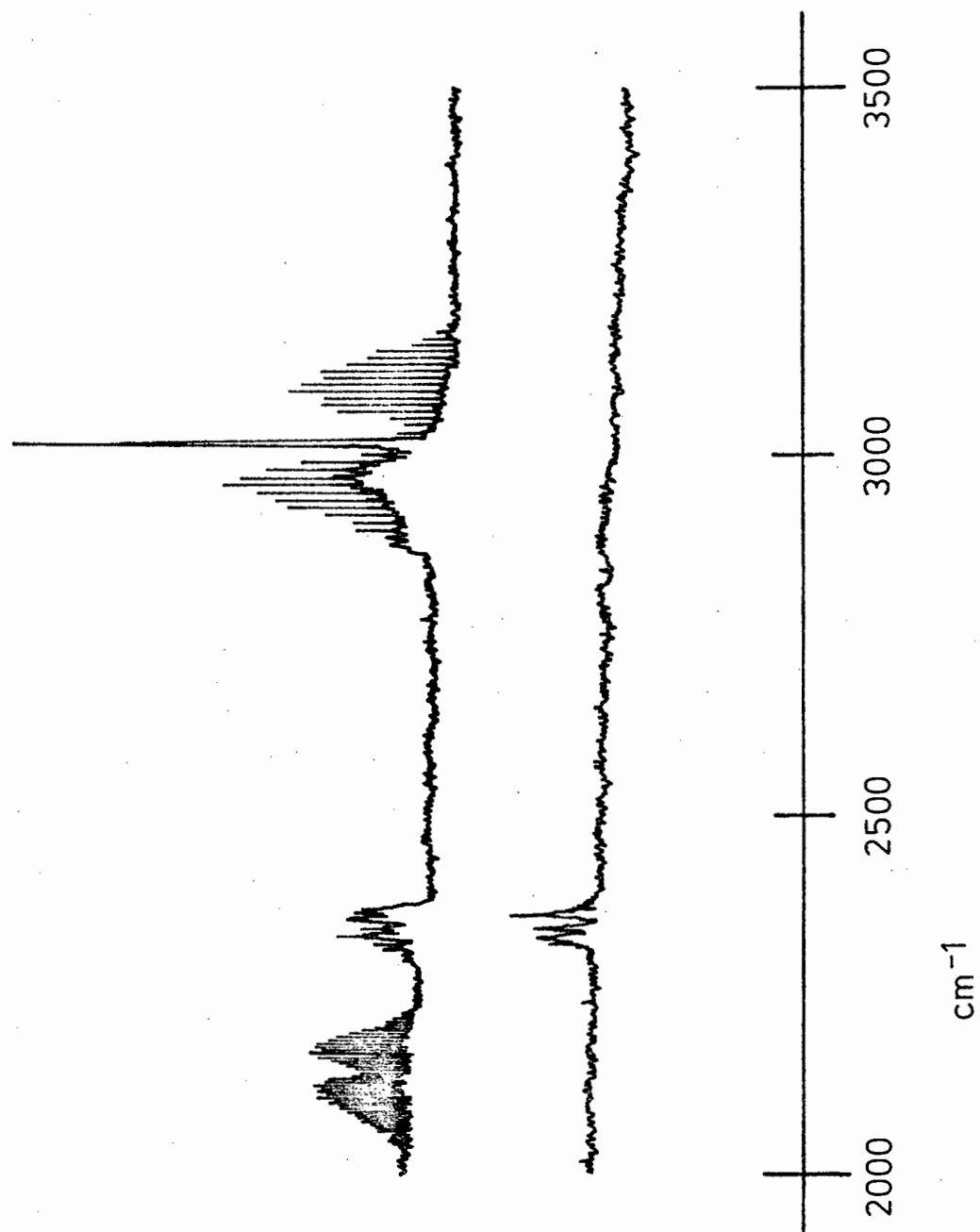
400°C. By monitoring at $3017,5\text{ cm}^{-1}$ methane was first detected at temperatures higher than those given for a nickel catalyst. The temperature ranges in which methane was first detected were (i) 200 to 220°C for a freshly reduced sample; and (ii) 220 to 250°C for an aged/sintered sample. These temperatures were common for all catalyst types.

Another common feature was that methane was detected by infrared as being the only hydrocarbon produced at high temperatures on applying the procedure $\text{H}_2 - \text{CO} - \Delta\text{H}$, whereas for procedures $\text{CO} - \text{H}_2 - \Delta\text{H}$ and $\text{CO}/\text{H}_2 - \Delta\text{H}$, when using catalysts FeII and III, trace amounts of ethane and propane were also given during the reaction. Invariably far more ethane was produced than was propane, and their presence was shown by broad but very weak absorptions in the infrared with maxima at about 2970 and 2880 cm^{-1} . These absorptions correspond to the CH_3 and CH_2 symmetric and asymmetric stretching frequencies. A typical spectrum recorded when the reactor had reached 400°C is given by Figure 29. The weak absorptions below 3000 cm^{-1} , although partly masked by the CH_4 P branch, are clearly shown; compare Ni, Figures 7 and 9.

Confirmation of C_2H_6 and C_3H_8 as by products in the reaction was revealed by mass spectrometry, see Figure 30. Thus for a FeII catalyst the cracking, or fragmentation, pattern produced is indicative of a methane/ethane/propane mixture. See Section 4.4 for further details.

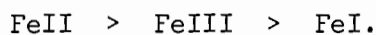
Type FeI catalysts were found to be less 'active' than the

FIGURE 29. Spectrum of products at 400°C from CO and H₂ adsorbed on Fe/Cu/SiO₂, with background offset.



other two in a much that methane was usually the only hydrocarbon detected on applying the two procedures $\text{CO} - \text{H}_2 - \Delta\text{H}$ and $\text{CO}/\text{H}_2 - \Delta\text{H}$. Only occasionally were there trace amounts of ethane produced, detected by infrared and confirmed by mass spectroscopy. The order of catalytic activity with respect to methane production, i.e., the relative amounts of CH_4 formed, using freshly prepared samples, after the reactor had reached 400°C , was found to be in the order:

catalyst type,



None of the iron catalysts were as 'active' as the nickel with respect to methane formation. However, catalyst FeII compared favourably, producing at least 2/3rds the amount of methane as that normally formed over a nickel catalyst.

No iron carbonyls were detected by infrared during any experiment either at room or elevated temperatures. This can be compared with the nickel results in which $\text{Ni}(\text{CO})_4$ was readily produced on allowing CO to come into contact with the surface at room temperatures. Furthermore, for all catalysts, no significant increase in intensity was observed of the vibrations attributable to $\text{H}_2\text{O}_{\text{vap}}$ and CO_2 over that given by a 'background' spectrum for any procedure involving the two reactants CO and H_2 . On one occasion only were there trace amounts of CO_2 and $\text{H}_2\text{O}_{\text{vap}}$ detected by mass spectroscopy on applying the procedure $\text{CO}_2 - \text{H} - \Delta\text{H}$ to a type FeI catalyst.

Usually no products were detected when applying the procedure $\text{CO} - \Delta\text{H}$ to all catalysts, except occasionally a small increase in intensity of the CO_2 fundamental was given at a frequency of 2345 cm^{-1} .

4.2.2 In situ cell experiments - Iron:

A background spectrum was first recorded over the frequency range 2300 to 1730 cm^{-1} ; also a 'blank' silica disc was housed in the reference beam as before, with the spectrometer conditions set as for the nickel *in situ* experiments. Transmittance was usually very good for iron catalysts prepared by the 'dip' method, and varied between 70 and 90% over the range of interest. However, discs prepared directly from powders, type FeIII and IV catalysts, were completely opaque to infrared radiation.

(a)

The first set of experiments were performed on F2 catalysts, (Fe/Cu/SiO₂). They were chosen because of the greater catalytic activity exhibited by copper promoted catalysts which was revealed by the reactor experiments. Initially sample discs were reduced for periods of 10 to 13 hours only, a reduction time found sufficient for nickel. On admission of about 1 Torr CO pressure a very weak absorption was observed having its maximum at $2169 \pm 1 \text{ cm}^{-1}$. This was classified as band B and appeared within a few minutes of admitting CO. However, no other absorptions were observed, even after allowing the system to stand at room temperatures for 1 hr. Evacuation for a period of 10 min. caused band B to disappear completely. Clearly the adsorbed CO species giving rise to B was very weakly held onto the metal surface. The very high frequency of this band (greater than that for free CO) is also indicative of a weakly held surface species.

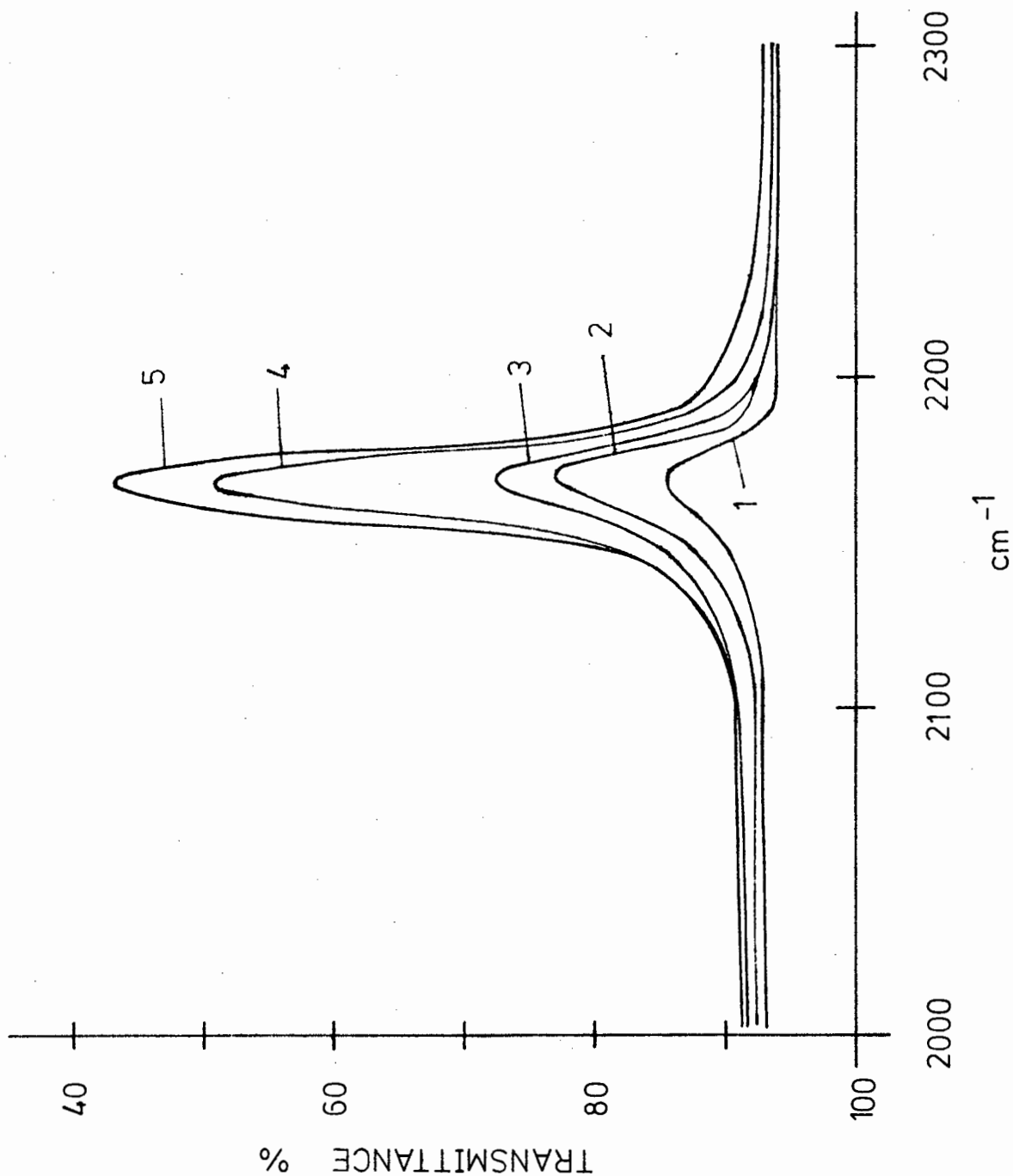
The experiment was repeated several times, often using fresh samples, and the effect of varying the CO pressure was studied. Band B was found to increase in intensity with pressure, and always disappeared completely on evacuation. Even with relatively high pressures, 40 to 50 Torr, no other absorptions were given. Figure 31 clearly shows the change in intensity with increasing pressure for band B. It is interesting to note that the higher reduction temperature, $\sim 450^{\circ}\text{C}$ as opposed to 400°C , appears to enhance catalytic activity with respect to band B, cf. plots 4 and 3.

By monitoring at a constant frequency of 2169 cm^{-1} during the heating programme, band B was observed to decrease in intensity over the temperature range 25 to 185°C . A full spectrum recorded at 185°C showed that B had almost disappeared. This decrease in intensity was not accompanied by a band shift to lower frequencies. On cooling back to room temperatures B reappeared. Furthermore, by allowing the system to stand overnight at room temperatures when at a CO pressure of 22 Torr, band B remained unchanged and still no other absorptions were observed. Thus the weakly held CO species appeared to be temperature and pressure dependent only.

(b)

Sample discs were then reduced for longer periods, 20 - 24 hr. at temperatures of about 450°C , and then subjected to between 40 and 45 Torr pressures of CO. The spectrum was recorded over the range 2300 to 1730 cm^{-1} after allowing the system to stand at room temperatures for $\frac{1}{2}$ hr., and then again after a further 2 hr. This was followed by an evacuation period of 10 min. The system was then

FIGURE 31. Effect of CO pressure on band B at 2169 cm^{-1} for CO on Fe/Cu/SiO_2 : (1) >1 Torr, (2) 5-6 Torr, (3) 19 Torr - reduced at 410°C ; (4) 20 Torr. (5) 46 Torr - reduced at 450°C .



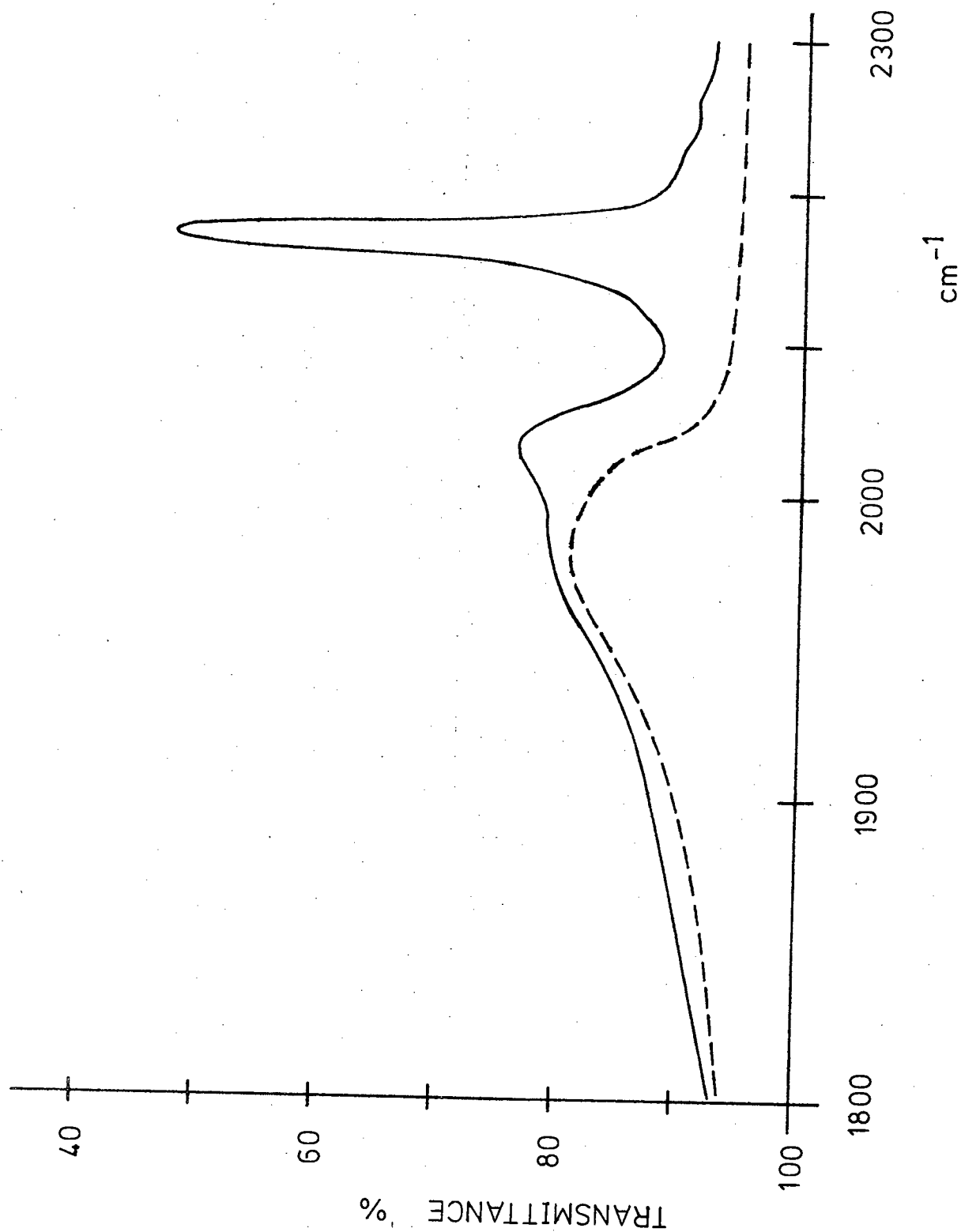
heated using the 'thermal programme' after being allowed to stand overnight at room temperatures.

The initial spectrum showed band B as a narrow band of medium intensity occurring as before, (a), at 2169 cm^{-1} . This was accompanied by a very broad but weak band having its maximum in the range 2030 to 2040 cm^{-1} . This latter absorption was classified as band A and is shown in Figure 32. In addition, band A showed a broad inflection at about 1980 cm^{-1} together with a low frequency tail. Band A increased slightly in intensity after the longer standing period. The effect of evacuation was to cause B to disappear as before, and A to shift to lower frequencies after which its maximum was then found in the region 1970 to 1980 cm^{-1} . Also a decrease in intensity was observed but the band still retained its broad appearance, see Figure 32.

These results clearly demonstrated the necessity for longer reduction times, and experience showed that $20 - 24\text{ hr.}$ was an ideal reduction period, as no appreciable improvement in the appearance of A was shown by discs reduced for both longer and shorter times. The problem of ageing and/or sintering had also to be considered. Thus it was necessary to find a balance between (i) attempts at increasing the sample's catalytic activity, which usually involved the use of increasingly severe reduction conditions; and (ii) ensuring that the ageing/sintering effect be kept at a minimum.

No further change in the appearance of band A was observed after the overnight standing period. Therefore this band was monitored at 1980 cm^{-1} as the system was heated. A gradual decrease in intensity

FIGURE 32. Effect of evacuation on the spectrum for CO (41 Torr) adsorbed on Fe/Cu/SiO₂ reduced for >20 hr. at 450°C : (—) before evacuation; (---) after evacuation.



was shown to start within the temperature range 100 to 140°C. Unfortunately, at temperatures > 200°C the 'background' shift, similar to that found with nickel catalysts, masked any further observations. However, it was clear that at 200°C, band A had only decreased by about half its original intensity. On one occasion the system was allowed to cool after heating to see if band A reappeared, but this was not so - a result contrary to that given by nickel.

Regretably type F2 catalysts lost their 'activity' very rapidly, and this limitation together with band A's very broad appearance made further work unsatisfactory.

(c)

An F1 sample disc, reduced for 6 hr., was treated with 12 Torr CO at room temperatures. Only band B was given at 2169 cm^{-1} as a very weak absorption, which disappeared on evacuation. The sample's inactivity was obviously in part due to the short reduction time. For some reason the sample failed to transmit at frequencies below 2000 cm^{-1} . On repeating the experiment with a freshly prepared sample the same limitation occurred. Both sample discs had a mottled appearance prior to their reduction.

(d)

A few discs were prepared directly from the powders, catalyst type FeIII and IV containing 5 and $2\frac{1}{2}$ wt. % iron respectively. Only powders prepared from the acetate/alcohol mixture gave firm discs, suitable and thin enough for reduction. However, these samples were found to be opaque over the entire range of interest. Different reduction times, between 6 and 24 hr., still failed to produce transparent discs.

4.3 THE REACTIONS OF CO AND H₂ ON SILICA SUPPORTED COBALT CATALYSTS.

Cobalt catalysts were found to be less 'active' than nickel but more 'active' than iron with respect to the interaction of chemisorbed CO and H₂ to give hydrocarbons. This corresponds with the ease of reducibility of cobalt oxide¹⁰⁷ in relation to the other two metal oxides. It has been found that at 350°C cobalt oxide had a P_{H_2O}/P_{H_2} value midway between values calculated for nickel and iron oxides¹⁰⁷. Despite cobalt's relative inactivity (more noticeable in the *in situ* experiments) some very interesting spectra were obtained which led to a possible interpretation on the type of chemisorbed species prevalent on cobalt under different experimental conditions.

4.3.1 Reactor experiments - Cobalt:

The four procedures; CO - H₂ - ΔH, CO/H₂ - ΔH, H₂ - CO - ΔH, and CO - ΔH, were applied in turn to the cobalt catalysts type CoI. As usual spectra were scanned over the frequency range 4000 to 1000 cm⁻¹ before and after the reactant gases were admitted at room temperatures, and also when the reactor had reached 400°C. During the heating programme the methane Q branch was always monitored at 3017,5 cm⁻¹. The results are given below for CoI type catalysts containing 5 wt.% Co:

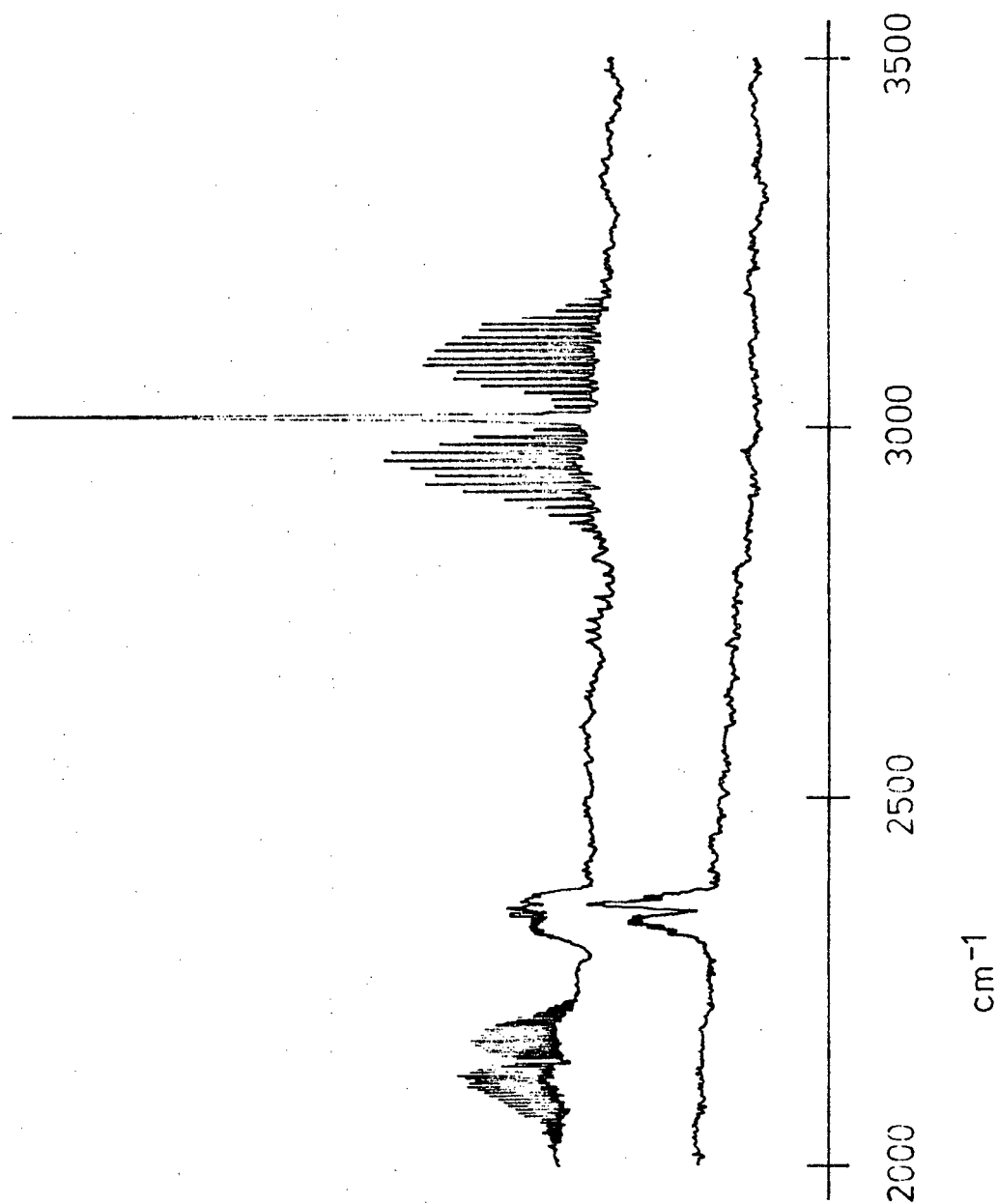
- (i) No carbonyls were detected by infrared at any stage throughout the four procedures described above.
- (ii) There was no apparent increase in intensity of the H₂O_{vap.} bands at the end of each experiment over that given by a 'background' spectrum.

- (iii) The only product observed on applying the procedure CO - ΔH was carbon dioxide. This was observed by the increase in intensity of the CO₂ fundamental at 2345 cm⁻¹ after the heating programme, over that given by the 'background' spectrum. Furthermore, the amount of CO₂ formed was dependent on the 'age' of the sample. The fresher the sample the greater the amount of CO₂ given.

Occasionally traces of CO₂ were detected by infrared for the procedures CO - H₂ - ΔH and CO/H₂ - ΔH . For the latter this was contrary to that found for nickel.

- (iv) On heating the catalyst, methane was found to be the chief product for all experiments in which CO and H₂ were present. A considerable amount of methane was formed as shown in Figure 33 for the procedure CO - H₂ - ΔH . This compares well with that given by a nickel catalyst under the same conditions, see Figure 7. When the thermal programme was used, methane was first detected within the temperature range 195 to 215°C.
- (v) No other hydrocarbons, either saturated or unsaturated, were detected by infrared spectroscopy. However, trace amounts of ethane were detected by mass spectroscopy together with trace amounts of H₂O_{vap.} and CO₂. The fragmentation pattern is given in Figure 34. The fragmentation pattern of species given by a nickel catalyst can be seen in Figure 35. All mass spectroscopy results have been collated in Section 4.4.

FIGURE 33. Spectrum of products at 400°C from CO followed by H₂ adsorbed on Co/SiO₂, with background offset.



- (vi) The procedure 3.4 (1.7) in which a CO/H₂ mixture was admitted, with the catalyst at a fixed temperature, revealed that methane was produced, although in limited quantities, at temperatures well below 195°C. A plot of absorbance with temperature is shown in Figure 36, and represents the varying amounts of methane produced at given temperatures. This was obtained simply by monitoring the CH₄ Q branch at 3017,5 cm⁻¹ over a period of 2 hr. at five different temperatures. It can be seen from the figure that only trace amounts of methane would be formed at temperatures of 100 - 130°C, (370 - 400 K), and none below those temperatures.

4.3.2 In situ cell experiments - Cobalt:

Sample discs of catalyst type Cl, ~ 5 wt. % Co, were studied. These were prepared by the 'dip' method. Usually spectra were scanned over the frequency range 2300 to 1700 cm⁻¹ when the system was at room temperatures, and a given species was monitored at a constant wavenumber during the heating programme. The disappearance of an adsorbed species was observed by monitoring at either 2181 or 2020 cm⁻¹. These frequencies corresponded to bands designated B and A respectively. Cobalt's inactivity was shown by three factors:

- (i) The relatively high CO pressures (40 - 50 Torr) required to produce absorption bands of medium intensity; cf. nickel which required only 1 - 2 Torr CO pressures.
- (ii) A cobalt catalyst could only withstand one heating programme/degassing period before it was rendered inactive. A nickel catalyst could be heated frequently without showing any sign of ageing or loss in activity.

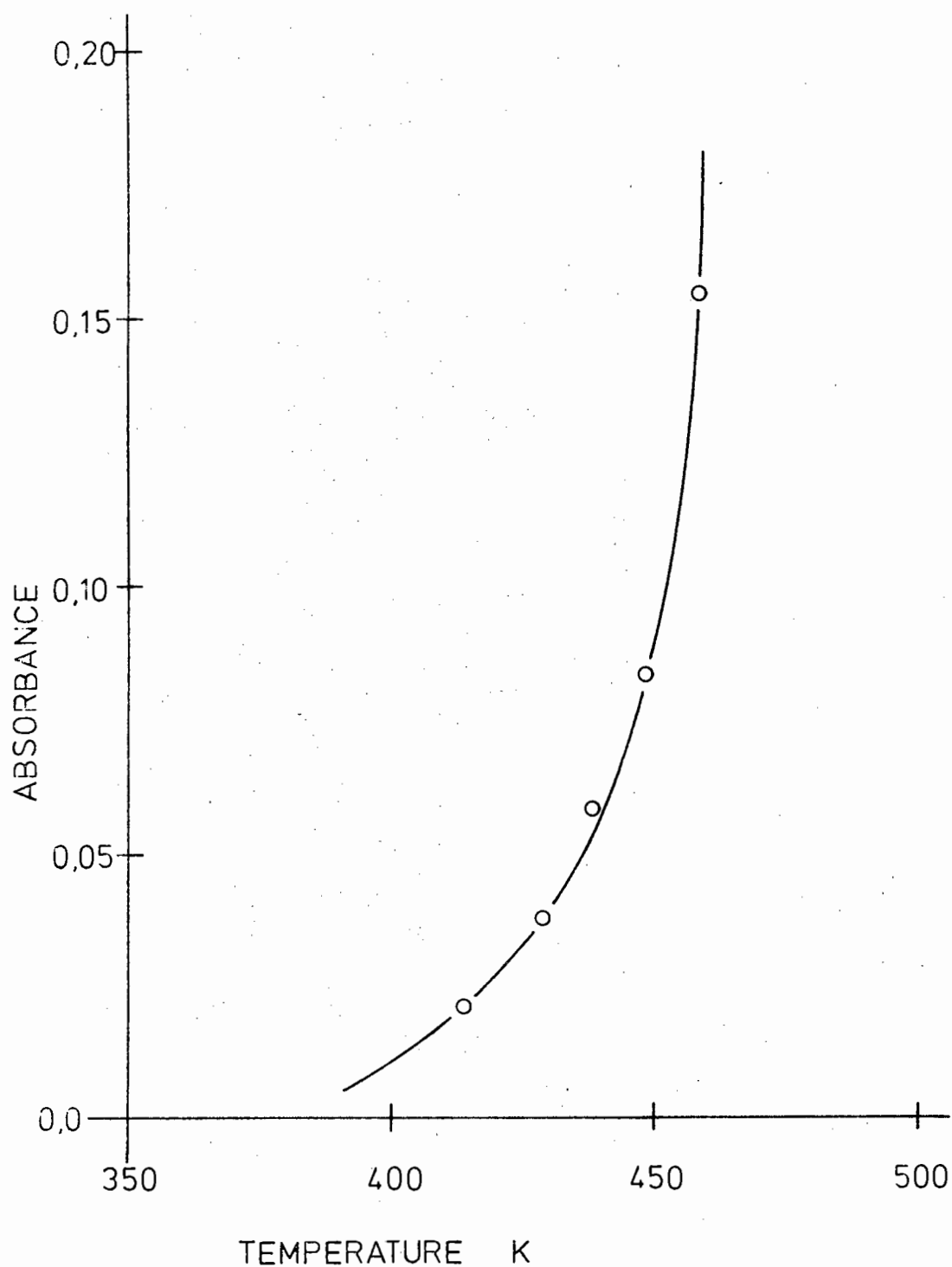


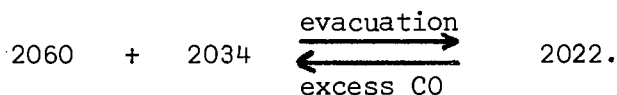
FIGURE 36. Plot of absorbance as a function of temperature at $3017,5 \text{ cm}^{-1}$ due to adsorbed CO and H_2 on Co/SiO_2 over a 2 hr. period.

(iii) Long reduction periods were necessary (20 - 24 hr.), cf. iron, Section 4.2.2 (b).

(a)

The spectrum of CO chemisorbed on cobalt at room temperatures is shown in Figure 37. A sharp narrow band at a frequency of $2181 \pm 1 \text{ cm}^{-1}$ was given together with a broad medium band having maxima within the frequency ranges $2062 - 55 \text{ cm}^{-1}$ and $2037 - 32 \text{ cm}^{-1}$. These two bands were assigned B and A respectively. A low frequency tail was also observed, which had a broad inflection at about 1900 cm^{-1} .

On evacuation (10 min.) band B almost disappeared and band A was shifted to lower frequencies accompanied by a change in its appearance. Band A now appeared as a narrower absorption having only one maximum (and not two) which occurred in the range $2027 - 20 \text{ cm}^{-1}$. There was also a slight increase in intensity, which was both unexpected and interesting. Bands attributed to CO in the gas phase had also disappeared. On addition of a further aliquot of CO at room temperatures the original spectrum was again observed, viz., band B at 2181 cm^{-1} and band A with two maxima at about 2060 and 2034 cm^{-1} . Consequently a reversible effect was shown to take place which can be represented, using approximate band positions, as follows:



On evacuation for longer periods (1 hr.) there was little further change in the appearance of band A. A slight decrease in intensity was observed, but no apparent frequency shift.

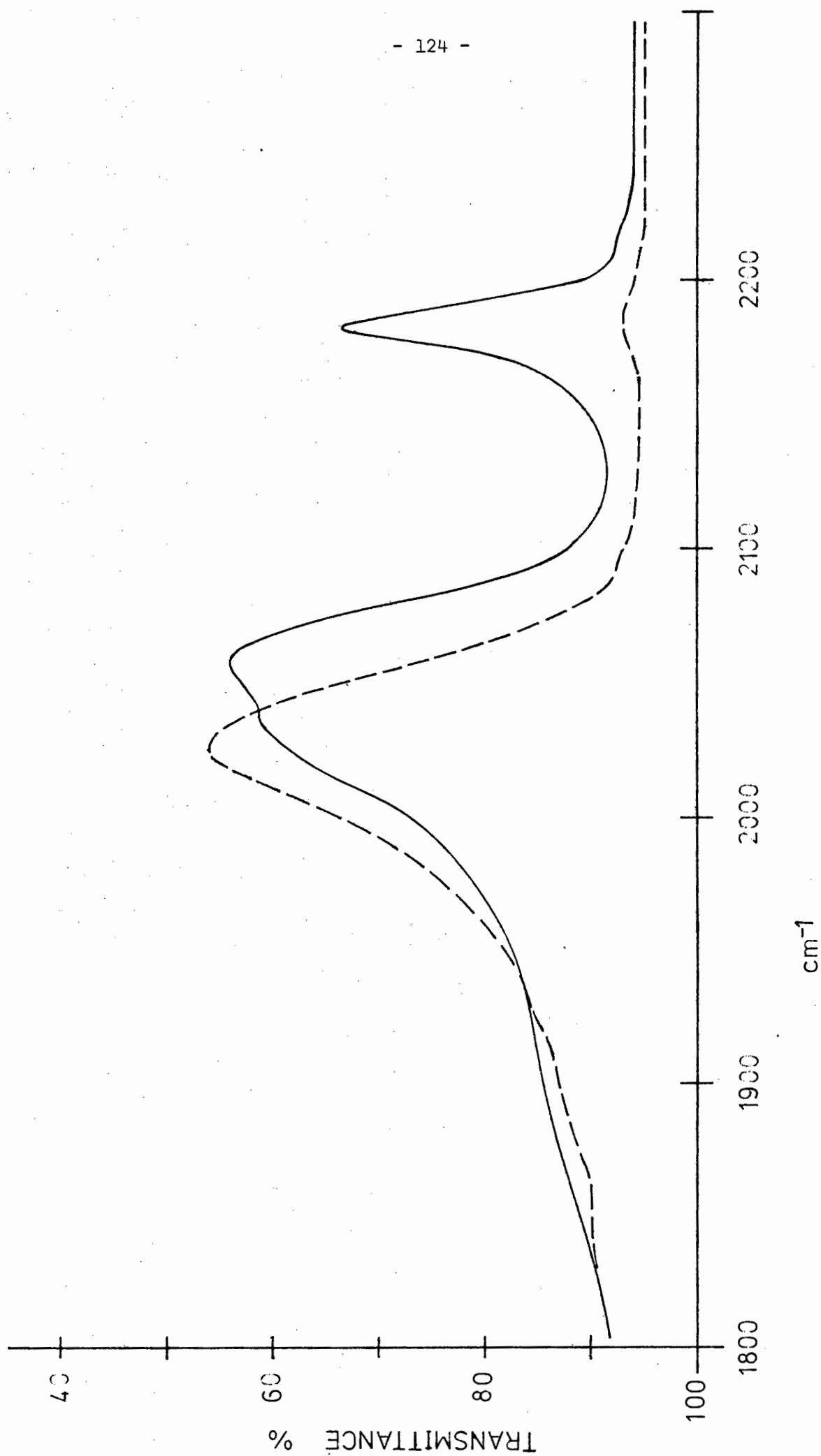


FIGURE 37. Effect of evacuation on the spectrum of CO adsorbed on Co/SiO₂ : (—) before evacuation; (---) after evacuation.

(b)

The procedure CO - evacuate - ΔH was then carried out and band A was monitored at 2020 cm^{-1} during the heating programme. A decrease in band intensity only occurred at temperatures between $115 - 125^{\circ}\text{C}$. This continued until temperatures of $280 - 290^{\circ}\text{C}$ were reached, by which time band A had completely disappeared. A plot of absorbance with temperature, Figure 38, showed A as decreasing linearly on increasing the temperature.

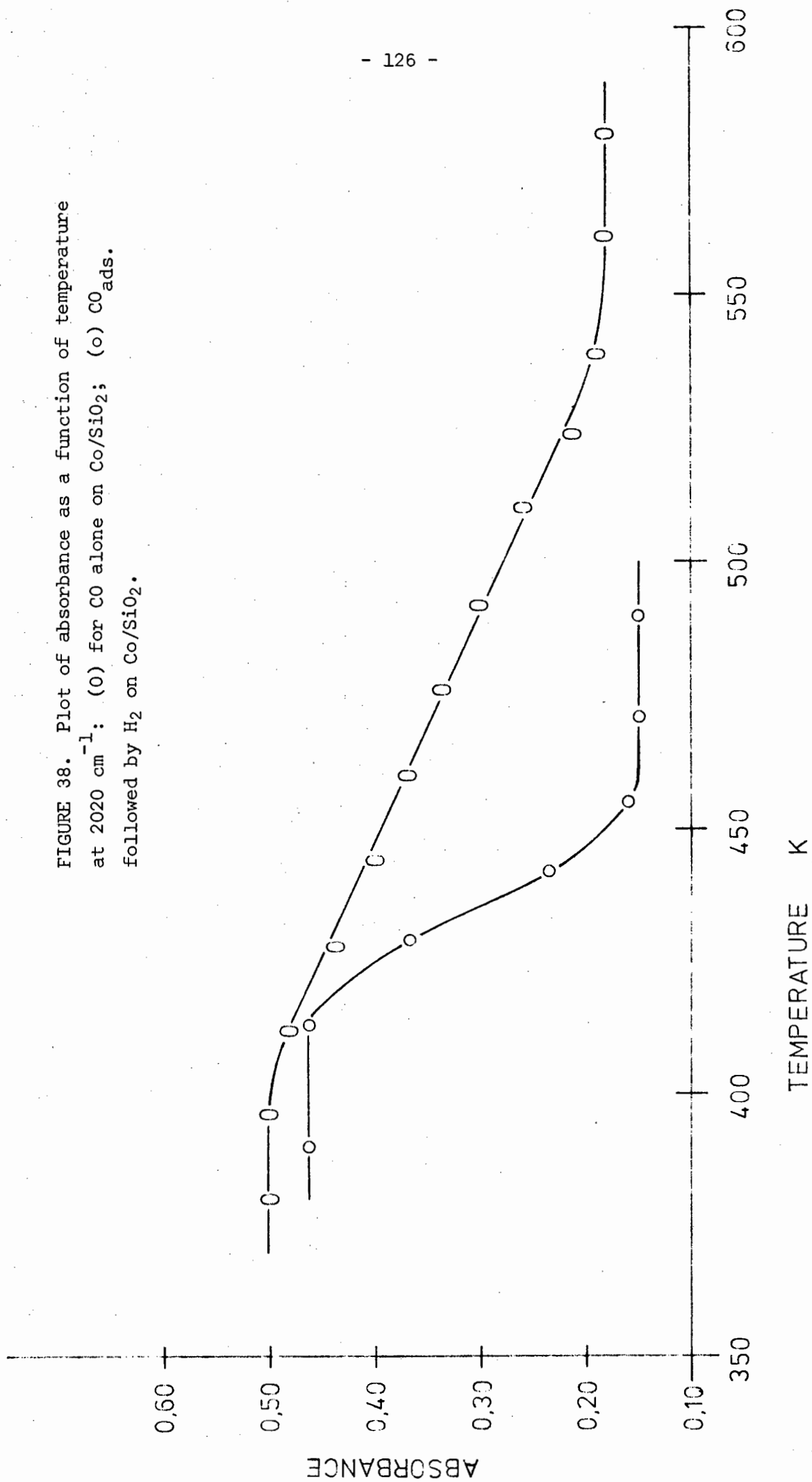
By monitoring at a frequency of 2181 cm^{-1} , while heating the catalyst in the presence of excess CO (50 Torr pressure), band B was observed to decrease in intensity, slowly at first, over the temperature range 25 to 180°C . Its disappearance was rapid at temperatures $> 70^{\circ}\text{C}$. Clearly the species giving rise to B were less firmly held on the surface than those responsible for band A.

(c)

The effect of varying the CO pressure on the spectra is shown in Figure 39. Band B was found to increase with pressure until a maximum was reached at about 55 Torr. Band A also increased with pressure, but this was accompanied by changes in shape which can be described as follows:

- (i) at low pressures, < 10 Torr, band A was broad with a table-top maximum centered about 2040 cm^{-1} ;
- (ii) at medium pressures, $10 - 30$ Torr, two maxima were observed of almost equal intensity at 2030 and $2055 - 50\text{ cm}^{-1}$;
- (iii) at higher pressures, > 30 Torr, the high frequency maximum predominated at 2060 cm^{-1} , and the low frequency maximum appeared almost as a shoulder at 2034 cm^{-1} .

FIGURE 38. Plot of absorbance as a function of temperature at 2020 cm^{-1} : (O) for CO alone on Co/SiO₂; (o) CO_{ads} followed by H₂ on Co/SiO₂.



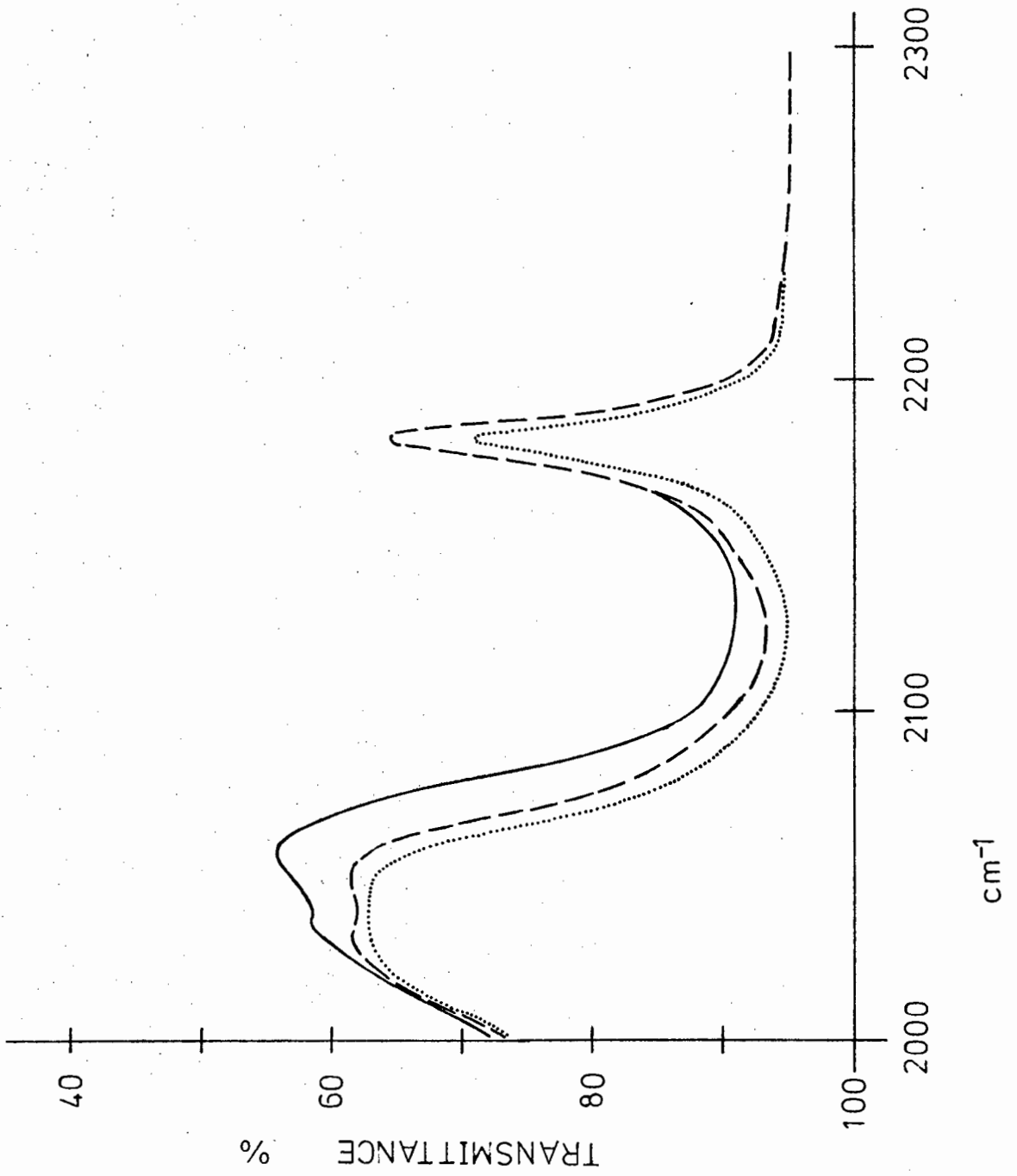


FIGURE 39. Effect on the spectra on varying CO pressure:
(.....) <10 Torr; (---) 10 - 30 Torr; (—) >30 Torr.

(d)

The addition of hydrogen to the system was investigated at both room and elevated temperatures. Firstly, H_2 was added to the system in which CO had previously been admitted, allowed to remain in contact with the catalyst and then evacuated for 10 min. The effect of H_2 on band A at 2022 cm^{-1} is clearly shown in Figure 40. (All three spectra are shown in the Figure for comparison, i.e. CO alone before and after evacuation, and $CO_{ads.}$ plus H_2 .) Hence the addition of H_2 caused band A to decrease in intensity and exhibit a high frequency hump. Only on one occasion did band A shift to higher frequencies by about 6 cm^{-1} . For reasons unknown, this band frequency shift could not be reproduced. At this stage the system comprised essentially of $CO_{ads.}$ with an excess of H_2 . On heating, during which band A was monitored at 2020 cm^{-1} , a decrease in intensity first occurred within the temperature range $125 - 140^\circ\text{C}$. The intensity decreased rapidly until temperatures of $195 - 215^\circ\text{C}$ were reached, by which time band A had disappeared. This effect is shown by the second plot in Figure 38, and can be compared with the system in which no hydrogen was added. Clearly the presence of hydrogen does affect the rate of disappearance of band A at elevated temperatures. However, it must be remembered that the observed temperature of $125 - 140^\circ\text{C}$ was much lower than that normally associated with methane formation ($>195^\circ\text{C}$ - reactor experiments) when using the 'thermal programme'.

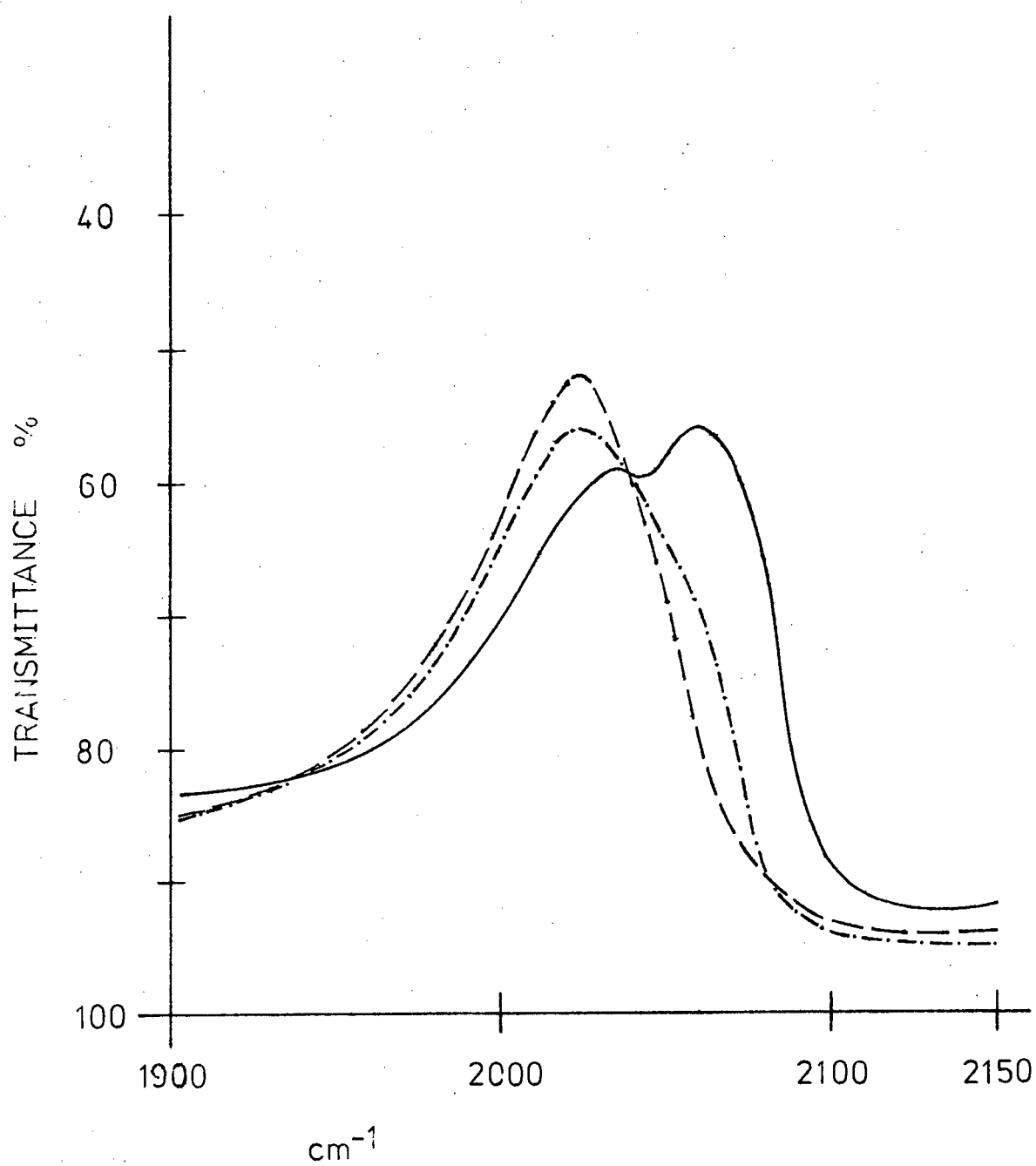
The order of addition of reactant gases was varied to investigate the effect, if any, on the spectrum of CO on cobalt. For both CO and H_2 pretreatments there was no apparent change in the spectrum,

FIGURE 40. Effect of H_2 on band A for CO on Co/SiO_2 :

(—) CO alone before evacuation;

(---) CO alone after evacuation;

(—•) on addition of H_2 .



except a slight overall increase in intensity for the experiment which involved CO pretreatment, followed by H₂. Similarly on H₂ pretreatment followed by an evacuation period prior to the admission of CO, the spectrum of CO chemisorbed on cobalt resembled that given in Figure 37, i.e. no change was observed.

(e)

Signs of ageing and/or sintering of the sample disc were clearly shown in an experiment which involved the admission of CO after pretreatment with H₂. The CO spectrum is given in Figure 41. Band B was found to occur as before at 2181 cm⁻¹, but band A was observed as a very broad weak band with a maximum in the region 2020 to 2025 cm⁻¹ and a shoulder at about 2050 cm⁻¹. On evacuation a frequency shift was observed in which band A then narrowed and showed a single maximum at 2000 cm⁻¹.

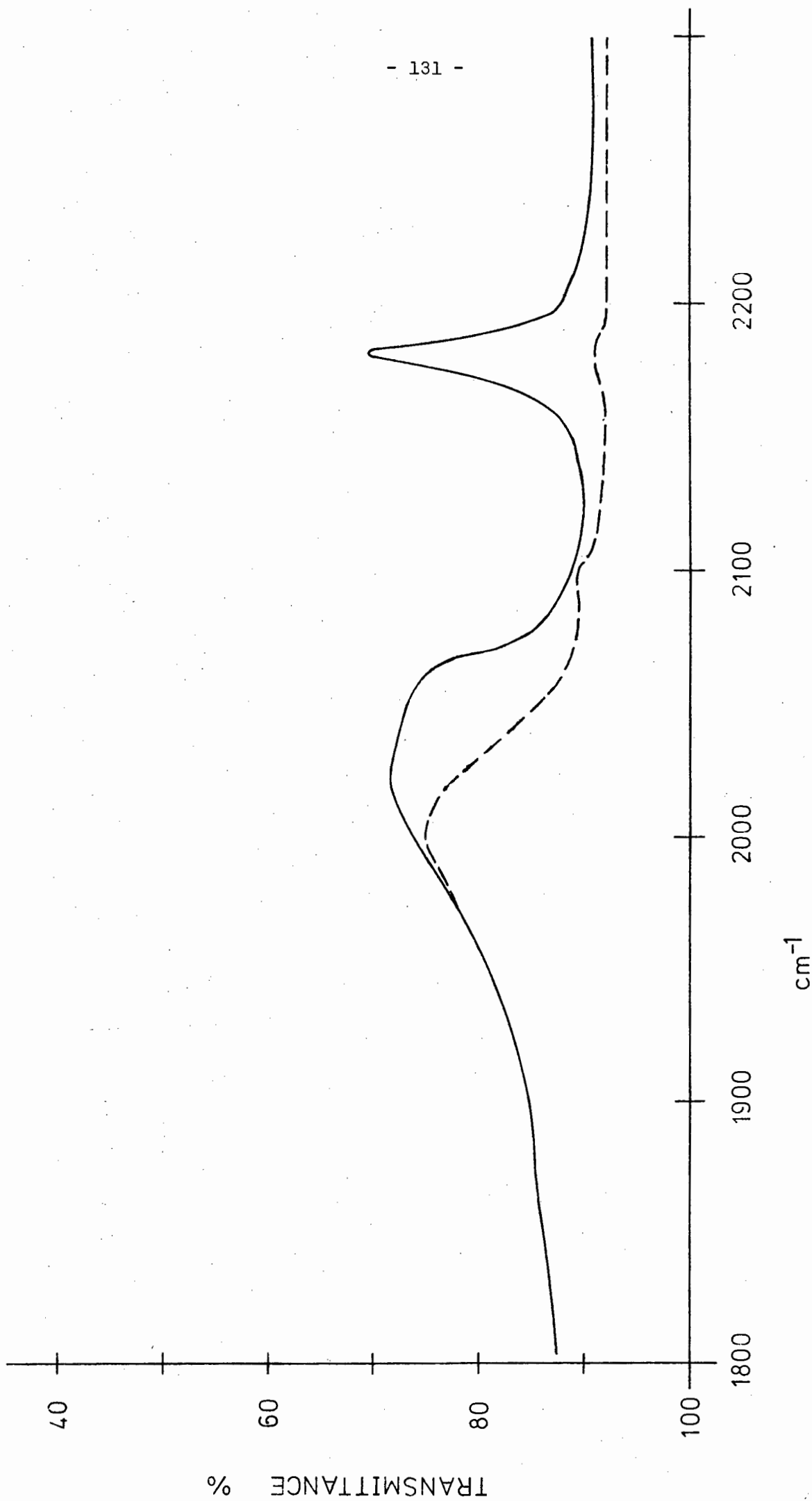


FIGURE 41. Spectra of CO adsorbed on an aged/sintered Co/SiO₂ disc after pretreatment with H₂; and (---) after evacuation.

4.4 MASS SPECTROSCOPY RESULTS

Occasionally it was necessary to analyse the reactants and products which occurred in the gas phase (obtained from the reactor experiments) by mass spectroscopy in order to detect trace amounts of hydrocarbons other than methane, formed from the interaction of CO and H₂ on some of the metal catalysts. Thus the following procedure was adopted: after recording the final infrared spectrum over the frequency range 4000 to 1000 cm⁻¹, when the reactor had reached 400°C, the 10 cm path length infrared gas cell was isolated from the system, removed, and its contents were then analysed using mass spectroscopy.

The products given by the various catalysts, Fe, Co, and Ni, after carrying out the procedure CO - H₂ - ΔH, were analysed in this way for comparison purposes, and their fragmentation patterns are shown in Figures 30, 34, and 35 respectively. The mass to charge ratio (m/e) and the relative abundance of each ion (R.A.%) together with the group commonly associated with the mass are given in Table 6. The most abundant ion, referred to as the base peak, in the spectrum was arbitrarily assigned as 100%.

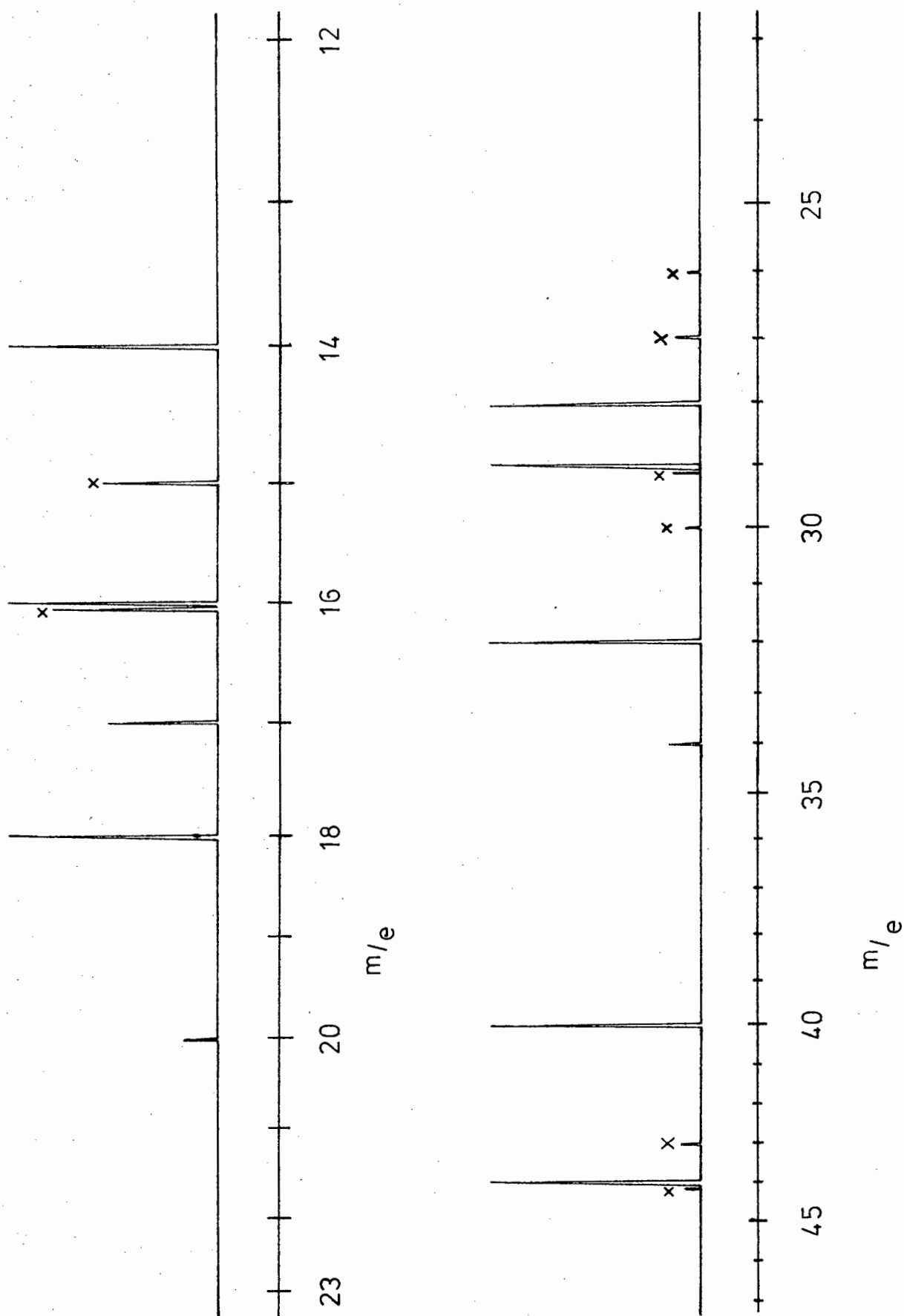


FIGURE 30. Fragmentation pattern of products, at 400°C, from CO H₂ adsorbed on Fe/Cu/SiO₂; (X) signifies a sample peak, other peaks are background.

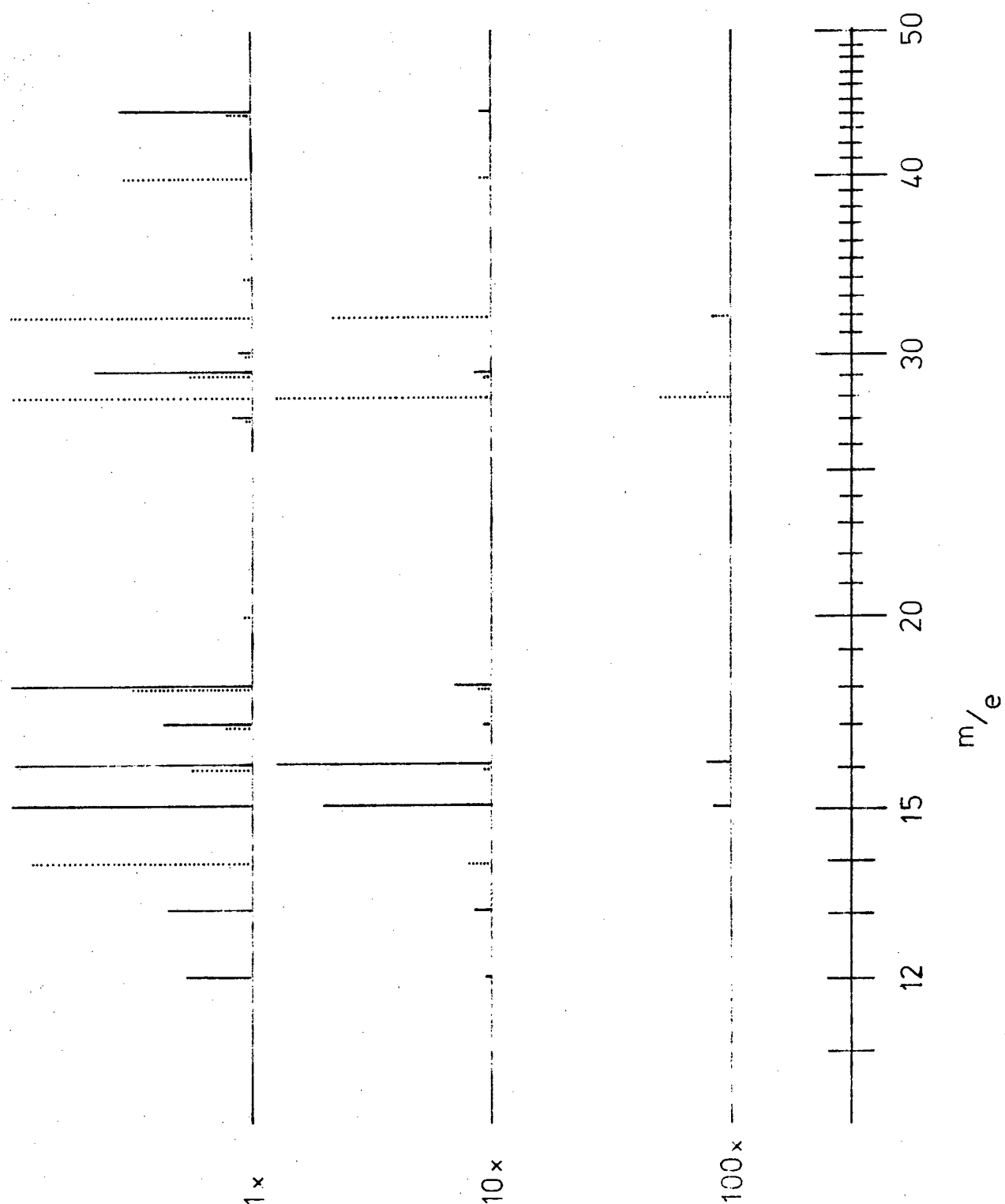


FIGURE 34. Fragmentation pattern of products, at 400°C, from CO and H₂ adsorbed on Co/SiO₂; (—) sample peaks, (.....) background.

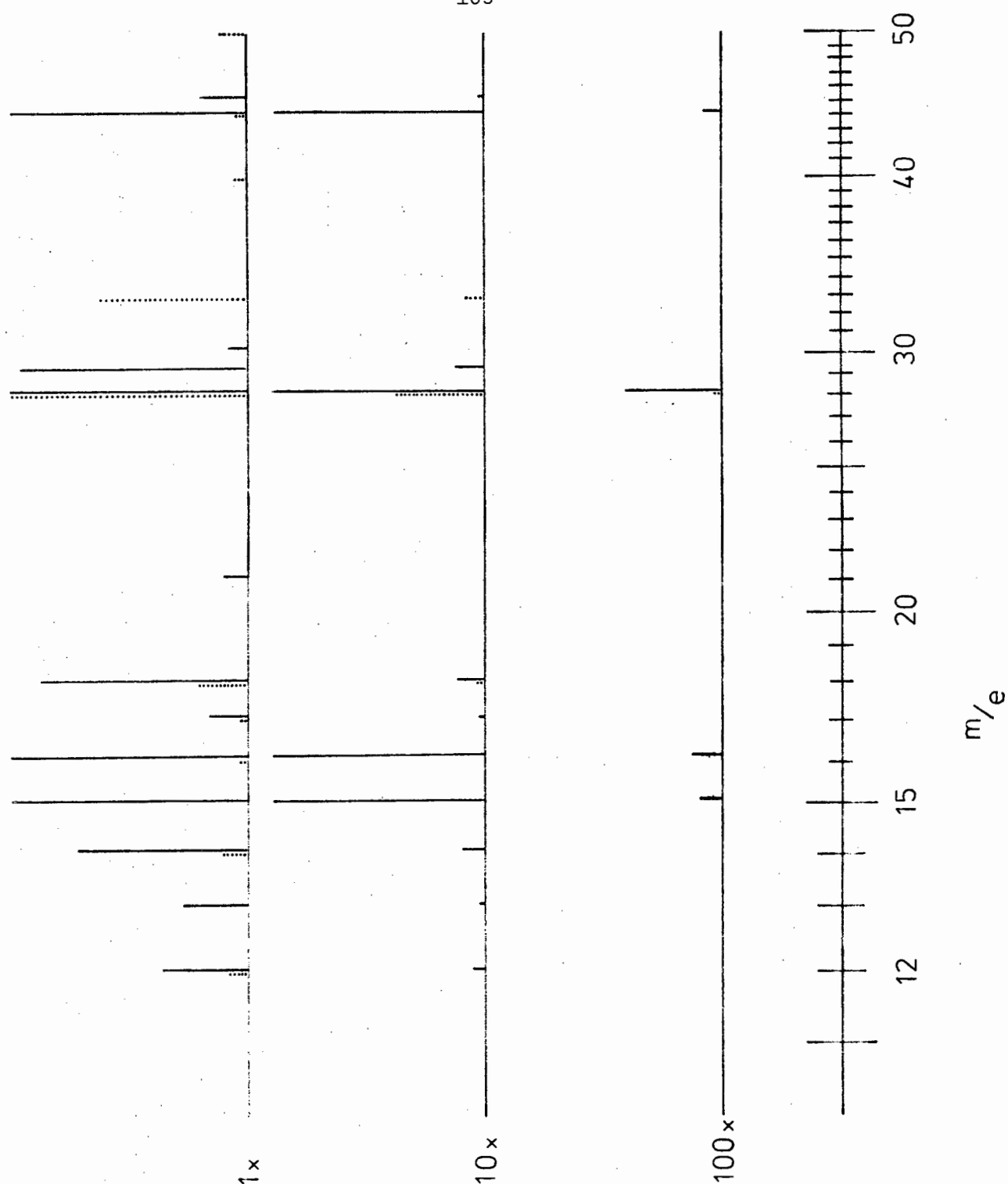


FIGURE 35. Fragmentation pattern of products, at 400°C, from CO and H₂ adsorbed on Ni/SiO₂; (—) sample peaks, (.....) background.

TABLE 6

Groups commonly associated with the Mass	m/e	Relative Abundance R.A. %		
		Iron, FeII	Cobalt, CoI	Nickel NiI
CH^+	13		8	3
CH_3^+	15	69	78	81
CH_4^+	16	100	100	100
OH^+	17		3	2
H_2O^+	18		17	8
C_2H_2^+	26	7		
C_2H_3^+	27	14	1	
C_2H_5^+	29	17	7	9
C_2H_6^+	30	9	<1	<1
C_3H_7^+	43	10		
C_3H_8^+	44	9		
CO_2^+	44		6	60

The table shows that:

1. odd electron ions, i.e., those ions which contain an unpaired electron and include molecular ions (M^+) and fragment ions (A^+) formed from M^+ by loss of an even-electron molecule. For example, C_2H_6^+ is a molecular ion and C_2H_2^+ a fragment ion formed from it;
2. the hydrocarbon ion series in which the values m/e 15, 29, and 43 correspond to the precursor ions CH_3^+ , C_2H_5^+ and C_3H_7^+ respectively;

3. from these precursor ions decomposition products can occur, of moderate abundance, according to the ion series $C_n H_{2n-1}^+$. These would be found at m/e 13, 27 and 41 which correspond to the ions CH^+ , $C_2H_3^+$ and $C_3H_5^+$ respectively. The ion $C_3H_5^+$ was not detected even from the fragmentation pattern produced by the iron catalyst probably because the amount of propane formed was too low;
4. the base peak in all cases was found to be the molecular ion CH_4^+ (m/e 16).

The table also shows that, from the interaction of CO and H_2 on various catalysts previously subjected to the procedure

CO - H_2 - ΔH :

1. the iron catalyst produced a methane/ethane/propane mixture in quantities where methane > ethane > propane;
2. cobalt and nickel catalysts gave methane as the chief product with only very small amounts of ethane. Propane was not detected with these two catalysts;
3. the amounts of ethane formed when using cobalt and nickel were lower than that formed from iron;
4. nickel produced relatively large amounts of CO_2 in the reaction, (see result 4.1 (1.1)). Only trace amounts of CO_2 were detected for cobalt;
5. small amounts of water vapour were detected for both nickel and cobalt catalysts.

CHAPTER 5

DISCUSSION OF RESULTS AND CONCLUSIONS

5.1 INTRODUCTION:

Infrared spectra of carbon monoxide, either chemisorbed onto metal surfaces or as metal carbonyl compounds, give intense absorption bands in the region 2200 to 1700 cm^{-1} . The frequency of 2000 cm^{-1} has often been used as the dividing line for distinguishing between linear and bridging CO groups, although under certain conditions linear CO can give rise to bands below 2000 cm^{-1} . This occurrence was explained in Section 2.2, together with an argument for and against the existence of bridged CO structures chemisorbed on metals, and their giving rise to bands in the infrared below 2000 cm^{-1} .

In this work, infrared absorption bands found below 2000 cm^{-1} were usually assigned to bridging carbonyl species. This decision was based on the substantial evidence given by infrared, magnetic data, LEED, and secondary ion mass spectrometry. The infrared studies of CO on alloys by Soma-Noto and Sachtler^{84,89,90} were particularly convincing on this issue. In support of this decision, for nickel catalysts, CO bands given below 2000 cm^{-1} did not readily disappear on evacuation or heating. In contrast, bands above 2000 cm^{-1} were more sensitive under these conditions. The results given in Section 4.1.2(2) demonstrate this, and are in accordance with the 'bridging' theory.

The classification of CO absorption bands for CO on nickel

catalysts, i.e., bands A to F, was based according to the assignment of Yates and Garland on nickel⁹⁷. Similarly, for CO on iron and cobalt, classification was made according to the frequency position of significant absorptions, where band A was assigned to that absorption which occurred at the lowest frequency. This did not necessarily mean that band A should be assigned to a bridged structure, as was the case for nickel. The classification scheme excluded absorptions which appeared either as shoulders or inflection points.

With carbon monoxide chemisorbed onto any metal of the transition series, the multiplicity of the band structure found at frequencies above 2000 cm^{-1} has been ascribed to single linear species on different crystalline sites^{115,97,83,27}. A molecular orbital description of the metal to CO bond was proposed by Blyholder⁸³, which was similar to that given for metal carbonyls¹⁶⁸. It was proposed that the M - C bond is comprised of a dative σ bond and a dative π bond. The net effect is that a charge shift occurs in opposite directions, which would strengthen each other mutually. The metal to carbon π bond, which involves the sharing of electrons between a filled $d\pi$ or hybrid $dp\pi$ metal orbital and an empty $p\pi^*$ orbital of CO, tends to weaken the carbon to oxygen bond, but strongly influences the chromophore relative to the σ bond formed between a filled carbon p-orbital and an empty metal d-orbital. Thus, formation of the σ bond originates from the lone pair of electrons of the carbon sp_z - hybrid orbital with suitable acceptor d orbitals on the metal atom. The π bond orders of adjacent M - C and C - O bonds, in M - CO surface species,

were thought to be complimentary.

As the π character of the metal to carbon bond increases, the bond order of the carbon to oxygen bond decreases because this results in a lowering of the CO bond strength and hence its stretching frequency. Therefore, CO chemisorbed onto metal sites rich in d- electron density, i.e., edges, corners, or sites in crystallographic planes of low coordination number, was considered to form a stronger metal to carbon bond, and therefore give rise to bands at lower frequencies than when chemisorbed onto sites of high coordination number. In addition, Blyholder⁸³ proposed that if the σ bond between the metal and carbon atoms remained constant then the increase in frequency of the carbonyl would result from a lesser number of d- electrons participating in the M - C bonding.

Guerra⁸⁶, however, in a recent study of collective data on the adsorption of CO by transition metals, obtained results showing an opposite trend, i.e., a decrease was observed in the CO frequency with a decrease in the number of metal d- electrons. The results referred to the chief absorption found above 2000 cm^{-1} , which could be assigned to chemisorbed species having a linear structure. It appeared that an increase in the metal to carbon bond strength resulted mainly from increased M - C σ bonding, which was promoted by emptier metal d orbitals. For charge neutrality, it was suggested that this increased M - C σ bonding would then cause greater M - C π bonding, as shown by an observed decrease in the C - O bonding and vibrational frequency when there were fewer d- electrons available in the metal orbitals. Furthermore, the estimated bond orders of the C - O bond, of

adsorbed CO, were shown to decrease in a manner proportional to the number of missing d- electrons of the metal across the series.

CNDO - molecular orbital calculations, for both carbon monoxide¹⁶⁹ and hydrogen¹⁷⁰ adsorbed on a cluster of nickel atoms, suggested that bonding of the carbon or hydrogen atoms to the nickel atom largely involved the nickel s and p orbitals with little contribution arising from the d orbitals. The calculated pattern of valence orbital energy levels agreed well with experimental results, using photoelectron spectroscopy, which allowed the energies obtained to be assigned to specific orbitals. However, the fact that metal d orbitals were considered to play a minor role was contradictory to the theory also proposed by Blyholder⁸³.

From a study¹³² of the oxygen (1s) binding energies with respect to the Fermi level, ($BE_{(F)}$), in the non-dissociative adsorption of CO on metals, it was again suggested that π bonding (back donation) was the major contribution to the M - CO bond. Results showed that as the enthalpy increased (M - C bond strength increasing) the $BE_{(F)}$ decreased, which indicated that the electron density on the oxygen was increasing. Furthermore, when the energy of the M - CO bond increased, so did the electron transfer from the metal to CO, i.e., there was enhanced back bonding into the 2π molecular orbital of CO. The σ contribution, which would cause a chemical shift in the opposite direction, was considered to be less important. There was no evidence for the operation of the synergic effect¹²⁰.

The controversy over whether π or σ bonding is the main

contribution to the M - CO bond (although evidence does favour the former) presents an interesting 'question-mark' on the interpretation of the multiplicity of infrared bands, usually found above 2000 cm^{-1} . CO chemisorbed on sites of low coordination number may well give bands at lower frequencies, but to what degree this shift is caused solely by increased π back bonding appears to be open to conjecture.

5.2 NICKEL CATALYSTS:

It has been shown in this work that, when either CO alone or CO followed by H₂ was allowed to contact the nickel surface, there occurred two main bands in the range above 2000 cm⁻¹, viz., bands at 2080 and 2055 cm⁻¹, (result 4.1(2.1), Figure 14). The band at 2055 cm⁻¹ (band C) did not occur when H₂ was admitted first, or even when a CO/H₂ mixture was used, Figure 15. Nor under these conditions was Ni(CO)₄ observed to form, (results 4.1 (1.2 and 1.3)). It was also observed that band C readily disappeared on evacuation or heating, (result 4.1 (2.1), Figures 19 and 22). Thus, it was concluded that band C must have been due to a species which was less firmly bound than was the species which gave rise to band B at 2080 cm⁻¹. It also seemed likely that band C was involved in gaseous Ni(CO)₄ formation. The fact that the species producing this band was less firmly held than B, at 2080 cm⁻¹, was contrary to the usual sequence of strongly held - lower frequency; indicative that the species which gave rise to band C was, not merely CO adsorbed, but, possibly due to either several CO groups attached to a single metal atom or adsorbed Ni(CO)₄. This was in agreement with Ferreira²⁷ who assigned a strong sharp band at 2058 cm⁻¹, (± 2 cm⁻¹), to either two, three, or even four ligands chemisorbed onto single nickel atoms. In addition, he suggested that it was possible that at least part of this band may have been due to physically adsorbed Ni(CO)₄, with the major contribution being due to more than one weakly chemisorbed CO molecule per metal site. Nevertheless, there are major differences between the two sets of results. Whereas the 2058 cm⁻¹ band was only observed²⁷ at high CO pressures, and usually after the

appearance of other bands, band C at 2055 cm^{-1} was strong even at pressures <1 Torr and appeared almost immediately the CO was brought into contact with the catalyst. Also, over and above the results of Ferreira²⁷, the reactor experiments clearly demonstrated that Ni(CO)_4 was formed rapidly at room temperatures. The readiness of Ni(CO)_4 formation in CO - Ni systems is obviously more acute than was originally considered^{27,109}. Preadsorption of hydrogen, prior to the admission of CO, must therefore either block specific sites on which adsorbed Ni(CO)_4 and/or its precursors can be held, or become co-adsorbed with CO on admission of the latter, thus preventing Ni(CO)_4 formation.

Coadsorption is the preferred explanation. This is supported by the observed frequency shift of band B to lower wavenumbers on evacuation at room temperatures, (result 4.1 (2.2)). Apart from the disappearance of band C, band B decreased in intensity only slightly on evacuation, the main effect was that of the band shift to lower frequencies. The cobalt results also support this hypothesis (see Section 5.4), and led to the following conclusion for CO on nickel, which can be stated:

"that band B, found at either 2080 cm^{-1} (on CO preadsorption) or at 2074 cm^{-1} (on H_2 preadsorption, or on treatment with a CO/ H_2 mixture), can be ascribed to co-adsorbed species having the structures Ni(CO)_X and $\text{H}_Z\text{Ni(CO)}_Y$ respectively, where $4 > X > Y > 1$, and $Z \geq 1$."

The above conclusion was reached for the following reasons:

(i) Coadsorption of H and CO, or adsorption of more than one CO per single nickel atom, would cause a decrease in the M - C bond order, which in turn would increase the C - O bond strength and hence increase the CO frequency.

(ii) The lower frequency of 2074 cm^{-1} can be explained in terms of an uneven distribution in π back-bonding between the M - H and M - C bonds, where back donation of the nickel d- electrons favour the antibonding CO orbitals over those of hydrogen. The fact that hydrogen is less strongly adsorbed onto metals than is CO has been well established. For example, gravimetric studies¹⁷¹ of CO adsorbed on supported palladium showed that preadsorbed hydrogen was replaced by CO according to the equation : $\text{PdH} + \text{CO}_{(\text{g})} \rightarrow \text{PdCO} + \text{H}_{(\text{g})}$.

(iii) Coadsorption of hydrogen was observed by Primet and Sheppard¹²⁹. The higher frequency at 2070 cm^{-1} for the νCO band over that of 2040 cm^{-1} , given by CO on a "hydrogen-covered" surface as opposed to a "hydrogen-free" surface, suggested that the hydrogen was electron-attracting. The shift of the d- electrons of nickel to adsorbed hydrogen, revealed by ferromagnetic results¹⁷², implied that the polarity of M - H bonds was of the type $\text{M}^{\delta+} - \text{H}^{\delta-}$. The readsorption of H_2 , which displaced the 2040 cm^{-1} band (observed after evacuation for 30 min. at 100°C) to near 2070 cm^{-1} , corresponded to the effect found on cobalt (discussed in Section 5.4, p. 162), viz., a high frequency hump. The effect on cobalt was less marked, probably due to slight differences in experimental conditions and also cobalt's inability to coadsorb H_2 with CO over that of nickel.

(iv) The observed band shifts to lower frequencies on evacuation, Figures 19 and 20, result 4.1 (2.2), suggest in both cases a return, in part, to the structure Ni - CO. It cannot be stated categorically whether the further shift to even lower frequencies on heating, (result 4.1 (2.2.)), arises either from a redistribution of adsorption sites, or from the complete conversion of the CO : metal ratio to a value of 1 from that of >1 .

The above, (i) to (iv), suggests that band C, at 2055 cm^{-1} , is chiefly due to adsorbed $\text{Ni}(\text{CO})_4$, which is in accordance with the properties of a band found at the same frequency, by Primet and Sheppard¹²⁹, for CO adsorbed on a "bare" or "hydrogen-free" nickel surface. Alternatively, it can be argued that the multiplicity of bands found at frequencies above 2000 cm^{-1} , and the absence of band C at 2055 cm^{-1} on pretreatment with hydrogen, could be attributed to the nature of the adsorption sites according to the interpretation by Garland *et al*¹¹⁵. However, reasons for rejecting this hypothesis will be covered in Section 5.4.

An interesting result was observed after a heating/cooling procedure or after admission of CO to an already heated catalyst followed by cooling; result 4.1 (2.3), Figures 23 - 26. Here only one band was seen to occur in the range above 2000 cm^{-1} . This came close to 2050 cm^{-1} , Figure 24, but its properties were different from those of the original band C at 2055 cm^{-1} . Namely, it was not easily removed by evacuation or on heating, but instead its frequency merely decreased systematically with increasing temperature, with a much smaller rate of decrease in intensity than shown by band C. The heating/cooling experiments can be interpreted, in part, in terms of CO being adsorbed at

room temperatures only on sites of low heat of adsorption and low activation energy. At higher temperatures, sites of high heat of adsorption and high activation energy become available, and thus the band frequencies decrease, possibly because, as the species are more firmly held, the stronger metal to carbon bond gives rise to bands at lower frequencies. On cooling, the distribution obtained at the higher temperature persists, i.e., the CO becomes 'frozen', such that the band observed on returning to room temperatures will occur at a lower frequency. Also the frequency shifts on further heating and cooling will be temperature reversible, as observed in Figure 26.

This redistribution of CO on the surface after the heating/cooling treatment seems to be such that the sites, which when initially at room temperatures were occupied by adsorbed $\text{Ni}(\text{CO})_4$, become occupied by adsorbed CO, which thus blocks the readsorption of $\text{Ni}(\text{CO})_4$ as such. The CO species involved here were considered to be chemisorbed single linear groups per metal site.

Now it was expected that band B, on cooling the system, would have returned to its original position at 2080 cm^{-1} and also assume its original shape and intensity, thereby being attributable to the structure $\text{Ni} - (\text{CO})_X$ where $X < 4$ but ≥ 1 . For low CO pressures (about 1 Torr) this was not the case, as shown above, which suggested that a side reaction had occurred. To verify this possibility a higher CO pressure (12 Torr) was admitted, i.e., excess free CO then occupied the *in situ* cell, and the heating/cooling procedure repeated. The final maximum given by band B was observed in the frequency range 2065 to 2070 cm^{-1} , higher than that shown by the earlier results, but once

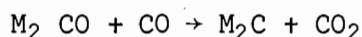
again the band's intensity was considerably reduced. A medium sharp band was found at a frequency of 2342 cm^{-1} together with an increase in the amount of free CO_2 . That CO_2 was formed on heating a Ni - CO system had been shown in the reactor experiments; result 4.1 (1.4), Figure 11. The sharp band observed at 2342 cm^{-1} was considered to be either physically adsorbed or weakly chemisorbed CO_2 species. Therefore, it seems likely that these species prevent the adsorption of more than one CO ligand per metal atom, by virtue of their own adsorption on nickel, probably through steric hindrance.

The chief product formed, by the interaction of adsorbed carbon monoxide and hydrogen on nickel, was methane. Its formation was demonstrated by results 4.1 (1.1) to (1.3) and shown by Figure 8, and only occurred at temperatures above $190^\circ \pm 5^\circ\text{C}$, but was still produced, although in limited quantities, at temperatures $\geq 430^\circ\text{C}$, result 4.1(1.6). Unlike iron, the nickel catalysts were very active with respect to methane formation, but only traces of ethane were detected using mass spectrometry, Figure 35. No other hydrocarbons, either saturated or unsaturated, were detected by infrared or mass spectrometry. Nevertheless, the activity of nickel with respect to CH_4 production was very marked as shown in Figure 7.

A by-product given in the reaction was CO_2 , Figure 7, providing CO had been preadsorbed at room temperatures, i.e. prior to the addition of hydrogen. CO_2 was also produced when the catalyst was heated in an atmosphere of CO alone, Figure 11, as mentioned earlier. Clearly this suggested that different 'active' sites became available

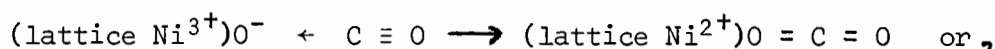
under these conditions, on or from which a second reaction mechanism could occur. Further evidence to support this was afforded by the results 4.1(1.2) and (1.3). Here it was shown that, on preadsorption of hydrogen or on admission of a CO/H₂ mixture, the hydrogen either became preferentially adsorbed onto those sites which favour CO₂ formation or coadsorbed with CO. In any event, these situations prevented a secondary reaction taking place.

The reaction mechanism responsible for CO₂ could proceed via one of two intermediates. The first possibility is via a surface carbide, which may be formed according to the equation:



i.e., involving a 'bridged' CO structure as opposed to a linear one. This mechanism was proposed by Ferreira²⁷ when he observed that CO₂ was the main reaction product under conditions of low H₂ : CO ratios. The other possibility could involve the thermally induced dissociation of adsorbed CO. Electron spectroscopy studies¹³² proved that, at temperatures of about 400 K, carbon monoxide dissociates on nickel to give surface carbon and oxygen. The authors' observations were in agreement with the formation of a surface carbide as suggested by Ramqvist¹⁷³, and in conclusion they pointed out the difficulty in obtaining nickel free traces of carbon and oxygen since their formation was relatively easy from CO_{ads} at 400 K. The above was also supported by Barber *et al*⁹³, in their studies of CO adsorbed on Ni and Cu, using secondary ion mass spectrometry. This technique revealed the formation of surface carbides on both metals, proceeding via a dissociation mechanism for Ni but one of disproportionation for Cu. Hence, formation of CO₂

could proceed via the surface oxygen, either in a manner similar to that shown for CO on a nickel oxide lattice²⁷ in which adsorption of CO was thought to occur followed by desorption of CO₂ :



on reduction of the oxygen by adsorbed carbon monoxide according to the equation $\text{CO} - \text{Ni} + \text{O} - \text{Ni} \rightarrow \text{CO}_2 + 2 \text{Ni}$. This was proposed by TQtttrup¹⁷⁴ as part of the sequence in which CO decomposes on nickel catalysts.

In addition, CO₂ formation was shown by a steady decrease in absorbance over the temperature range 100° (≈ 400 K) - 400°C, result 4.1(1.1), and it is interesting to note that the lower temperature limit corresponds closely with the temperature of dissociation of CO¹³².

If a surface oxygen species is formed then the catalyst can be considered as being partially oxidised. Therefore, when hydrogen is present, during a heating programme, reduction of the surface could also take place to give water as a by-product. For the nickel-reactor experiments water vapour could not be detected with any degree of accuracy using infrared, however, traces were detected by mass spectroscopy. The absence of water vapour in determinable amounts may be explained in terms of the competition between hydrogen and carbon monoxide to adsorb on, or react with, available Ni - O species. Thus, the reaction $\text{Ni} - \text{O} + \text{CO} \rightarrow \text{CO}_2$ probably occurs at a lower temperature than does surface reduction, $\text{Ni} - \text{O} + \text{H}_2 \rightarrow \text{H}_2\text{O}$. It is quite possible that, when higher temperatures are reached, the reaction with hydrogen is then favoured, providing some Ni - O species still remain available.

No evidence could be provided to determine exactly which type of adsorbed CO species was involved in CO₂ formation, either linear or bridged. However, Ansorge and Foerster¹⁴⁷, in their studies of CO on Co - Mg mixed salt catalysts, considered that the CO species which gave rise to low frequency bands in the infrared were responsible, thus supporting Ferreira's²⁷ hypothesis.

Evidence for the surface species involved in methane formation, using nickel catalysts, was obtained from the *in situ* cell experiments. The rapid decrease in absorbance at $\pm 190^{\circ}\text{C}$ given by the Absorbance - Temperature curve, Figure 21, on heating systems containing both CO and excess H₂, and the absence of such a decrease for the system containing only CO, indicated that band B, i.e., linear CO species, was involved in methane formation. This is contrary to the findings of others^{27,28}. It could be argued that linear CO ligands, when desorbed at high temperatures, readsorb as bridged CO species, which in turn then become the intermediates in the methane reaction mechanism. This redistribution of surface species seems unlikely for two reasons. Firstly, linear CO, giving rise to band B, still remained firmly held on the metal surface even when temperatures as high as 400°C were applied, result 4.1 (2.2). Furthermore, on increasing the temperature, the rate of decrease in intensity of band B was not only found to be similar to that of band A, but also occurred initially at about 20°C higher than the latter. Therefore, it appears that both linear and bridged CO are involved in hydrocarbon formation, but the reaction scheme may well be different for each intermediate. Nickel tetracarbonyl was not considered to be involved in the methane reaction mechanism in any way. Result 4.1 (1.7), Figure 13,

showed that Ni(CO)_4 decomposed rapidly over the temperature range 150 to 190°C , a range slightly lower than that required to initiate the reaction between CO and H_2 . It is also interesting to note that evidence for the interaction between CO and H_2 was provided by the two plots in Figure 18, which again suggested that band B was responsible in the catalytic reaction.

Despite the knowledge already obtained on the nature of the gas/solid surface, only occasionally has there been undisputed evidence to justify the concept of "surface complexes". This was provided recently by Queau and Poilblanc¹⁵⁴, and their findings were discussed earlier, Section 2.3. In this work, the result 4.1 (1.5) provided evidence of a similar nature. Namely, that a reaction between hydrogen (excess) and CO (adsorbed species only) on a nickel catalyst had occurred was shown by the considerable amount of methane detected at the end of the experiment, see Figure 12. The result verifies that, for a Ni/CO/H_2 system, interaction with a surface complex is definitely a stage in the reaction mechanism.

Of the many different types of metal site available, only some may be actively involved in reaction mechanisms and the formation of new compounds. Also it is widely known that specific catalysts favour a specific set of reactions, e.g., hydrogenation, oxidation, and dinitrogen fixation reactions. The author considers that the above can now be modified to read : either,

"that for a given metal catalyst specific 'active' sites
will favour a specific reaction under a given set of
conditions" or,

"providing a given state of adsorbed species (intermediate) is made available then a specific product will be formed under a given set of conditions".

Consequently catalysts need not only be 'tailor-made' for a set of reactions but even for a specific by-product or side-reaction. Some evidence for this has been provided in this work. The two by-products, CO_2 and Ni(CO)_4 , can be eliminated simply by preadsorbing H_2 before the addition of CO , or on admission of a CO/H_2 mixture, results 4.1 (1.2) and (1.3). Either the hydrogen is being preferentially adsorbed onto certain nickel sites, thus effectively blocking the route via which these by-products are formed, or, on coadsorption with CO , the state of the chemisorbed CO species is altered. A similar effect was shown in the *in situ* cell experiments in which one band above 2000 cm^{-1} , and not two, was observed on hydrogen preadsorption, result 4.1 (2.1).

The resolved absorption bands, given by a spectrum of an aged/sintered catalyst or by a catalyst having a low nickel content, Figure 27, can also be explained either in terms of different adsorption sites, or, can reflect differences in the $\text{CO} : \text{Ni}$ ratio. The latter explanation is preferred, in view of the evidence provided by the cobalt results.

5.3 IRON CATALYSTS :

The iron catalysts were found to be far less 'active' with respect to methane formation than was nickel. This was attributed to the ease of reducibility of nickel oxide relative to the oxides of iron which has been discussed earlier, p. 118. However, there was one advantage in using iron catalysts, over nickel and cobalt, which was that other hydrocarbons were produced in relatively large amounts, namely ethane and propane. This was shown by the weak absorptions occurring at frequencies of 2970 and 2880 cm^{-1} ; result 4.2.1, Figure 29.

Kölbel and Tillmetz¹⁵⁷ observed a special catalytic activity for chain propagation, which occurred on Fe(111) surface clusters, and was deduced from the geometrical and electronic structure of the Fe - CO complex. They showed that no stable complex containing oxygen could be formed with nickel. This implied that no chain propagation within a condensation mechanism could occur on nickel catalysts, although hydrocarbon chains of moderate lengths have been produced^{100,175}. Therefore, they suggested that a different reaction mechanism occurred on nickel proceeding via primary complexes having a methylene structure.

In the case of iron and cobalt a relatively short C - O bond length and partial double bond character in both complexes pointed to an enolic behaviour. These complexes were also reported as being highly reactive and were involved, especially when adsorbed onto Fe(111) planes, in chain propagation via condensation mechanisms; with probably the first step occurring only after splitting of water. This would leave, as

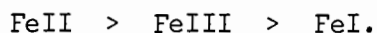
shown by Kölbel's representation of complexes on iron, an aldehyde and methylene functional group close to one another on the surface. It was also stated that the higher stability and strongly marked enolic behaviour of the iron complex relative to the cobalt complex seemed to be responsible for the production of longer hydrocarbon chains, with a higher content of oxygenated species in the spectrum on iron.

Therefore the observed, (see mass spectroscopy results 4.4), enhanced activity of the iron catalysts, relative to nickel and cobalt, with respect to the formation of hydrocarbons other than methane is well supported by the above explanation.

Allied to this was the interesting phenomenon given on hydrogen preadsorption with all catalyst types. Here only methane was formed, and no other hydrocarbon was detected either by infrared or mass spectroscopy. Although no supporting evidence was obtained, it would appear that either the hydrogen blocked those sites which would favour the formation of higher hydrocarbons, or, on coadsorption with CO, a new complex would be formed which would not be able to take part in condensation mechanisms, thus inhibiting chain propagation. Once again, results suggest that either different adsorbed CO species are responsible for the formation of different products, or specific adsorption sites favour specific reactions.

The introduction of small amounts of copper to an iron catalyst was found to increase the catalytic activity markedly. The copper may either be acting as a promoter, i.e., encouraging the formation of surface complexes, or simply facilitates the reduction of iron. In any case, results showed that copper containing iron catalysts, type FeII,

were more 'active' such that the comparison between the different catalysts, with respect to their catalytic activity, was of the order :



Contrary to that found for nickel, no iron carbonyls were detected throughout the reactor experiments, and only traces of CO_2 were given (as a by-product), even on admission of CO alone. This suggests that iron is unable to form specific complexes with CO on its surface, which can be readily formed on a nickel surface. Evidence of iron's 'inactivity', relative to nickel, was shown by the higher temperature required, ($> 200^\circ\text{C}$ for a freshly-prepared sample), to initiate methane formation, cf. 190°C for nickel.

Spectra obtained in the *in situ* cell experiments were rather disappointing, and only two absorption bands, attributed to adsorbed CO, were observed at frequencies of 2169 and 2030 cm^{-1} . Both bands were found unsuitable for use for correlation with the 'reactor' results. This was due either to their behaviour under certain conditions, such as evacuation and heating, or to their poor appearance.

The sharp band found at 2169 cm^{-1} , band B, was attributed in part to very weakly chemisorbed CO ligands, with perhaps some CO existing in a physisorbed state. The band's high frequency position, together with the fact that it was extremely sensitive to CO pressure, heating, and evacuation, indicated that physisorbed species may have been present. On the other hand, band A, observed at 2030 cm^{-1} , was more strongly held; result 4.2.2 (b), Figure 32, and it may therefore be

assigned solely to CO ligands chemisorbed onto iron. The CO species responsible for band A was considered to have a linear structure. This is in agreement with Blyholder and Marvin¹⁶¹ who assigned the first main infrared band to linear CO on iron. Band A also shifted to lower frequencies on evacuation at room temperatures, see Figure 32, in a similar manner to that given by band B for CO on nickel. This result supported the assignment of a linear structure.

Voroshilov *et al*¹⁵⁸, in their studies of adsorbed CO on ferric oxide of different reduction states, attributed absorption bands found at 2180 and 2020 cm^{-1} to CO adsorbed on Fe_2O_3 and Fe respectively. For the former the C - O bond was strengthened in comparison with the free C - O bond, whereas in the latter case it was weakened. They suggested that differences occurred in the electronic structure of chemisorbed CO forms due to the surface of iron oxides; with maximum differences being observed in the Fe_2O_3 - SiO_2 catalysts. Because of the difficulty encountered in obtaining well reduced iron samples, it seems likely that CO adsorbed on iron oxide would be responsible for band B at 2169 cm^{-1} , but that band A was due to CO adsorbed on an oxygen free iron surface. Between Voroshilov's and these results there was a difference in frequency of $\pm 10 \text{ cm}^{-1}$ for the high wave-number absorption. This may have been due either to differences in sample preparation or differences in the Fe_2O_3 : FeO ratio. The assignment of very high frequency absorptions to CO species adsorbed onto oxides is in agreement with Ferreira²⁷.

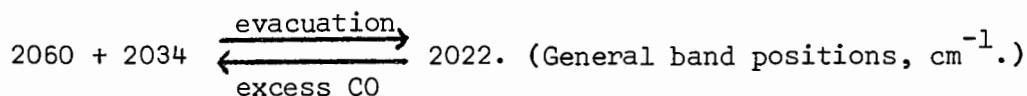
The results given in 4.2.2 (a) and (b) clearly demonstrated the necessity for longer reduction times and higher temperatures, but further attempts to increase the 'activity' of sample discs proved to be unsuccessful.

5.4 COBALT CATALYSTS:

The cobalt catalysts displayed a degree of "activity" midway between that shown by nickel and iron catalysts. Relatively high CO pressures were required to produce absorption bands of medium intensity. This was observed during the *in situ* cell experiments. Also long reduction times at high temperatures were necessary to produce "active" samples. On the other hand, considerable amounts of methane were formed, in the reactor, from the interaction of CO and H₂ on cobalt which compared favourably with the amounts formed on nickel.

When carbon monoxide was allowed to contact a cobalt surface there occurred three main absorption bands in the region above 2000 cm⁻¹, viz., bands at 2181, 2060, and 2034 cm⁻¹, (result 4.3.2 (a), Figure 37). The latter two appeared as maxima belonging to a broad band of medium intensity which was assigned band A. Linear CO species were considered to be responsible for band A. This is in agreement with Ferreira²⁷.

The most significant result obtained from cobalt was the reversible band frequency shift, observed when the catalyst was subjected to the alternating conditions of CO admission and evacuation, see Figure 37. Thus to recapitulate : on evacuation, band B at 2181 cm⁻¹ disappeared, and the low frequency bands were replaced by a narrower absorption having its maximum at about 2022 cm⁻¹. The CO species giving rise to this latter band were very firmly held onto the catalyst surface, being unaffected by prolonged evacuation periods and also on heating at temperatures $\leq 120^{\circ}\text{C}$. However, on addition of a further aliquot of CO, the original spectrum was re-established, according to the equation:



The above result, and indeed the multiplicity of the band structure found above 2000 cm^{-1} , cannot be adequately explained in terms of single linear CO groups adsorbed onto different crystalline sites as had been proposed earlier by others^{97,27,83}. The reasons for rejecting their hypothesis are given below.

(1) The species responsible for the band found at 2022 cm^{-1} was very firmly held onto the surface. This complies with the argument that the strong M - C bond results in a weakening of the C-O bond and hence lowers the C - O frequency. Assuming that these strongly held ligands were then occupying sites of low coordination number, i.e., crystal edges or corners, it is very unlikely that the shift to higher frequencies can be considered as a redistribution of sites, i.e., to metal atoms lying in crystal lattice planes and which have a higher coordination number. A strongly held species would not move to sites where it would be less strongly held than before.

(2) The high energy required to break a strong M - C bond, and then to establish a new single C - O species in which the M - C bond is weaker, cannot be attributed to the admission of low CO pressures ($\leq 50\text{ Torr}$) as would appear to be the case, especially as this bond was unaffected by more severe conditions such as evacuation or heating to temperatures of 120°C .

(3) By assigning the 2022 cm^{-1} band mainly to CO adsorbed onto edge or corner sites, and the bands at 2060 and 2034 cm^{-1} to CO on different crystalline planes, the spectra revealed that, under certain conditions, most plane sites remained vacant while edge and corners were occupied, and vice-versa. If this were so, then, the fairly high ratio of atoms adsorbed onto planes to that of atoms adsorbed on corners and

edges would be reflected by a marked difference in relative band intensities. This effect was not shown in the results. In fact, the opposite was observed, viz., the band at 2022 cm^{-1} was slightly more intense than the other two instead of being less so as would be expected.

Therefore, in view of the above, a new interpretation is proposed for the observed infrared spectra of CO chemisorbed on cobalt:

The multiplicity and frequencies of infrared bands given by carbon monoxide chemisorbed onto silica supported cobalt catalysts can be explained in terms of the CO : metal ratio, whereas only their shape is dependent on factors such as ligand - ligand interaction, metal to metal distances, and the nature of the adsorption sites, e.g., planes, corners and edges.

Therefore for CO on cobalt, the bands found above 2000 cm^{-1} have been attributed to the species $M(\text{CO})_Z$, $M(\text{CO})_Y$, and $M(\text{CO})_X$ corresponding to the frequencies 2060, 2034, and 2022 cm^{-1} respectively, and where $Z > Y > X \geq 1$. Thus the M - C bond strengths would be in the order $M(\text{CO})_X > M(\text{CO})_Y > M(\text{CO})_Z$.

The interpretation can be applied to the infrared spectra of CO adsorbed onto other metals, e.g., nickel, which has been discussed in Section 5.2. The interpretation also includes bridging carbonyl structures, $M_2\text{CO}$, because the lower the CO frequency the lower the CO : metal ratio. All the experimental results can be adequately explained by this hypothesis, such as varying the CO

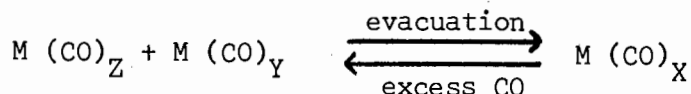
pressure, evacuation, temperature effects, and the influence of additional gases, e.g., hydrogen. However, before the evidence is presented, further discussion is required, which not only substantiates the points made on page 159, (1) to (3), but also favours this hypothesis.

Within a system $M-(CO)_n$, any change in the value of n can be described as an "internal" change and one which should greatly influence the relative bond strengths, $M - C$ and $C - O$. On the other hand, influences on the bond strengths such as ligand-ligand interactions, metal to metal distances, and the nature of the adsorption sites can be described as being "external" to the system, and so it is reasonable to assume that their influence would be less marked than the former. The position of infrared absorption bands depends solely on the $C - O$ bond strength which, in turn, is mainly influenced by the $M - C$ bond strength. This is the main argument to justify the assignment of band frequency positions and band shifts to changes in the value of n , or more correctly the $CO : metal$ ratio. For example, the influence shown by the $CO : metal$ ratios $1 : 2$ and $1 : 1$, i.e., between bridged and linear species, is demonstrated by the large differences observed in band positions, e.g., about 130 cm^{-1} for CO on Ni^{101} .

Because the "external" forces must be much weaker, then their influence is not shown in the band positions or frequency shifts but by the shape of these bands. As a result of the large number of forces of this nature bands attributed to adsorbed CO are usually broad in appearance.

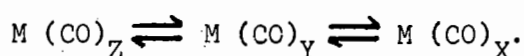
The following results, given in Section 4.3.2., provided evidence to support the new interpretation :

(i) The reversible frequency shift, Figure 37, suggested that a reaction had taken place according to the equation :



A similar effect was observed by Soma-Noto and Sachtler⁸⁹, in their studies of CO adsorbed on Pd and Pd - Ag alloys.

(ii) Studies on the effect of band A on varying the CO pressure exhibited the expected equilibria :



This was shown in result 4.3.2 (c), Figure 39, in which the shape of band A varied according to whether low (<10 Torr), medium (10-30 Torr), or high (>30 Torr) CO pressures were used. On increasing the pressure the peak at higher frequencies predominated while the low frequency peak at 2022 cm^{-1} decreased in intensity.

(iii) The effect on band A, at 2022 cm^{-1} , on the addition of hydrogen was studied. Essentially the system then comprised of CO_{ads} . plus excess H_2 . Band A, at 2022 cm^{-1} , was observed to decrease slightly in intensity and exhibit a high frequency hump. This is shown in Figure 40, and can be explained in terms of the partial coadsorption of hydrogen with CO. Coadsorption, producing band A to shift to higher frequencies, was similar to that shown by the addition of a further aliquot of CO, see above. The effect suggests that back-donation from the metal to a hydrogen atom had occurred, which reduced the π bonding between the metal and carbon atom and thereby increased the C - O bond order and CO frequency. Although the spectra indicated that only a small proportion of H - M - CO species were formed, the

extent of the shift would be dependent on two competing factors :

(i) the ability of hydrogen to accept d- electrons from the metal, and the effective d electron density required to maintain an M - H bond which can then be attributed to an M - H species in a chemisorbed state; and (ii) the relative amounts of d electron density distributed between the M - H and M - C bonds within an H - M - CO species. Dalmon *et al*¹³⁸ calculated the heats of adsorption for H₂ and O on Co and Ni catalysts deposited on SiO₂. They concluded that the O formed a surface oxide layer. Similarly, the results of the H - Ni system were also interpreted in terms of the formation of a surface hydride layer; but with H - Co this did not occur. The latter was attributed to the greater energy required to break down the ferromagnetic coupling between surface cobalt atoms. In any case, adsorption of hydrogen on cobalt was less strongly felt than on nickel, and this has been confirmed for both metals by the results given here.

(iv) The loss of "activity" of a sample, characteristic of an ageing and/or sintering process, is shown in Figure 41. The shape of band A and its low frequency position suggests that the catalyst did not have the ability to form as many M (CO)_n species having high values of n as would a fresh, less sintered catalyst. The frequency shift to lower wavenumbers on evacuation indicated a tendency to form bridged carbonyls at the expense of linear ones.

(v) Band A shifted to lower frequencies on increasing the temperature. Thus the peaks at 2060 and 2034 cm⁻¹ gradually disappeared, i.e., decreased in intensity, to be replaced by the peak at 2022 cm⁻¹, which increased in intensity. This effect is best shown by the nickel results, 4.1 (2.1), but both sets indicated the gradual decrease in the

value of n , until possibly a value of 1 was obtained.

The sharp band, band B, found at a frequency of 2181 cm^{-1} , exhibited the same characteristics as had band B for CO on iron. Namely, it readily disappeared on evacuation at room temperatures, (result 4.3.2 (a)); it increased in intensity with an increase in CO pressure, (result 4.3.2 (c)); and decreased in intensity over the temperature range $25 - 180^{\circ}\text{C}$, (result 4.3.2 (b)). Therefore, the band was attributed partly to weakly chemisorbed CO, and also to some physisorbed CO species. In addition, the chemisorbed CO species may well have been adsorbed onto cobalt oxide surfaces because it was very difficult to obtain well reduced samples.

Methane was found to be the chief product formed by the interaction of adsorbed carbon monoxide and hydrogen on cobalt catalysts. Its formation, shown in Figure 33, on using the "thermal programme" only occurred at temperatures above the range $195 - 215^{\circ}\text{C}$ (slightly higher than for nickel but lower than iron), and can be represented by an Absorbance-Temperature curve similar to that plotted for nickel, Figure 8. Methane could also be formed at temperatures below 195°C , as shown by Figure 36. This result simply demonstrates that its formation is dependent on both time and temperature.

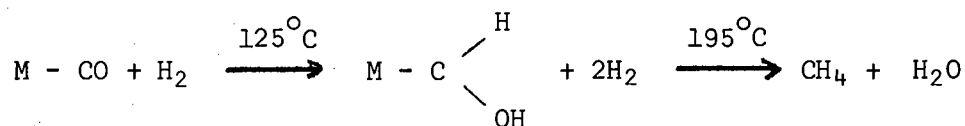
Carbon dioxide was the only product given by CO alone on cobalt. No carbonyls were detected, contrary to that found with nickel. Occasionally trace amounts of CO_2 were produced when applying the procedures $\text{CO} - \text{H}_2 - \Delta\text{H}$ and $\text{CO}/\text{H}_2 - \Delta\text{H}$. For the latter, CO_2 formation may well have proceeded via surface oxygen atoms, probably due to

incomplete reduction of the catalyst. Only trace amounts of ethane were found, detected by mass spectroscopy. This is shown by the fragmentation pattern in Figure 34. Therefore, cobalt's reduced "activity" with respect to chain propagation, relative to that exhibited by iron, confirms the observations made by Kölbel and Tillmetz¹⁵⁷.

Strong evidence was provided to show that linear CO species were involved in methane formation, which was similar to that proved for nickel catalysts, Section 5.2. The rapid decrease in absorbance of band A at 2020 cm^{-1} over the temperature range 125 to 215°C , given by the Absorbance-Temperature curve, Figure 38, on heating systems containing both CO and excess H_2 , and the absence of such a decrease for the system containing only CO, confirmed that the species giving rise to band A was involved in methane formation. With only CO contained in the system, band A decreased linearly over the range 115 to 290°C , again shown in Figure 38.

The low temperature range ($125 - 215^{\circ}\text{C}$) observed for systems containing both H_2 and CO did not coincide with the methane formation temperature of $+ 195^{\circ}\text{C}$, which was revealed in the reactor experiments, considering that the 'thermal programme' had been used for both sets of experiments. Compare the nickel results in which band B at 2030 cm^{-1} decreased in intensity at temperatures above 190°C , a temperature corresponding closely with that of methane formation, $190 \pm 5^{\circ}\text{C}$. Thus it appears that, within the range $125 - 195^{\circ}\text{C}$, an intermediate complex was formed between the adsorbed CO and hydrogen, which did not absorb in the frequency range $2300\text{ to }1750\text{ cm}^{-1}$. The complex may well have been

of an enolic nature, i.e. $\text{H} - \text{C} - \text{OH}$ as reported by Farrauto¹⁸⁰ when he studied a nickel/alumina methanation catalyst. Balaji Gupta *et al*¹⁸¹, who studied the interaction of H_2 and CO on cobalt catalysts, also suggested that a complex of the type $-\text{C}(\text{H})\text{OH}$ was formed on the surface. Assuming this to be correct, the methanation process could be summarised, provided thermal programming conditions were used, as follows:



It has been shown in Section 4.1 that from the interaction of CO and H_2 on nickel catalysts, band B, at 2030 cm^{-1} , decreased at a temperature which did coincide with the methane formation temperature of $\geq 190^\circ\text{C}$. Possibly the intermediate complex formed on nickel was less stable, and the reaction rate for its conversion to methane was fast. This implies that, for nickel, the rate determining step was the formation of the intermediate.

APPENDIX 1.

EXPERIMENTS ON THE RATE OF DIFFUSION OF

CARBON MONOXIDE

Test spectra were carried out in the absence of catalyst to examine the rate of diffusion of CO in relation to the various procedures applied in the reactor experiments. For convenience only vol. D of the vacuum line was used with vol. (D - C) comprising the 10 cm path length infrared gas cell. At the start of each experiment vol. D was evacuated to a pressure of 10^{-6} Torr. A schematic diagram of the gas line is given in Figure 6.

For the actual reactor experiments both reactant gases were admitted into the gas line so that, just prior to mixing, the line contained the following:

- (a) CO in vol. (E - C) and H₂ in vol. C, for procedure CO - H₂ - ΔH.
- (b) CO in vol. (D_r - C) and H₂ in vol. C, for procedure CO/H₂ - ΔH.
- (c) H₂ in vol. (E - A) and CO in vol. A, for procedure H₂ - CO - ΔH.

This was then altered to give H₂ in vol. (E - B) with CO in vol. B.

These systems may now be compared with the test systems described below.

1.

With about 31 Torr CO pressure occupying vol. (D - C), the spectrum was recorded over the frequency range 2210 to 2010 cm⁻¹. This frequency range suitably covered the absorption band due to free CO. On re-evacuating vol. C to a pressure of 10^{-6} Torr, H₂ was then

admitted and the stopcock opened between the two volumes to allow mixing. The CO spectrum was recorded immediately and also at half-hourly intervals thereafter. The procedure was repeated, maintaining an initial CO pressure at 30 - 35 Torr in vol. (D - C), but varying the pressures and/or gas in vol. C prior to mixing. Also a 'blank' was recorded in which CO, previously held in vol. (D - C), was then allowed to occupy vol. D. Prior to this step vol. C had been pre-evacuated to 10^{-6} Torr.

The results are given in Table 4.

TABLE 4.

Initial CO pressure, vol.(D-C), Torr	Initial Air or H ₂ pressure vol.C,Torr	Total pressure after mixing Vol.D, Torr	Absorbance CO band, before mixing	Absorbance CO band after mixing	Standing period, after mixing, hr.
31,5	10^{-6}	2	0,80	0,06	0, (nil)
31,5	<u>H₂</u> , 84	78	0,78	1,02	0, (nil)
31,0	<u>H₂</u> , 57	55	0,73	0,88	0, (nil)
				0,60	0,75
				0,54	1,5
				0,47	2,5
				0,40	3
				0,32	4
				0,29	5
31,0	<u>Air</u> , 62	59	0,74	0,92	0, (nil)
				0,68	0,75
34,0	<u>Air</u> , 25	26	0,81	0,66	0, (nil)
				0,55	0,5
				0,41	1,5
				0,36	2,5
				0,35	3,5

The results showed that on mixing CO with H₂ or air, providing the pressure ratio CO : other gas was <1, an immediate increase in intensity was observed of the CO fundamental. This is analogous to a

pressure broadening effect. Thereafter the intensity decreased exponentially with an increase in time due to the slow diffusion rate of CO when in the presence of another gas. The 'blank' gave the expected decrease in band intensity, which occurred immediately on opening the stopcock, and corresponded closely to the relative volumes (D - C) : D of 1 : 15.

2.

A 'background' spectrum was first recorded over the same frequency range as before, 2210 to 2010 cm^{-1} . H_2 was then admitted into vol. (D - B) and the spectrum again recorded. With CO occupying vol. B the stopcock was then opened between these two volumes to allow mixing. The spectrum was recorded immediately and also at half-hourly intervals thereafter. Two 'blanks' or standard spectra were recorded for comparison. The first involved the admission of CO into vol. B at a known pressure. This quantity of CO was then allowed to occupy vol. D and both the spectrum and new pressure was recorded. The second 'blank' simply involved the recording of 'background' spectra when vol. D was either evacuated to 10^{-6} Torr or occupied by a known amount of H_2 .

These results are given in Table 5.

TABLE 5.

Initial CO pressure in vol.B Torr	Initial pressure in vol.(D-B), Torr	Total pressure after mixing, vol.D. Torr	Absorbance CO band, before mixing.	Absorbance CO band, after mixing.	Standing period, after mixing, hr.
34	69 (H ₂)	42	0,09	0,11 0,29 0,49 0,56	0, (nil) 0,5 1 1,5
'Blank'1 → 50	10 ⁻⁶	39	0,07	0,92	0, (nil)
-	-	92	0,09	0,09	0, (nil)
	→ 'Blank'2 (H ₂)				

Once again the results showed the slow diffusion rate of CO on mixing with H₂. Whereas in the absence of H₂ the CO pressure ratio of 50 : 39, observed by recording the spectrum immediately on allowing CO to fill vol. D, corresponds closely with the volume ratio D : B.

'Blank' 2 confirmed that the H₂ was not contaminated with CO, and neither did it produce any interference bands within the frequency range studied. even at relatively high pressures.

3.

The same procedure was adopted as for 1. An immediate increase was observed of the CO band intensity on mixing CO and H₂. This time, however, vol. (D - C) was isolated from the line after allowing the gases to mix for only 1 min. The increase in band intensity was maintained even after a 1 hr. standing period. A further aliquot of H₂, (previously occupying vol. C), was then allowed to mix with the contents in vol. (D - C) by opening the

stopcock between these volumes and keeping it open. No immediate change in intensity was observed, the pressure broadening effect was not heightened, but an expected decrease was given on allowing the system to stand for 1 hr. This was due to the slow diffusion of CO from vol. (D - C) into vol. C. The fact that the band intensity remained unaltered on allowing the system to stand in the first instance provides further evidence to support the theory of pressure broadening.

The conclusions to the above experiments are given in Section 3.4.3.

APPENDIX 2.

THE SILICA DISC REFERENCE.

Test spectra were carried out on the silica disc reference to check instrument noise and drift levels when monitoring at a constant frequency for long periods, and also to ensure that the silica provided no interference fringes over the range of interest, (2300 - 1700 cm^{-1}).

1.

Three freshly prepared silica discs of varying thickness were placed in turn in the sample beam of the spectrometer and their spectra recorded over the frequency range 3000 to 1500 cm^{-1} . A typical spectrum is given in Figure 42. Very little absorption occurred over the range 2600 to 2100 cm^{-1} . At lower frequencies the silica was found to absorb strongly giving two maxima at 1860 and 1635 cm^{-1} . The two maxima did not shift in frequency relative to one another as the sample thickness varied. A frequency shift of this nature would have been indicative of interference 'fringes' which in turn would have caused errors in the observed spectra of CO on silica supported metal samples.

2.

A freshly prepared silica disc was placed in a 10 cm path length infrared gas cell fitted with CaF_2 windows, and this cell evacuated to at least 10^{-3} Torr pressures. The disc was held in a brass sample holder similar to that used in the *in situ* cell and its dimensions are shown in Figure 3. With the cell placed in the sample beam of the spectrometer, the instrument was set to monitor at a constant frequency of 2056 cm^{-1} . This frequency was chosen because

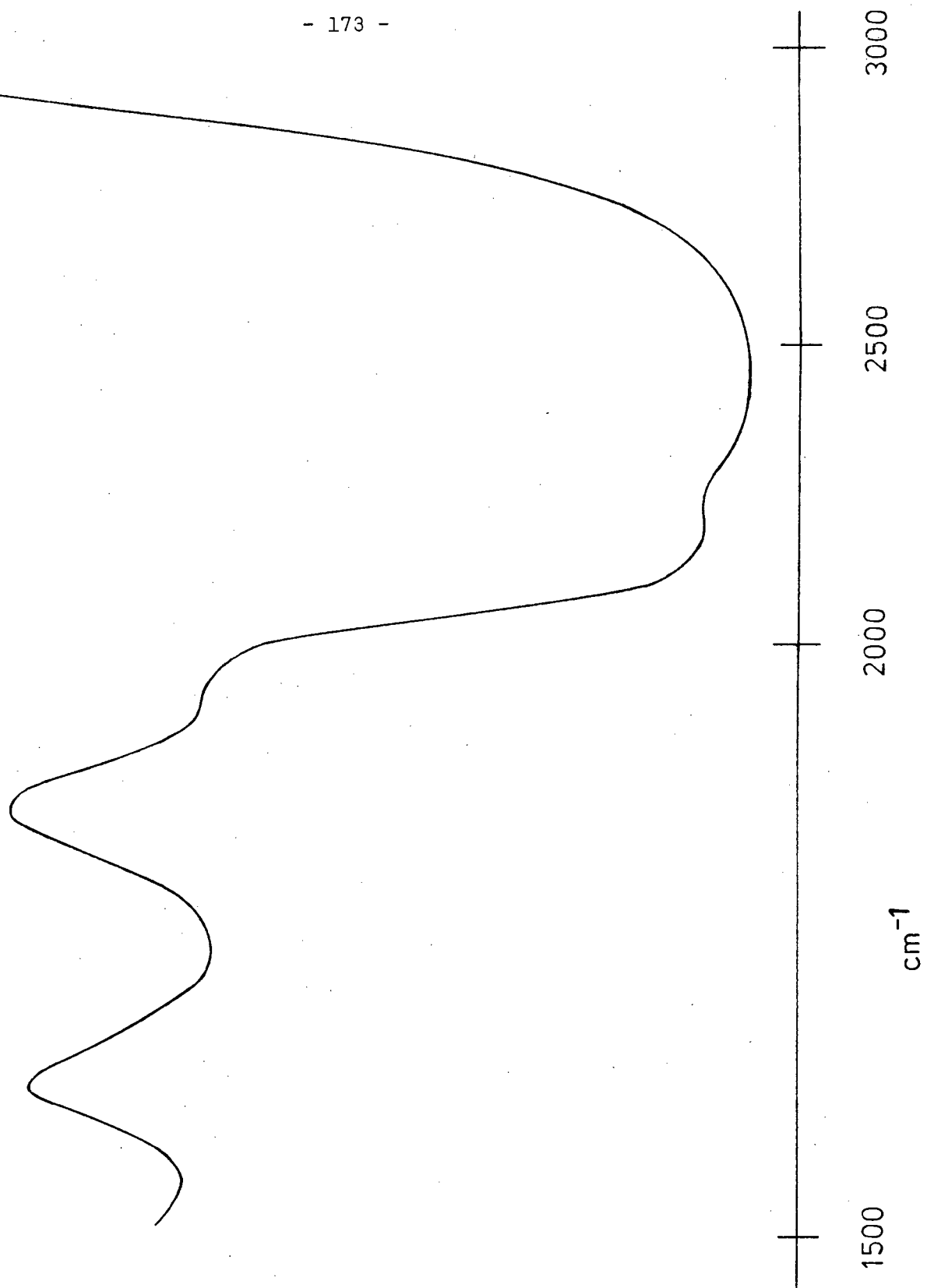


FIGURE 42. Spectrum of a thin SiO_2 disc.

it coincided with that of band C for CO on Ni (Section 4.1.2), a band which occurred almost centre of the range of interest.

After monitoring for a period of 16 hr. the 'noise' and 'drift' levels were measured and found to be 1% and $\pm 1.5\%$ Transmittance respectively. Both values were considered to be low enough and did not produce any unwanted interference.

It was concluded that a silica disc, of comparable thickness to the sample, provided a satisfactory reference in flattening the 100% Transmittance line and establishing the more sensitive differential technique.

APPENDIX 3

Frequently the Perkin-Elmer 180 infrared spectrometer was calibrated in order to assess its performance. The tests carried out included:

1. Baseline check, over the frequency range 4000 to 180 cm^{-1} , at 100 and 0% Transmittance.
2. The recording of a spectrum of a thin polystyrene film. This was regarded as a 'spot' check.
3. Frequency repeatability - precision.
4. Abscissa accuracy.
5. Resolution.

Results for tests (3) to (5) inclusive were obtained by recording the spectra of gases, e.g., HCl, CO, CO₂, H₂O_{vap.}, NH₃, and CH₄, over specific frequency ranges and varying spectrometer conditions.

It was found, at all times, that the instrument's performance was good and that the specifications given by the manufacturer were met. Two important criteria were abscissa accuracy and frequency repeatability. For these it was found that :

1. frequency repeatability was within $0,03\text{ cm}^{-1}$;
- and
2. abscissa accuracy, over the range $2500 - 1000\text{ cm}^{-1}$ was $\pm 0,25\text{ cm}^{-1}$;
and $>2500\text{ cm}^{-1}$ was $\pm 0,7\text{ cm}^{-1}$.

R E F E R E N C E S

1. V. HAENSEL; Ind. Engng. Chem., 57(6), 18, (1965).
2. S. GLASSTONE; K. J. LAIDLER, and H. EYRING; "Theory of Rate Processes", McGraw-Hill, (1941).
3. J. M. THOMAS and W. J. THOMAS; "Introduction to the Principles of Heterogeneous Catalysis", Chap., 1, Academic Press, London, (1967).
4. R. M. BAMER and E.K. Rideal; Proc. Roy. Soc., 149A, 231, (1935).
5. E. A. MOELWYN-HUGHES; "Physical Chemistry", p. 1107, Pergamon, (1957).
6. S. MATSUSITA; Japan Chem. Soc. Meeting, Tokyo, (Apr. 1952), see Advan. in Catal., 6, 82, (1954).
7. R. T. DAVIS; J. Amer. Chem. Soc., 68, 1395, (1946).
8. O. BEECK; Disc. Faraday Soc., 8, 118, (1950).
9. G. K. L. CRANSTOWN and S. J. THOMSON; Trans. Faraday Soc., 59, 2403, (1963).
10. F. H. CONSTABLE; Proc. Roy. Soc., 108A, 355, (1925).
11. H. S. TAYLOR; Proc. Roy. Soc., 108A, 105, (1925).
12. O. BEECK, A. E. SMITH, and A. WHEELER; Proc. Roy. Soc., 177A, 62, (1940).
13. G. H. TWIGG and E. K. RIDEAL; Trans. Faraday Soc., 36, 533, (1940).
14. H. LEIDHEISER and A. T. GWATHMEY; J. Amer. Chem. Soc., 70, 1200, (1948).
15. R. E. CUNNINGHAM and A. T. GWATHMEY; Advan. in Catal., 9, 25, (1957).
16. A. COUPER and D. D. ELEY; Disc. Faraday Soc., 8, 172, (1950).
17. G. M. SCHWAB; Disc. Faraday Soc., 8, 167, (1950).
18. G. KEMBALL; Proc. Roy. Soc., 214A, 413, (1952).
19. M. E. DRY and S. F. STONE; Disc. Faraday Soc., 28, 192, (1959).
20. W. E. GARNER; Proc. Roy. Soc., 197, 294, (1949).
21. W. E. GARNER; Proc. Roy. Soc., 211, 472, (1952).
22. Z. KNOR; Advan. in Catal., 22, 51, (1972).
23. H. H. STORCH, N. GOLUBIC, and R. B. ANDERSON; "The Fischer-Tropsch and Related Syntheses", J. Wiley & Sons Inc., N.Y., (1951).

24. R. B. ANDERSON; "Catalysis", Ed. P.H. EMMETT, 4, 257, Reinhold, N.Y., (1956).
25. M. E. DRY, T. SHINGLES, L. J. BOSCHOFF, and G. J. OOSTHUIZEN; J. Catal., 15, 190, (1969).
26. H. W. STERNBERG and I. WENDER; Abst. Papers, Int. Conf. Coord. Chem., London, (1959); Chem. Soc. Spec. Publ., 13, 35.
27. L. C. FERREIRA; Ph.D. Thesis, University of Cape Town, Cape Town, R.S.A., (1970).
28. L. C. FERREIRA and E. C. LEISEGANG; J. South African Chem. Inst., 23, 136, (1970).
29. C. A. COULSON; "Valence", 2nd Ed. Oxford University Press, London, (1961).
30. F. A. COTTON and G. WILKINSON; "Advanced Inorganic Chemistry", 2nd Ed. Interscience, (1966).
31. F. A. COTTON and R. M. WING; Inorg. Chem., 4, 314, (1965).
32. K. NAKAMOTO; "Infrared Spectra of Inorganic and Coordination Compounds", Wiley, N.Y., (1961).
33. F. A. COTTON and G. WILKINSON; J. Amer. Chem. Soc., 79, 752, (1957).
34. W. F. EDGEELL, W. E. WILSON, and R. SUMMITT; Spectrochim. Acta, 19, 863, (1963).
35. L. H. JONES; Spectrochim. Acta, 19, 329, (1963).
36. E.W. ABEL, M. A. BENNETT, and G. WILKINSON; J. Chem. Soc., Part 3, 2323, (1959).
37. C. S. KRAIHANZEL and F. A. COTTON; Inorg. Chem., 2, 533 (1963).
38. R. D. FISCHER; Chem. Ber., 93, 165, (1960).
39. R. K. SHELINE and K. S. PITZER; J. Amer. Chem. Soc., 72, 1107, (1950).
40. E. R. COREY and L. F. DAHL; Inorg. Chem., 1, 521, (1962).
41. R. R. MYERS; Ann. N.Y. Acad. Sci., 72, 339, (1958).
42. R. A. GARDNER and R. H. PETRUCCI; J. Amer. Chem. Soc., 82, 5051, (1960).
43. R. A. GARDNER; J. Phys. Chem., 64, 1120, (1960).
44. TH. WOLKENSTEIN; Advan. in Catal., 9, 807, (1957).
45. R. A. GARDNER and R. H. PETRUCCI; J. Phys. Chem., 67, 1376. (1963).

46. R. A. GARDNER; J. Catal., 3, 22, (1964).
47. G. M. BARROW; "Introduction to Molecular Spectroscopy", McGraw-Hill, (1962).
48. M. L. HAIR; "Infrared Spectroscopy in Surface Chemistry", E. Arnold, London, (1967).
49. S. J. GREGG; "The Surface Chemistry of Solids", Chapman and Hall, London, (1965).
50. D. J. SHAW; "Introduction to Colloid and Surface Chemistry", 2nd Ed., Butterworths, (1970).
51. A. D. CROSS; "Introduction to Practical Infrared Spectroscopy", Butterworths, (1969).
52. G. HERZBERG; "Infrared and Raman Spectra of Polyatomic Molecules", Van Nostrand, Princeton, N.J., (1945).
53. R. G. J. MILLER; "Laboratory Methods in Infrared Spectroscopy", 2nd Edit., Heyden and Son, London, (1972).
54. R. G. WHITE, "Handbook of Industrial Infrared Analysis", Plenum Press, N.Y., (1964).
55. L. H. LITTLE, "Infrared Spectra of Adsorbed Species", Academic Press, N.Y., (1966).
56. G. WEBB; Sci. Progress, 60, No. 239, 337, (1972).
57. R. P. EISCHEMS; Accounts Chem. Res., 5 (2), 74, (1972).
58. N. D. PARKYNS; "Laboratory Methods in Infrared Spectroscopy", 2nd Ed., 318-39 and 373-4, (1972).
59. H. KNOEZINGER, Acta. Cient. Venez., 24 (2), 76, (1973).
60. T. B. GRIMLEY; Proc. Phys. Soc. (Lon.), 79, 1203, (1965).
61. G. DUYCKEARTS; Analyst, (Lond.), 84, 201, (1959).
62. L. H. LITTLE; Platinum Metals Review, 12, 136, (1968).
63. F. SOLYMOSI; Catalysis Rev., 1, 233, (1967).
64. G. M. SCHWAB and K. KOLLER; J. Amer. Chem. Soc., 90, 3078, (1968).
65. D. TARINA, E. WEISSMAN, and D. BARB; J. Catal., 11, 348, (1968).
66. W. N. DELGASS, and M. BOUDART; Catalysis Rev., 2, 129, (1968).
67. V. C. F. HOLM and A. CLARK; J. Catal., 11, 305, (1968).
68. J. K. A. CLARKE, G. M. FARREN, and H. E. RUBALCAVA; J. Phys. Chem., 72, 327, (1968).

69. G. BLYHOLDER; Proc. 3rd International Cong. on Catal., Nth. Holland, Amsterdam, 657, (1965).
70. W. N. DELGASS; M. BOUDART, and G. PARRAVANO, J. Phys. Chem., 72, 3563, (1968).
71. R. GRECU; Studii Si Cert. De Chim., 18 (8), 815, (1970).
72. M. CUKR; Chemické Listy, 64 (8), 785, (1970).
73. M. CUKR; Chemické Listy, 64 (4), 337, (1970).
74. V. GYORGY; Khem. Kozlem, 31 (2), 153, (1969).
75. L. H. LITTLE; Chemisorption React. Metal Films, 1, 489 (1971).
76. J. PRITCHARD; Surface Defect. Prop. Solids, 1, 222, (1972).
77. G. E. EWING; Annu. Rev. Phys. Chem., 23, 141, (1972).
78. C. H. ROCHESTER and M. S. SCURRELL; Surface Defect. Prop. Solids, 2, 114, (1973).
79. N. TAKEZAWA and I TOYOSHIMA; Shinku, 16 (5), 168, (1973).
80. R. P. EISCHENS, S. A. FRANCIS, and W. A. PLISKIN; J. Chem. Phys., 22, 1786, (1954).
81. R. P. EISCHENS, S. A. FRANCIS, and W. A. PLISKIN; J. Phys. Chem., 60, 194, (1956).
82. G. BLYHOLDER; J. Chem. Phys., 36 (8), 2036, (1962).
83. G. BLYHOLDER; J. Phys. Chem., 68, 2772, (1964).
84. Y. SOMA-NOTO and W. H. M. SACHTLER; Proc. Int. Conf. Solid Surf., 2nd, 241, (1974).
85. R. P. EISCHENS and W. A. PLISKIN; Adv. Catal., 10, 1, (1958).
86. C. R. GUERRA; J. Colloid Interface Sci., 29 (2), 229, (1969).
87. G. ERTL and J. KOCH; Z Naturforsch., 25a, 1906, (1970).
88. R. F. BADDOUR, M. MODELL, and R. L. GOLDSMITH; J. Phys. Chem., 74, 1787, (1970).
89. Y. SOMA-NOTO and W. M. H. SACHTLER; J. Catal., 32 (2), 315, (1974).
90. Y. SOMA-NOTO and W. M. H. SACHTLER; J. Catal., 34 (1), 162, (1974).
91. H. HOBERT; Z. Chem., 6, 73, (1966).
92. J. ANSORGE, M. PRIMET, J. A. DALMON, and G. A. MARTIN; C. R. Hebd. Seances Acad. Sci., Ser. C., 281 (15), 607, (1975).
93. M. BARBER, J. C. VICKERMAN, and J. WOLSTENHOLME; J. Chem. Soc., Faraday Trans. 1, 72 (1), 40, (1976).

94. J. A. DALMON, M. PRIMET, G. A. MARTIN, and B. IMELIC; *Surf. Sci.*, 50 (1), 95, (1975).
95. N. P. SOKOLOVA; *J. Mol. Struct.*, 19 (2), 591, (1973).
96. R. M. HAMMAKER, S. A. FRANCIS, and R. P. EISCHEMS; *Spectrochim. Acta*, 21, 1295, (1965).
97. J. T. YATES Jr., and C. W. GARLAND; *J. Phys. Chem.*, 65, 617, (1967).
98. C. E. O'NEILL and D. J. C. YATES; *J. Phys. Chem.*, 65, 901, (1961).
99. A. J. REST and J. J. TURNER; (*Chem. Comm.*), 1026, (1969).
J. Chem. Soc. D (18), (1969).
100. G. BLYHOLDER and L.D. NEFF; *J. Catal.*, 2, 138, (1963).
101. M. J. HEAL, E. C. LEISEGANG, and R. G. TORRINGTON; *J. Catal.*, 42 (1), 10, (1976).
102. C. W. GARLAND; *J. Phys. Chem.*, 63, 1423, (1959).
103. J. B. PERI; *Disc. Faraday Soc.*, 41, 121, (1966).
104. J. B. PERI; *J. Phys. Chem.*, 70, 3168, (1966).
105. M. UCHIDA and T. IMAI; *Bull. Chem. Soc., Japan*, 35, 989, (1962).
106. I. G. VOROSHILOV, L. M. ROEV, G.M. KOZUB, M.T. RUSOV, and N. K. LUNEV; *Kinet. Katal.*, 16 (5), 1267, (1975).
107. P. H. EMMETT; "Catalysis", Vol. IV, Reinhold Publishing Corp., New York, (1956).
108. S. S. DERBENEVA, L. G. KARAKCHIEV, B. N. KUZNETSOV, and Yu. I. ERMAKOV; *Kinet. Katal.*, 16 (1), 262, (1975).
109. K. H. LUDLUM and R. P. EISCHEMS; *Surface Sci.*, 40 (2), 397, (1973).
110. G. MARX, H. HOBERT, V. HOPFE, B. KNAPPE, W. VOGELSBERGER, P. MACKRODT, and K. MEYER; *Z.Chem.*, 12 (12), 444, (1972).
111. H. L. PICKERING and H.C. ECKSTROM; *J. Phys. Chem.*, 63, 513, (1959).
112. H. C. ECKSTROM; *J. Phys. Chem.*, 70, 594, (1966).
113. L. H. JONES; *J. Chem. Phys.*, 28, 1215, (1958).
114. J. B. SARDISCO; *Perkin-Elmer Inst. News*, 15, 3, (1963).
115. C. W. GARLAND, R. C. LORD, and P. F. TROIANO; *J. Phys. Chem.*, 69, 1195, (1965).

116. F. S. BAKER, A. M. BRADSHAW, and J. PRITCHARD; Surface Sci., 12 (3), 426, (1968).
117. A. M. BRADSHAW and J. PRITCHARD; Surface Sci., 17 (2), 372, (1969).
118. G. BLYHOLDER, M. TANAKA, and J. D. RICHARDSON; J. Chem. Soc. D., 10, 499, (1971).
119. G. G. POSSLEY; Dist. Abst. Int. B, 31 (1), 155, (1970).
120. A. M. BRADSHAW and J. PRITCHARD; Proc. Roy. Soc., Ser. A, 316 (1525), 169, (1970).
121. A. M. BRADSHAW and O. VIERLE; Ber. Bunsengesellschaft Phys. Chem., 74, 630, (1970).
122. N. N. KAVTARADZE and N. P. SOKOLOVA; Russ. J. Phys. Chem., 44, 1485, (1970).
123. W. A. PLISKIN and R. P. EISCHENS; Z. Phys. Chem. Frankf. Ausg., 24, 11, (1960).
124. R. van HARDEVELD and A. van MONTFOORT; Surface Sci., 4, 396, (1966)
125. J. LAPUJOULADE and K. S. NEIL; J. Chim. Phys. Physicochim. Biol., 70 (5), 798, (1973).
126. D. D. CASEY; Diss. Abstr. Int. B, 33 (12), (Part 1), 6026, (1973).
127. M. PROCOP and J. VOELTER; Z. Phys. Chem. (Leipzig), 253 (1-2), 33, (1973).
128. K. SHIRONO, T. YAMABE, M. UEHARA, T. IKAWA, and S. SUZUKI; Nippon Kagaku Kaishi, 1, 35, (1975).
129. M. PRIMET and N. SHEPPARD; J. Catal., 41 (2), 258, (1976).
130. M. DE VIJLDER and K. F. VANDEN; Bull. Soc. Chim. Belg., 84 (12), 1165, (1975).
131. E. F. McCOY and R. St.C. SMART; Surface Sci., 39 (1), 109 (1973).
132. R. W. JOYNER and M. W. ROBERTS; J. Chem. Soc., Faraday Trans. 1, 70, 1819, (1974).
133. K. KISHI and M. W. ROBERTS; J. Chem. Soc. Faraday Trans. 1, 71 (8), 1715, (1975).
134. R. W. JOYNER and M. W. ROBERTS; Chem. Phys. Lett., 29 (3), 447, (1974).

135. Yu. I. ERMAKOV and B. N. KUZNETSOV; *React. Kinet. Catal. Lett.*, 1 (1), 87, (1974).
136. S. V. BATYCHKO, M. T. RUSOV, and L. M. ROEV; *Dokl. Akad. Nauk. SSSR*, 191 (6), 1309, (1970).
137. D. V. POZDNYOKOV and V. N. FILIMONOV; *Kinet. Katal.*, 13 (2), 522, (1972).
138. J. A. DALMON, G. A. MARTIN, and B. IMELIK; *Colloq. Int. Cent. Nat. Rech. Sci.*, 593, 1971, (Pub. 1972).
- 139.* R. P. EISCHENS and W. A. PLISKIN; *Adv. Catal.*, 10, 1, (1958).
140. G. BLYHOLDER and L. D. NEFF; *J. Phys. Chem.*, 66, 1464, (1962).
141. G. BLYHOLDER and L. D. NEFF; *J. Phys. Chem.*, 66, 1664, (1962).
142. F. FISCHER and H. TROPSCH; *Brennstoff-Chem.*, 7, 97, (1926).
143. R. J. KOKES, W. K. HALL, and P. H. EMMETT; *J. Amer. Chem. Soc.*, 79, 2989, (1957).
144. H. KÖLBEL, M. RALEK, and P. JIRU; *Erdöl u. Kohle, Erdgas, Petrochem.*, 23, 580, (1970).
145. H. KÖLBEL, M. RALEK, and P. JIRU; *Z. Naturforsch.*, 25a, 670, (1970).
146. H. KÖLBEL, M. RALEK, and P. JIRU; *Collect. Czech. Chem. Commun.*, 36 (2), 512, (1971).
147. J. ANSORGE and H. FOERSTER; *Z. Phys. Chem. (Frankfurt am Main)*, 95 (4-6), 255, (1975).
148. W. H. SMITH and H. C. ECKSTROM; *J. Chem. Phys.*, 46, 3657, (1967).
149. D. W. PASHLEY; *Advan. Phys.*, 14, 327, (1965).
150. L. M. ROEV, S. V. BATYCHKO, and M. T. RUSOV; *Theor. Eksp. Khim.*, 7 (2), 232, (1971).
151. G. BLYHOLDER; *J. Phys. Chem.*, 76 (22), 3180, (1972).
152. G. C. BOND; *"Catalysis by Metals"*, Academic Press, N.Y., (1962).
153. R. R. FORD; *Adv. Catal.*, 21, 51, (1970).
154. R. QUEAU and R. POILBLANC; *J. Catal.*, 27 (2), 200, (1972).
155. Y. - Y. HUANG and J. R. ANDERSON; *J. Catal.*, 40 (2), 143, (1975).
156. G. I. KOVALEV, Yu. B. KAGAN, and A. V. KRYLOVA; *Izv. Otd. Khim. Nauki, Bulg. Akad. Nauk.*, 6 (1), 235, (1973).
157. H. KÖLBEL and K. D. TILLMETZ; *J. Catal.*, 34 (2), 307, (1974).
158. T. G. VOROSHILOV, N. K. LUNEV, L. M. ROEV, and M. T. RUSOV; *Dopov. Akad. Nauk. Ukr. RSR, Ser. B*, 4, 319, (1975).

159. M. R. BASILA; Appl. Spectr. Rev., 1 (2), 289, (1968).
160. G. BLYHOLDER and W. V. WYATT; J. Phys. Chem., 70 (6), 1745, (1966).
161. G. BLYHOLDER and A. MARVIN; J. Amer. Chem. Soc., 91 (2), 3158, (1969).
162. J. F. HARROD, R. W. ROBERTS, and E. F. RISSMAN; J. Phys. Chem., 71, 343, (1967).
163. A. IGARASHI, Y. OGINO, and S. ONODERA; Rev. Sci. Instrum., 44, 321, (1973).
164. J. B. PERI and R. B. HANNAN; J. Phys. Chem., 64, 1526, (1960).
165. M. J. HEAL, E. C. LEISEGANG, and R. G. TORRINGTON; J. Phys. E: Sci. Instrum., 7, 352, (1974).
166. L. H. JONES; J. Chem. Phys., 23, 2448, (1955).
167. A. H. NIELSON and H. H. NIELSON; Phys. Rev., 48, 864, (1935).
168. H. STAMMERICH, K. KAWAI, OSW. SALA, and P. KRUMHOLZ; J. Chem. Phys., 35, 2168, (1961).
169. G. BLYHOLDER; J. Vac. Sci. Technol., 11 (5), 865, (1974).
170. G. BLYHOLDER; J. Chem. Phys., 62 (8), 3193, (1975).
171. R. GOMEZ, F. FIGUERAS, and H. CHARCOSSET; Rev. Inst. Mex. Petrol., 5 (3), 66, (1973).
172. Yu N. ARTYUKH and N. K. LUNEV; Kinet. Katal., 12, 253, (1971).
173. L. RAMQVIST; J. Appl. Phys., 42, 2113, (1971).
174. P. B. TQTTTRUP; J. Catal., 42 (1), 29, (1976).
175. H. KÖLBEL: in "Winnacker-Küchler, Chem. Technologie", Vol. 3, p. 457. Carl Hanser, München, (1959).
- 176.* H. KNÖZINGER; Acta. Cient. Venez., 24 (2), 76, (1973).
177. N. I. KOBOZEV; Acta Physicochim. U.S.S.R. 9, 805, (1938).
178. D. A. DOWDEN; "Catalysis", (G. W. Hightower, Ed.), Vol. 41, 621, Proc. 5th Int. Congr. Catalysis. Florida, (1972).
179. W. M. H. SACHTLER and P. Van Der PLANK; Surface Sci., 18, 62, (1969).
180. R. J. FARRAUTO; J. Catal., 41, 482, (1976).
181. R. BALAJI GUPTA, B. VISWANATHAN, and M.V.C. SASTRI; J. Catal., 26, 212, (1972).

* These references have been repeated elsewhere, viz 139 (85) and 176 (59).